PAPER

Qubit models of weak continuous measurements: markovian conditional and open-system dynamics

To cite this article: Jonathan A Gross *et al* 2018 *Quantum Sci. Technol.* **3** 024005

View the article online for updates and enhancements.

Recent citations

Quantum Science and Technology

PAPER

Qubit models of weak continuous measurements: markovian conditional and open-system dynamics

Jonathan A Gross[1,2,5] , Carlton M Caves[1,2], Gerard J Milburn[2] and Joshua Combes[1,2,3,4]

[1] Center for Quantum Information and Control, University of New Mexico, Albuquerque NM 87131-0001, United States of America
[2] Centre for Engineered Quantum Systems, School of Mathematics and Physics, The University of Queensland, St. Lucia QLD 4072, Australia
[3] Institute for Quantum Computing, Department of Applied Mathematics, University of Waterloo, Waterloo, ON, Canada
[4] Perimeter Institute for Theoretical Physics, 31 Caroline St. N, Waterloo, Ontario, N2L 2Y5 Canada
[5] Author to whom any correspondence should be addressed.

E-mail: jagross@unm.edu, ccaves@unm.edu, milburn@physics.uq.edu.au and joshua.combes@gmail.com

Abstract

In this paper we approach the theory of continuous measurements and the associated unconditional and conditional (stochastic) master equations from the perspective of quantum information and quantum computing. We do so by showing how the continuous-time evolution of these master equations arises from discretizing in time the interaction between a system and a probe field and by formulating quantum-circuit diagrams for the discretized evolution. We then reformulate this interaction by replacing the probe field with a bath of qubits, one for each discretized time segment, reproducing all of the standard quantum-optical master equations. This provides an economical formulation of the theory, highlighting its fundamental underlying assumptions.

1. Introduction and motivation

The strength of a projective measurement is made known in weakness. Although we are taught from youth that quantum measurements project the target system onto an eigenstate of the measured observable as an irreducible action, closer inspection reveals a more nuanced reality. Measurements involve coupling quantum systems to macroscopic devices via finite-energy interactions, these devices have finite temporal resolution, and a host of imperfections lead to encounters with the classical world that violate unitarity without conforming to the projective-measurement mold.

Of course, in many scenarios these discrepancies are fleeting and the projective description is all that is needed—and sometimes all that can be observed! Modern experiments, however, show projective measurements for what they are, and if we are to glory in this revelation, we need tools like the theory of quantum trajectories, which generalizes measurement projection to weak, continuous monitoring of a quantum system.

Consider using a transition-edge sensor to detect photons. As a photon is absorbed by the detector, the output current begins to drop. At first it is difficult to tell the difference between a photon and thermal fluctuations, but as the current continues to drop we become more and more confident of the detection prognosis until we have integrated enough current deficiency to announce a detection. The accumulating current deficiency is the result of a continuous sequence of *weak measurements* (sometimes called *gentle* or *fuzzy*), where the name signifies that each measurement outcome (in this case output current integrated over a short time interval) contains little information about the system being measured and consequently only gently disturbs that system. Many repetitions of such weak measurements, however, do have an appreciable effect upon the system, sometimes as dramatic as a projective measurement. Because these measurements are nearly continuous, differential equations are used to track the cumulative effect on the system, and because quantum theory tells us the measurement results are random, these differential equations are stochastic.

The system's time-dependent state (or some expectation value thereof) conditioned on a continuous measurement record is called a *quantum trajectory* in the continuous-measurement literature. Physically, this continuous measurement record is written on successive probes that interact weakly with the system. The stochastic differential equations that generate quantum trajectories take a variety of forms, going by names such as *stochastic Schrödinger equations*, *quantum-filtering equations*, or in this paper *stochastic master equations* (SMEs). A great deal of attention has been devoted both to deriving stochastic equations for and to observing trajectories in a variety of physical systems, e.g., cavity QED [1], circuit QED (superconducting systems) [2–4], fermionic systems [5–7], and mechanical systems [8–11].

The ability to resolve these subprojective effects opens up many possibilities, including feedback protocols and continuous-time parameter estimation. An example of feedback control is continuous-time quantum error correction. Ahn *et al* [12] investigated using continuous-time quantum measurements for this purpose, thus pioneering a fruitful line of research [13–21]. Feedback control additionally allows one to view weak measurements as building blocks for constructing other generalized measurements, as explored by Brun and collaborators [22–25]. Continuous weak measurements have also been pressed into service for parameter and state estimation [26–32]. One notable example is the single-shot tomography of an ensemble of identically prepared qubits [33].

Error correction, parameter estimation, and state tomography are important subjects in quantum computation and information. Unfortunately, much of the literature on continuous weak measurements, which would otherwise be of interest to this community, suffers from needlessly arcane terminology and interpretations. We take the refiner's fire to trajectory theory, revealing a foundation of finite-dimensional probe systems, unitary gates between the system and successive probes, and quantum operations to describe the system state after the probe is measured—all three familiar to the quantum information scientist of today. This process also distills the essence of trajectory theory from its origins in field-theoretic probes, yielding insights that can be appreciated even by veterans of the subject. A particularly useful tool that arises naturally within our approach is the quantum circuit diagram, and we take pains throughout our presentation to illustrate relevant principles with this tool.
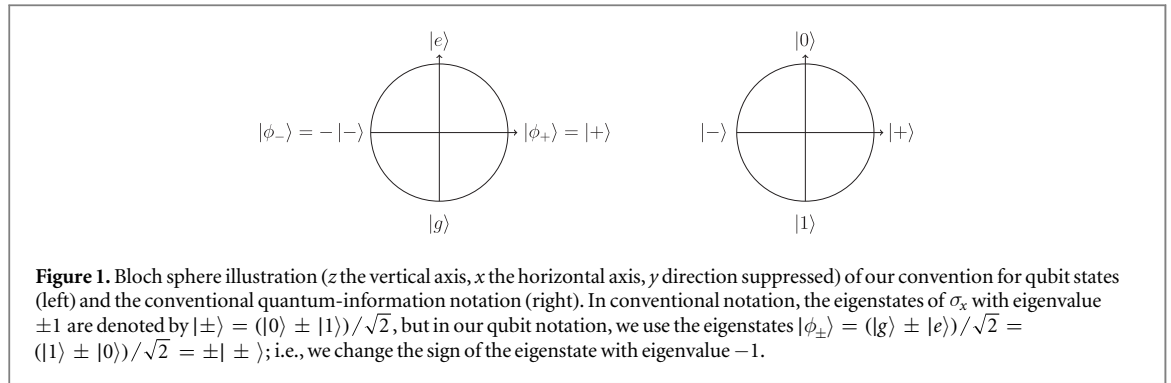
Of all the prior work on this subject, our paper is most related to—and indeed inspired by—Brun's elegant work on qubit models of quantum trajectories [34]. In sections 3 and 5 we describe the connection between his work and ours. Looking further back to the origin of this line of research, one might identify an important precedent in the work [35] of the great theorists, Scully and Lamb (Lamb also did experiments), in which they considered systems interacting with a spin bath. The mathematics literature has a related body of work that studies approximating Fock spaces with chains of qubits known as 'toy Fock spaces' [36–44].

The physics and mathematical-physics communities have a rich history of deriving the stochastic equations of motion for a system subject to a continuous measurement. So rich, in fact, that these equations have been discovered and rediscovered many times. Historically, the theory was developed in the 80's and early 90's by a number of authors: Mensky [45, 46], Belavkin [47], Srinivas and Davies [48], Braginskiĭ and Khalili [49], Barchielli *et al* [50], Gisin [51], Diósi [52, 53], Caves [54, 55], Caves and Milburn [56], Milburn [57], Carmichael [58], Dalibard *et al* [59], and Wiseman [57]. The most recent rediscovery was by Korotkov [60, 61], who dubiously introduced yet more terminology by christening his rediscovery 'quantum Bayesian theory.'

Many other good references on the topic are available for the interested reader. We recommend the following articles: Brun [34], Jacobs and Steck [62], Wiseman's PhD thesis [63], and for the mathematically inclined reader, Bouten *et al* [43, 64]. Helpful books include [58, 65, 66], and [67].

This paper is structured as follows: section 2 lays out our notational conventions. Section 3 gives a unified description of strong and weak measurements via ancilla-coupled measurements, followed by quantum-circuit depictions of the iterated interactions that limit to continuous quantum measurements and their relation to Markovicity. Section 4 develops the continuous-measurement theory in terms of a system undergoing successive weak interactions with a probe field.

Sections 5 to 7 are the heart of the paper: they show how to replace a probe field with probe qubits in constructing quantum trajectories, and they explore the consequences of changing the parameters of the formalism, i.e., using different probe initial states, different interaction unitaries, and different measurements on the probes. Section 5 contains the first derivation of a SME in our model, focusing on the vacuum SMEs. These arise when probe initial states are vacuum (ground state for probe qubits); the probe undergoes a weak interaction with the system and then experiences one of several kinds of measurements, which lead to different quantum trajectories. The theme of section 5 is thus exploring the effect of different kinds of measurements on the probes. Section 6 considers the Gaussian SMEs, in which a probe field starts in a Gaussian state, undergoes a weak interaction with the system, and then is subjected to homodyne measurements. The theme of this section is thus exploring the effect of different probe initial states, but the main contribution of this section is a technique to accommodate all the Gaussian field states in probe qubits and to show that, since qubits have too small a Hilbert space to achieve this by only changing the initial state, one must also modify aspects of the weak system/

Figure 1. Bloch sphere illustration (*z* the vertical axis, *x* the horizontal axis, *y* direction suppressed) of our convention for qubit states (left) and the conventional quantum-information notation (right). In conventional notation, the eigenstates of σ_x with eigenvalue ± 1 are denoted by $|\pm\rangle = (|0\rangle \pm |1\rangle)/\sqrt{2}$, but in our qubit notation, we use the eigenstates $|\phi_\pm\rangle = (|g\rangle \pm |e\rangle)/\sqrt{2} = (|1\rangle \pm |0\rangle)/\sqrt{2} = \pm|\pm\rangle$; i.e., we change the sign of the eigenstate with eigenvalue -1.

probe interaction unitary. Section 7 explores a radical departure that allows interactions between the probe qubits and the system that are strong, but occur randomly.

As an aid to intuition, section 8 presents visualizations of numerical solutions to some of the SMEs derived in the previous sections. Finally, section 9 summarizes lessons learned from our approach and suggests promising related approaches.

2. Notational conventions

Confusion can arise when denoting the states of quantum-field modes and two-level systems (qubits) in the same context. In particular, that $a|n\rangle = \sqrt{n}|n-1\rangle$ and thus $a|1\rangle = |0\rangle$, yet $\sigma_-|0\rangle = |1\rangle$, can lead to momentary confusion and even persistent perplexity. The standard qubit states are the eigenstates of $\sigma_z = |0\rangle\langle 0| - |1\rangle\langle 1| = \sum_{a=0,1}(-1)^a|a\rangle\langle a|$; since the qubit Hamiltonian is often proportional to σ_z—this is why one chooses $|0\rangle$ and $|1\rangle$ to be the standard states—it is natural to regard $|1\rangle$ (eigenvalue -1 of σ_z) as the ground state and $|0\rangle$ (eigenvalue $+1$) as the excited state. In doing so, one is allowing the multiplicative label $(-1)^a$ to trump the bitwise label a, which gives an opposite hint for what should be labeled ground and excited.

To allay this confusion, one good practice would be to label the standard qubit states by the eigenvalue, $(-1)^a$, of σ_z, but instead we choose the more physical labeling of $|g\rangle = |1\rangle$ as the 'ground state' and $|e\rangle = |0\rangle$ as the 'excited state.' In this notation, $\sigma_-|e\rangle = |g\rangle$, as expected; this notation plays well with the correspondence we develop between field modes and two-level systems. Our notation is illustrated in figure 1. As a further check on confusion, we often label the vacuum state of a field mode as $|vac\rangle$ instead of $|0\rangle$.

Some useful relations between qubit operators are given below:

$$\sigma_+ = |e\rangle\langle g| = |0\rangle\langle 1| = \tfrac{1}{2}(\sigma_x + i\sigma_y),$$
$$\sigma_- = |g\rangle\langle e| = |1\rangle\langle 0| = \tfrac{1}{2}(\sigma_x - i\sigma_y),$$
$$\sigma_x = \sigma_+ + \sigma_- = |e\rangle\langle g| + |g\rangle\langle e|,$$
$$\sigma_y = -i\sigma_+ + i\sigma_- = -i|e\rangle\langle g| + i|g\rangle\langle e|,$$
$$\sigma_z = |e\rangle\langle e| - |g\rangle\langle g|,$$
$$[\sigma_-, \sigma_+] = \tfrac{1}{2}i[\sigma_x, \sigma_y] = -\sigma_z. \tag{2.1}$$

When writing qubit operators and states in their matrix representations, we order the rows and columns starting from the top and left with $|e\rangle = |0\rangle$ followed by $|g\rangle = |1\rangle$. Thus $\sigma_- = |g\rangle\langle e|$ has the representation

$$\begin{array}{cc} & \langle e| \quad \langle g| \\ \begin{array}{c} |e\rangle \\ |g\rangle \end{array} & \begin{pmatrix} 0 & 0 \\ 1 & 0 \end{pmatrix}. \end{array} \tag{2.2}$$

The first place our notation has the potential to confuse is in how we denote the eigenstates of σ_x. These eigenstates are conventionally written as $|\pm\rangle = (|0\rangle \pm |1\rangle)/\sqrt{2}$, but we choose to denote them by

$$|\phi_\pm\rangle := \frac{1}{\sqrt{2}}(|g\rangle \pm |e\rangle) = \frac{1}{\sqrt{2}}(|1\rangle \pm |0\rangle) = \pm|\pm\rangle; \tag{2.3}$$

i.e., we change the sign of the eigenstate with eigenvalue -1. This notation is illustrated in figure 1.

In our circuit diagrams, each wire corresponds to an individual system; a collection of those wires corresponds to a tensor product of the systems. To keep track of the various systems when moving between circuit and algebraic representations, the tensor-product order equates systems left-to-right in equations with
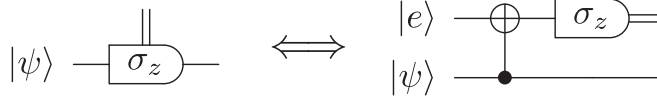
Figure 2. Equivalence between a direct (left) and ancilla-coupled (right) measurement of σ_z. Note that for the CNOT gate in the ancilla-coupled measurement, the application of the NOT gate to the probe is controlled on $|g\rangle = |1\rangle$, as shown algebraically in equation (3.1). The single wires carry systems in quantum states, while the double wires carry classical information. In both the direct and the ancilla-coupled measurement, the double wire emerging from the measurement apparatus carries the result of the measurement, either e (0) or g (1). After the measurement, the system is left in the corresponding state, $|e\rangle$ ($|0\rangle$) or $|g\rangle$ ($|1\rangle$); this state is carried by the system wire emerging from the right of the measurement apparatus in the direct measurement and by the system wire proceeding to the right in the ancilla-coupled version.

the systems bottom-to-top in the circuits. We also reserve the left-most/bottom position for the system in our discussions, putting the probe systems to the right/above. True to conventional quantum-circuit practice, single wires carry quantum information (i.e., systems in quantum states), whereas double wires carry classical information (typically measurement outcomes).

We use the notation $\mathbb{E}[\Delta A]$ to denote the expectation value of a classical random variable ΔA, which need not correspond to a Hermitian observable. Typically ΔA can be thought of as a map from measurement outcomes to numbers, in which case sampling from ΔA involves performing said measurement and mapping the outcome to the appropriate value. For a measurement defined by a POVM $\{E_j\}$ (see section 3.3) and corresponding random-variable values denoted by ΔA_j, the expectation value evaluates to

$$\mathbb{E}[\Delta A] = \sum_j \Delta A_j \, \mathrm{Tr}\,[\rho E_j]. \tag{2.4}$$

The implicit dependence on quantum state ρ and measurement POVM $\{E_j\}$ should be clear from context.

3. Measurements and the quantum-circuit depiction

3.1. Indirect and weak measurements

The instantaneous direct measurement of quantum systems, still the staple of many textbook discussions of quantum measurement, is only a convenient fiction. As discussed in the Introduction, one typically makes a measurement by coupling the system of interest to an ancillary quantum system prepared in a known state and then measuring the ancilla. This is called an *indirect* or *ancilla-coupled* measurement. For brevity we refer to the system of interest as the *system*. Although the ancillary system goes by a variety of names in the literature, we refer to such systems here as *probes* to evoke the way they approach the system to interrogate it and depart to report their findings. When additional clarity is helpful, we use subscripts to identify states with various systems, so $|\psi\rangle_{\mathrm{sys}}$ and ρ_{sys} designate system states and $|\phi\rangle_{\mathrm{pr}}$ and σ_{pr} designate probe states.

Ancilla-coupled measurements can be used to effect any generalized measurement, including the direct measurements of textbook lore. Suppose one wants to measure σ_z on a qubit system. This can be accomplished by preparing a probe qubit in the state $|e\rangle$, performing a controlled-NOT (CNOT) gate from the system to the probe, and finally measuring σ_z directly on the probe. The CNOT gate is defined algebraically as

$$\mathrm{CNOT} := |e\rangle\langle e| \otimes \mathbf{1} + |g\rangle\langle g| \otimes \sigma_x = |0\rangle\langle 0| \otimes \mathbf{1} + |1\rangle\langle 1| \otimes \sigma_x. \tag{3.1}$$

Doing nothing when the probe is in the excited state might feel strange, but this convention is chosen to harmonize with the quantum-information notation that is shown in the second form of equation (3.1), in which the NOT gate (σ_x) is applied to the probe when the system is in the state $|1\rangle = |g\rangle$; this is called control on $|1\rangle$ or, in this context, control on $|g\rangle$. Figure 2 depicts in quantum circuits the equivalence between a direct measurement of σ_z and the ancilla-coupled measurement.

For an arbitrary initial system state

$$|\psi\rangle_{\mathrm{sys}} := \alpha \, |g\rangle_{\mathrm{sys}} + \beta \, |e\rangle_{\mathrm{sys}}, \tag{3.2}$$

the joint state of the system and probe after the interaction is

$$|\Psi\rangle := \mathrm{CNOT} \, |\psi\rangle_{\mathrm{sys}} \otimes |e\rangle_{\mathrm{pr}} = \alpha|gg\rangle + \beta|ee\rangle. \tag{3.3}$$

Local σ_z measurements on the probe are described by the projectors $\Pi_g^{(\mathrm{pr})} := \mathbf{1} \otimes |g\rangle\langle g|$ and $\Pi_e^{(\mathrm{pr})} := \mathbf{1} \otimes |e\rangle\langle e|$ (the superscript indicates projection only on the probe). These measurements give the following probabilities and post-measurement system states:

$$\mathrm{Pr}(g) = \langle\Psi|\Pi_g^{(\mathrm{pr})}|\Psi\rangle = |\alpha|^2, \qquad \frac{\mathrm{Tr}_{\mathrm{pr}}[\Pi_g^{(\mathrm{pr})}|\Psi\rangle\langle\Psi|\,\Pi_g^{(\mathrm{pr})}]}{\mathrm{Pr}(g)} = |g\rangle_{\mathrm{sys}}\langle g|, \tag{3.4}$$

$$\Pr(e) = \langle\Psi|\Pi_e^{(\mathrm{pr})}|\Psi\rangle = |\beta|^2, \qquad \frac{\mathrm{Tr}_{\mathrm{pr}}[\Pi_e^{(\mathrm{pr})}|\Psi\rangle\langle\Psi|\ \Pi_e^{(\mathrm{pr})}]}{\Pr(e)} = |e\rangle_{\mathrm{sys}}\langle e|. \qquad (3.5)$$

These are the same probabilities and post-measurement system states as for a direct measurement of σ_z on the system. This equivalence comes about because the CNOT gate produces perfect correlation in the standard qubit basis.

More general interactions between the system and probe do not produce perfect correlation. A specific example of an imperfectly correlating interaction,

$$U_{\mathrm{CNOT}}(\theta) \coloneqq \exp\left(-i\theta\ \mathrm{CNOT}\right) = \cos\theta\ \mathbf{1}\otimes\mathbf{1} - i\sin\theta\ \mathrm{CNOT}, \qquad (3.6)$$

was presented by Brun [34]; $\theta = 0$ gives the identity, i.e., no correlation between system and probe, and $\theta = \pi/2$ gives (up to the global phase $-i$) CNOT, i.e., perfect correlation between system and probe. For $0 < \theta < \pi/2$ the probe becomes partially correlated with the system. This kind of partial CNOT can be constructed because the CNOT gate is Hermitian as well as unitary, and therefore generates unitary transformations. The joint state of the system/probe after the interaction is

$$|\Psi_\theta\rangle \coloneqq U_{\mathrm{CNOT}}(\theta)|\psi\rangle_{\mathrm{sys}}\otimes|e\rangle_{\mathrm{pr}} = \cos\theta\ |\psi\rangle_{\mathrm{sys}}\otimes|e\rangle_{\mathrm{pr}} - i\sin\theta|\Psi\rangle = \beta e^{-i\theta}|ee\rangle + \alpha\cos\theta|ge\rangle - i\alpha\sin\theta|gg\rangle. \qquad (3.7)$$

A projective measurement on the probe after the interaction gives only partial information about the system and thus only partially projects the system state. As explained in the Introduction, such measurements have been called *weak*, *fuzzy*, or *gentle*. These measurements should not be equated with *weak values* [68, 69], a derivative concept utilizing weak measurements but with no additional relation to the continuous-measurement schemes we consider. The outcome probabilities and post-measurement system states are

$$\Pr(g) = \langle\Psi_\theta|\Pi_g^{(\mathrm{pr})}|\Psi_\theta\rangle = |\alpha|^2\sin^2\theta, \qquad \frac{\mathrm{Tr}_{\mathrm{pr}}[\Pi_g^{(\mathrm{pr})}|\Psi_\theta\rangle\langle\Psi_\theta|\ \Pi_g^{(\mathrm{pr})}]}{\Pr(g)} = |g\rangle_{\mathrm{sys}}\langle g|, \qquad (3.8)$$

$$\Pr(e) = \langle\Psi_\theta|\Pi_e^{(\mathrm{pr})}|\Psi_\theta\rangle = |\beta|^2 + |\alpha|^2\cos^2\theta, \qquad \frac{\mathrm{Tr}_{\mathrm{pr}}[\Pi_e^{(\mathrm{pr})}|\Psi_\theta\rangle\langle\Psi_\theta|\ \Pi_e^{(\mathrm{pr})}]}{\Pr(e)} = |\chi\rangle_{\mathrm{sys}}\langle\chi|, \qquad (3.9)$$

where

$$|\chi\rangle_{\mathrm{sys}} = \frac{\alpha\cos\theta\ |g\rangle_{\mathrm{sys}} + \beta e^{-i\theta}\ |e\rangle_{\mathrm{sys}}}{\sqrt{|\alpha|^2\cos^2\theta + |\beta|^2}}. \qquad (3.10)$$

For $\theta \ll 1$, we can expand these results to second order in θ to see more clearly what is going on in the case of a weak measurement. The outcome e is very likely, occurring with probability $\Pr(e) \simeq 1 - |\alpha|^2\theta^2$, and when this outcome is observed, the post-measurement state of the system is almost unchanged from the initial state

$$|\chi\rangle_{\mathrm{sys}} \simeq \alpha\left(1 - \tfrac{1}{2}|\beta|^2\theta^2\right)|g\rangle_{\mathrm{sys}} + \beta\left(1 - i\theta - \tfrac{1}{2}|\beta|^2\theta^2\right)|e\rangle_{\mathrm{sys}}. \qquad (3.11)$$
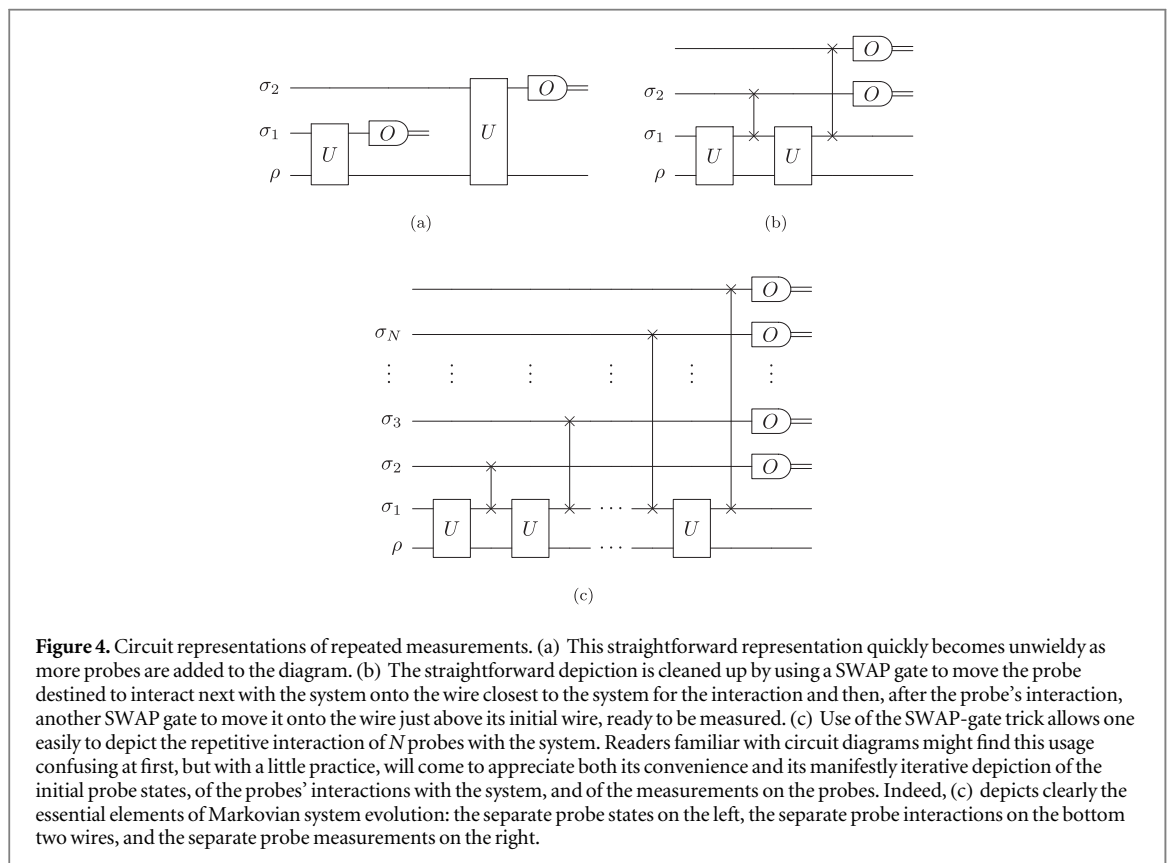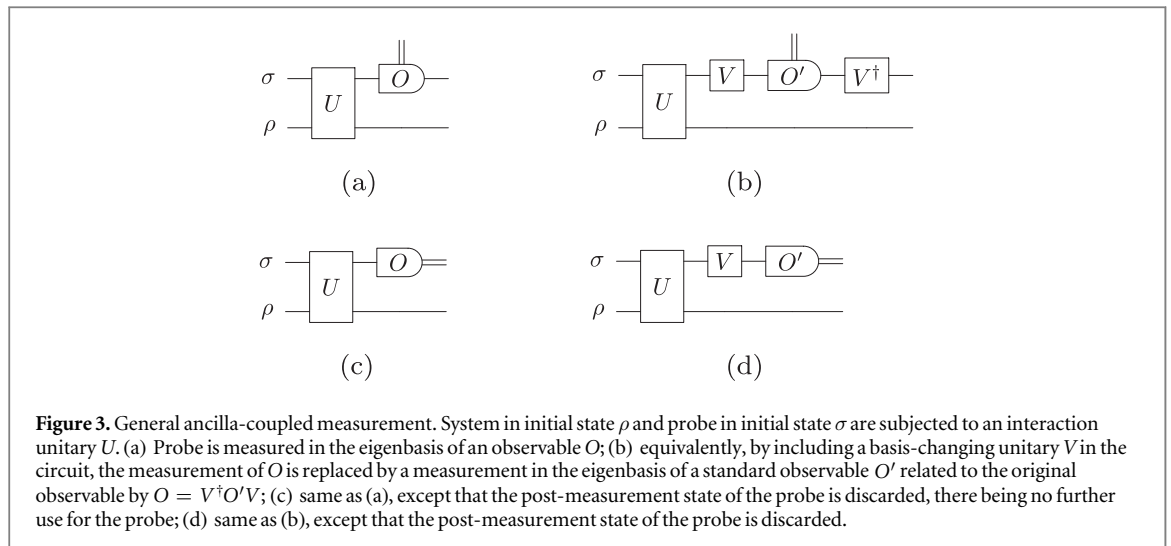
In contrast, the outcome g is very unlikely, occurring with probability $\Pr(g) \simeq |\alpha|^2\theta^2$, and when this outcome is observed, the system is projected into the state $|g\rangle_{\mathrm{sys}}$, which can be very different from the initial state. This kind of weak measurement can be thought of as usually providing very little information about the system, but occasionally determining that the system is in the ground state. These unlikely, discontinuous events in system evolution are often referred to as *quantum jumps* in the literature [70].

3.2. Quantum-circuit description of measurements

In the most general ancilla-coupled-measurement scheme, the system is initially in a (possibly mixed) state ρ and the probe begins in the (possibly mixed) state σ. System and probe interact via an interaction unitary U and then the probe is measured in the eigenbasis of an observable O. We illustrate and elaborate on this scheme in figure 3.

Because a weak measurement extracts partial information and thus only partially projects the system onto an observed eigenstate, we can learn more about the system by performing repeated weak measurements (contrast this with a projective measurement, where one gains no new information by immediately repeating the measurement). One method of extracting all the available information about the system is to repeat a weak measurement many times. Such iterated weak measurements are explored in more detail in section 4.

We introduce a circuit convention in figure 4 that makes it easy to depict iterated measurements. The naïve depiction, figure 4(a), is clumsy and distracts from the repetitive character of the probe interactions. For the remainder of the paper, we employ a cleaner convention by reserving one probe wire (usually the one nearest to the system) for all interactions with the system. We then use SWAP gates to bring probes into and out of contact with the system as necessary. Thus the circuit in figure 4(a) transforms to figure 4(b). Generally, the SWAP trick leads to circuit diagrams like figure 4(c). The SWAPs in all cases are purely formal and used only for convenience.

Figure 3. General ancilla-coupled measurement. System in initial state ρ and probe in initial state σ are subjected to an interaction unitary U. (a) Probe is measured in the eigenbasis of an observable O; (b) equivalently, by including a basis-changing unitary V in the circuit, the measurement of O is replaced by a measurement in the eigenbasis of a standard observable O' related to the original observable by $O = V^\dagger O' V$; (c) same as (a), except that the post-measurement state of the probe is discarded, there being no further use for the probe; (d) same as (b), except that the post-measurement state of the probe is discarded.

Figure 4. Circuit representations of repeated measurements. (a) This straightforward representation quickly becomes unwieldy as more probes are added to the diagram. (b) The straightforward depiction is cleaned up by using a SWAP gate to move the probe destined to interact next with the system onto the wire closest to the system for the interaction and then, after the probe's interaction, another SWAP gate to move it onto the wire just above its initial wire, ready to be measured. (c) Use of the SWAP-gate trick allows one easily to depict the repetitive interaction of N probes with the system. Readers familiar with circuit diagrams might find this usage confusing at first, but with a little practice, will come to appreciate both its convenience and its manifestly iterative depiction of the initial probe states, of the probes' interactions with the system, and of the measurements on the probes. Indeed, (c) depicts clearly the essential elements of Markovian system evolution: the separate probe states on the left, the separate probe interactions on the bottom two wires, and the separate probe measurements on the right.

The SWAP trick works because our system is distinct from the probes in an important way. We are assuming that the system is persistent and not directly accessible—i.e., we cannot directly measure or swap the state of the system—while the probes are transient, interacting with the system once and then flying away to be measured. In figure 4 we have included subscripts to individuate the probes, although we often omit these designations since the circuit wire already contains this information—e.g., in a circuit diagram, we can drop the probe designation n from σ_n since the diagram tells us which probe this density operator describes.

Under the repetitive measurements depicted in figure 4(c), the system undergoes a conditional dynamics, where the conditioning is on the results of the measurements on the probes. Discarding the results of the measurements on the probe is equivalent to not doing any measurements on the probe, and then the system dynamics are the unconditional open-system dynamics that come from tracing out the probes after they interact with the system.

Figure 5. Two different scenarios that produce non-Markovian system dynamics by changing the probe-system interactions away from the Markovian pattern in figure 4(c): (a) A finite environment (here consisting of three probes) forces the probes to return and interact repeatedly with the system. (b) Successive probes simultaneously interact with the system, making it impossible to separate the environment into disjoint modes that individually interact with the system.

The circuit diagram in figure 4(c) can be thought of as depicting probes that successively and separately scatter off the system and then are measured to extract the information picked up from the system in the scattering event. Indeed, the diagrams highlight the essential assumptions behind the Markovian system evolution that comes with this sort of scattering. Each probe, in its own state, uncorrelated with the other probes, scatters off the system and then flies away, never to encounter the system again; this happens, for example, when a vacuum or thermal field scatters off the system and propagates away to infinity. The result is Markovian unconditional evolution; to get Markovian conditional evolution, one requires in addition that the probes be measured independently. Markovian evolution is usually thought of in the context of continuous-time evolution, in which the interaction unitaries U correspond to repetitive Hamiltonian evolution for infinitesimal time intervals and thus are necessarily weak interactions that give rise to weak, continuous measurements on the system. Despite the importance of continuous-time evolution and continuous measurements, which are the focus of this paper, the circuit diagram in figure 4(c) allows one to see clearly what is involved in Markovian evolution even for finite-time interaction events: the separate probe states on the left, the separate probe interactions on the bottom two wires, and the separate probe measurements on the right. The circuit diagrams for infinitesimal time interactions are the foundation for the Markovian input-output theory of quantum optics, which we consider in section 6.1.

Various modifications to the circuit diagram of figure 4 give non-Markovian evolution. One modification is to initialize the probes in a correlated state, either via classical correlations or via the quantum correlations of entanglement. A second kind of modification, depicted in figure 5, is to allow the system to interact with each probe multiple times, by having a probe return and interact yet again after other probes have interacted with the system, as in figure 5(a), or to have a time window in which multiple probes interact with the system, as in figure 5(b). The first of these is the general situation when a finite environment interacts with the system; environment 'modes' acting as probes never exit cleanly, so a mode can interact with the system more than once. We note that the methods developed in [54, 55] allow probes to overlap in the same time window and thus might provide an avenue to describing non-Markovian dynamics. Finally, conditional evolution can be non-Markovian when one makes joint measurements, instead of independent measurements, on the probes after they depart from the system. This occurs when modeling finite detector bandwidth as discussed in [66, section 4.8.4].

3.3. Conditional evolution and Kraus operators

Suppose that, as is depicted in figure 4(c), we cause the system, initially in pure state $\rho = |\psi\rangle\langle\psi|$, to interact sequentially with N probes, initially in the product state $\sigma_1 \otimes \cdots \otimes \sigma_N$, where we assume, for the moment, that the initial probe states are pure, i.e., $\sigma_n = |\phi\rangle_n\langle\phi|$. The interaction of the nth probe with the system is described by the unitary operator $U^{(n)}$, and after the interaction, we measure the observable O on each probe, obtaining outcomes $o_{j_1}, \ldots, o_{j_N}$. We want to calculate probabilities for obtaining different sequences of measurement outcomes, as well as the conditional quantum state of the system after observing a particular sequence of outcomes. These probabilities can be derived in a variety of ways, some of which were explored in [54, 55], producing the following expressions [56]: the probability for the outcome sequence is

$$\Pr(o_{j_1},\ldots,o_{j_N}|\psi) = \langle\tilde{\psi}_N|\tilde{\psi}_N\rangle, \tag{3.12}$$

where

$$|\tilde{\psi}_N\rangle = \langle o_{j_1}|_1 \otimes \cdots \otimes \langle o_{j_N}|_N\, U^{(N)} \cdots U^{(1)}|\psi\rangle \otimes |\phi\rangle_1 \otimes \cdots \otimes |\phi\rangle_N \tag{3.13}$$

is the unnormalized system state at the end of the entire process and

$$|\psi_N\rangle = |\tilde{\psi}_N\rangle \Big/ \sqrt{\langle\tilde{\psi}_N|\tilde{\psi}_N\rangle} \tag{3.14}$$

is the corresponding normalized state after the process. As the number of probes increases, these expressions become pointlessly unwieldy, since in the Markovian situation of figure 4(c) we should be able to deal with the probes one at a time. The most efficient way to write the results is to use the system-only formalisms of *positive-operator-valued measures* (POVMs) and *quantum operations*, which were historically introduced as *effects* and *operations*.

The ingredient common to both POVMs and quantum operations that gives us this system-only description is the *Kraus operator*, which we define in the standard way using partial inner products:

$$K_j := \langle o_j|U|\phi\rangle. \tag{3.15}$$

As usual, these Kraus operators give rise to POVM elements,

$$E_j := K_j^\dagger K_j, \tag{3.16}$$

and the POVM elements resolve the identity,

$$\sum_j E_j = \mathbf{1}. \tag{3.17}$$

The POVM elements specify the quantum statistics of a generalized measurement on the system. The conditional (unnormalized) state of the quantum system after observing a single outcome o_j is

$$\tilde{\rho} = \langle o_j|U(\rho \otimes |\phi\rangle\langle\phi|)U^\dagger|o_j\rangle = \langle o_j|U|\phi\rangle\,\rho\,\langle\phi|U^\dagger|o_j\rangle \tag{3.18}$$

and is thus described by a quantum operation constructed from the single Kraus operator K_j,

$$\tilde{\rho} = K_j \rho K_j^\dagger. \tag{3.19}$$

One can easily see that the unnormalized system state (3.13) after observing a particular outcome sequence is

$$|\tilde{\psi}_N\rangle = K_{j_N} \cdots K_{j_1}|\psi\rangle. \tag{3.20}$$

Writing this in terms of the system's initial density operator—allowing us to accommodate mixed initial system states—we get the unnormalized final system state

$$\tilde{\rho}_N = K_{j_N} \cdots K_{j_1} \rho K_{j_1}^\dagger \cdots K_{j_N}^\dagger, \tag{3.21}$$

the probability of the outcome sequence

$$\Pr(o_{j_1},\ldots,o_{j_N}|\rho) = \mathrm{Tr}[\tilde{\rho}_N] = \mathrm{Tr}[K_{j_N} \cdots K_{j_1} \rho K_{j_1}^\dagger \cdots K_{j_N}^\dagger], \tag{3.22}$$

and the normalized final state of the system,

$$\rho_N = \frac{K_{j_N} \cdots K_{j_1} \rho K_{j_1}^\dagger \cdots K_{j_N}^\dagger}{\mathrm{Tr}[K_{j_N} \cdots K_{j_1} \rho K_{j_1}^\dagger \cdots K_{j_N}^\dagger]}. \tag{3.23}$$

The Markov nature of the model manifests itself algebraically as the decomposition of the collective Kraus operator for all N measurements into a product of separate Kraus operators for each probe. Indeed, the Kraus operators for the nth probe, $K_{j_n} = \langle o_{j_n}|U^{(n)}|\phi_n\rangle$, neatly display the elements of Markovian evolution: each probe has its own initial state, its own interaction with the system, and its own measurement. As a consequence, the results for a sequence of measurements can be dealt with one probe at a time; in particular, the system state after

$n + 1$ measurements is

$$\rho_{n+1} = \frac{K_{j_{n+1}} \cdots K_{j_1} \rho K_{j_1}^\dagger \cdots K_{j_{n+1}}^\dagger}{\Pr(o_{j_1},\ldots,o_{j_{n+1}}|\rho)}$$

$$= K_{j_{n+1}} \rho_n K_{j_{n+1}}^\dagger \frac{\Pr(o_{j_1},\ldots,o_{j_n}|\rho)}{\Pr(o_{j_1},\ldots,o_{j_{n+1}}|\rho)}$$

$$= \frac{K_{j_{n+1}} \rho_n K_{j_{n+1}}^\dagger}{\Pr(o_{j_{n+1}}|o_{j_1},\ldots,o_{j_n},\rho)}; \tag{3.24}$$

the final denominator here is the conditional probability for the $(n + 1)$th outcome, given the previous outcomes, which can be written as

$$\Pr(o_{j_{n+1}}|o_{j_1},\ldots,o_{j_n},\rho) = \mathrm{Tr}[\rho_n E_{j_{n+1}}]. \tag{3.25}$$

Notice that for consistency, we should denote the initial state as $\rho = \rho_0$.

Quantum trajectories are usually formulated as difference equations,

$$\Delta\rho_{n|j} := \rho_{n+1|j} - \rho_n, \tag{3.26}$$

or, in the continuous-time limit, as the corresponding differential equation. Here we have explicitly denoted the $(n + 1)$th measurement outcome by j and left all prior measurement results implicit in the density operator ρ_n. The object of this paper is to derive equation (3.26) for different choices of the elements that go into the Kraus operator (3.15), i.e., the measurement outcomes $\langle o_j|$, the interaction unitary U, and the initial state $|\phi\rangle$.

A final point that we need later on is how to find the Kraus operators when the probes begin in a mixed state. For a mixed probe initial state,

$$\sigma = \sum_k \lambda_k |k\rangle\langle k|, \tag{3.27}$$

the unnormalized post-measurement system state (3.18) becomes

$$\tilde{\rho} = \langle o_j|U\rho \otimes \sigma U^\dagger|o_j\rangle$$

$$= \sum_k \sqrt{\lambda_k}\,\langle o_j|U|k\rangle\,\rho\,\langle k|U^\dagger|o_j\rangle\,\sqrt{\lambda_k}$$

$$= \sum_k K_{jk}\rho K_{jk}^\dagger, \tag{3.28}$$

where the Kraus operators, defined by

$$K_{jk} := \sqrt{\lambda_k}\,\langle o_j|U|k\rangle, \tag{3.29}$$

act together to make up a quantum operation.

Armed with this language of Kraus operators, we can put forward alternative descriptions of projective and weak measurements. A projective measurement is one whose Kraus operators are one-dimensional projectors, and weakness (or gentleness or fuzziness) is measured by the extent to which this is not the case, by having Kraus operators that are either sub-unity multiples of one-dimensional projectors or operators higher than rank one. Typically, what is meant by a weak measurement is a measurement whose Kraus operators are mostly 'close' to some multiple of the identity operator, corresponding to outcomes that do not disturb the system much, although there might also be some which are very 'small,' corresponding to outcomes that might significantly disturb the system, but that occur infrequently.

3.4. Open-system dynamics

We finally note that every conditional dynamics gives rise to an unconditional, open-system dynamics that corresponds to throwing away information about measurement outcomes. In the Markovian scenarios we are considering, throwing away the probe information at timestep $n + 1$ gives evolution described by a quantum operation $\mathcal{A}$:

$$\mathcal{A}[\rho] := \sum_j K_j \rho K_j^\dagger, \tag{3.30}$$

$$\rho_{n+1} = \mathcal{A}[\rho_n]. \tag{3.31}$$

Notice that for a mixed-state probe, the Kraus operators K_{jk} of equation (3.29) go together in equation (3.28) to make an outcome-dependent quantum operator $\mathcal{A}_j[\rho] := \sum_k K_{jk}\rho K_{jk}^\dagger$ that can be thought of as coming from throwing away the information about the probe's initial state.

The differential equation corresponding to the evolution (3.31) is known as the *master equation*. As is well known [71], the Kraus decomposition (3.30) for the quantum operation $\mathcal{A}$ is not unique. Different Kraus

decompositions correspond to performing different measurements on the probes and result in different system dynamics. In the trajectory literature, these alternative stochastic dynamics are known by Carmichael's terminology of *unravelings* [58]. The relationship of the master equation to equation (3.26) is

$$\Delta \rho_n := \sum_j \Pr(j|\rho_n) \rho_{n+1|j} - \rho_n = \mathbb{E}[\Delta \rho_{n+1|j}]. \tag{3.32}$$

4. Continuous measurements with probe fields

We have now presented circuit-model and algebraic representations of the conditional evolution of a quantum system subjected to a sequence of weak measurements. In this section we formally describe sequences of weak interactions between a system and a probe field and discuss how the approximations made in quantum input-output theory allow us to use the circuit of figure 4(c) to describe the quantum trajectories arising from continuous measurement of the probe field. The probe field—and the probe qubits we use *in lieu* of a field—are often referred to as a reservoir or a bath.

We begin by writing the combined Hamiltonian for the system coupled to the field as

$$H = H_{\text{sys}} + H_{\text{field}} + H_{\text{interaction}}. \tag{4.1}$$

For simplicity, we assume that the interaction Hamiltonian is linear in the one-dimensional probe field a,

$$H_{\text{interaction}} = i\sqrt{\gamma}(c \otimes a^\dagger - c^\dagger \otimes a), \tag{4.2}$$

where c is a system operator. Representative examples are coupling to the angular momentum of a collection of atoms yielding $c = J_-$, coupling to the position of an oscillator yielding $c = a$, and nonlinear coupling to an optomechanical oscillator yielding an effective $c = x$ after several approximations [72]. Writing the interaction Hamiltonian in this form uses the rotating-wave approximation (RWA) to keep only the energy-conserving terms in the interaction. Typical interaction terms involve the product of a Hermitian system operator and a Hermitian field operator. Writing these Hermitian operators as sums of positive- and negative-frequency parts leads to four terms in the interaction Hamiltonian, only two of which conserve energy when averaged over times much longer than the system's characteristic dynamical time. The RWA retains these two energy-conserving, co-rotating terms and discards the two counter-rotating terms, leaving the interaction Hamiltonian (4.2). Making the RWA requires averaging over times much longer than the system's dynamical time. We say more about the RWA below.

It is useful to work in the interaction picture, where the free time evolution of the system and field (generated by $H_0 := H_{\text{sys}} + H_{\text{field}}$) is transformed into the operators, leaving a time-dependent interaction Hamiltonian,

$$H_I(t) := e^{iH_0 t} H_{\text{interaction}} e^{-iH_0 t} = i\sqrt{\gamma}[c(t) \otimes a^\dagger(t) - c^\dagger(t) \otimes a(t)]. \tag{4.3}$$

In the interaction picture, the system operator c acquires a free time dependence; we assume now that the system has a single transition (characteristic) frequency Ω, so that $c(t) = c\, e^{-i\Omega t}$. The field operators also acquire a time dependence; each frequency mode of the field oscillates at its angular frequency ω, i.e., as $e^{-i\omega t}$. Indeed, the positive-frequency part of the field appearing in equations (4.2) and (4.3) is constructed from the frequency-mode annihilation operators $a(\omega)$ and is given by

$$a(t) = \int_0^\infty \frac{d\omega}{2\pi}\, a(\omega) e^{-i\omega t}. \tag{4.4}$$

The field in equation (4.4) is written in photon-number units, by which we mean it is the Fourier transform of the frequency-domain annihilation operators, which obey the canonical commutation relations

$$[a(\omega), a^\dagger(\omega')] = 2\pi\delta(\omega - \omega'). \tag{4.5}$$

Writing the field in these units omits frequency-dependent factors in the Fourier transform, and this omission is called the *quasimonochromatic approximation*, which assumes that the coupling of the field to the system is weak enough, i.e., $\gamma \ll \Omega$, that only field frequencies near the system transition frequency Ω, i.e., those within a few linewidths γ of Ω, are important. This allows us to choose the averaging time required by the RWA much longer than the system's characteristic time $1/\Omega$, but much shorter than the inverse linewidth $1/\gamma$; i.e., the averaging time is long enough to average away the counter-rotating, energy-nonconserving parts of the interaction Hamiltonian, but short enough that not much happens to the system during the averaging time.

It is convenient to introduce a new field operator,

$$b(t) = e^{i\Omega t} a(t) = \int_{-\Omega}^\infty \frac{d\epsilon}{2\pi}\, a(\Omega + \epsilon) e^{-i\epsilon t}, \tag{4.6}$$

which has its zero of frequencies shifted to the transition frequency Ω. Within the quasimonochromatic approximation, we can extend the integral over ϵ to $-\infty$; introducing phantom modes at negative $\omega = \Omega + \epsilon$

does not make any difference because they do not participate in the narrow-bandwidth coupling to the system. This gives us

$$b(t) = \int_{-\infty}^{\infty} \frac{d\epsilon}{2\pi} a(\Omega + \epsilon) e^{-i\epsilon t}. \tag{4.7}$$

The advantage of extending the integral to $-\infty$ is that the field operators $b(t)$ become instantaneous temporal annihilation operators, obeying the canonical commutation relations,

$$[b(t), b^{\dagger}(t')] = \delta(t - t'). \tag{4.8}$$

These operators are often called 'white-noise operators' because of their delta commutator, which permits them to be delta-correlated in time like classical white noise. The interaction Hamiltonian now assumes the following continuous-time form:

$$H_I(t) = i\sqrt{\gamma}\,[c \otimes b^{\dagger}(t) - c^{\dagger} \otimes b(t)]. \tag{4.9}$$

The essence of the quasimonochromatic approximation is the use of the photon-units field operator (4.7). The notion of creating instantaneous photons at the characteristic frequency Ω clearly requires a bit of cognitive dissonance: it is valid only if 'instantaneous' is understood to mean temporal windows that are broad compared to $1/\Omega$, corresponding to a narrow bandwidth of frequencies near Ω.

   The discrete interactions in figure 4 arise from the continuous-time interaction Hamiltonian (4.9) by dividing the field into probe segments, starting at times $t_n = n\Delta t$, $n = -\infty, \ldots, \infty$, all of duration $t_{n+1} - t_n \coloneqq \Delta t$. We assume, first, that $\Delta t \gg \Omega^{-1}$ so that within each segment Δt, the interaction with the probe field is averaged over many characteristic times of the system, as required by the RWA, and, second, that $\Delta t \ll \gamma^{-1}$ so that the probe/system interaction over the time Δt is weak. Instead of using the frequency modes $a(\Omega + \epsilon)$ or the instantaneous temporal modes $b(t)$, we now resolve the field into discrete temporal modes $b_{n,k}$ as

$$b(t) = \sum_{n=-\infty}^{\infty} \sum_{k=-\infty}^{\infty} \frac{1}{\sqrt{\Delta t}} b_{n,k} \Theta(t - t_n) e^{-i2\pi kt/\Delta t}, \tag{4.10}$$

where $\Theta(u)$ is the step function that is equal to 1 during the interval $0 < u < \Delta t$ and is 0 otherwise. The discrete temporal modes are given by

$$
\begin{aligned}
b_{n,k} &\coloneqq \frac{1}{\sqrt{\Delta t}} \int_{t_n}^{t_{n+1}} dt\, e^{i2\pi kt/\Delta t} b(t) \\
&= \sqrt{\Delta t} \int_{-\infty}^{\infty} \frac{d\epsilon}{2\pi} a(\Omega + \epsilon) \exp\left[-i\left(\epsilon - \frac{2\pi k}{\Delta t}\right)\left(\frac{t_n + t_{n-1}}{2}\right)\right] \frac{\sin(\epsilon\Delta t - 2\pi k)/2}{\epsilon\Delta t - 2\pi k}.
\end{aligned}
\tag{4.11}
$$

These modes obey discrete canonical commutation relations,

$$[b_{n,k}, b_{m,l}^{\dagger}] = \delta_{nm}\delta_{kl}; \tag{4.12}$$

this is the discrete-time analogue of continuous-time white noise of equation (4.8). We now recall that the interaction is weak enough, i.e., $\gamma \ll \Omega$, that only frequencies within a few γ of Ω need to be considered; given our assumption that $1/\Delta t \gg \gamma$, this allows us to neglect all the discrete temporal modes with $k \neq 0$, reducing the probe field to

$$b(t) = \sum_{n=-\infty}^{\infty} \frac{1}{\sqrt{\Delta t}} b_n \Theta(t - t_n), \tag{4.13}$$

where

$$b_n \coloneqq b_{n,0} = \frac{1}{\sqrt{\Delta t}} \int_{t_n}^{t_{n+1}} dt\, b(t). \tag{4.14}$$

The neglect of all the sideband modes is illustrated schematically in figure 6. Plugging this expression for the probe field into the equation (4.9) puts the interaction Hamiltonian in its final form,

$$H_I(t) = \sum_{n=-\infty}^{\infty} H_I^{(n)} \Theta(t - t_n), \tag{4.15}$$

where

$$H_I^{(n)} \coloneqq i\sqrt{\frac{\gamma}{\Delta t}} (c \otimes b_n^{\dagger} - c^{\dagger} \otimes b_n) = i\left(\sqrt{\gamma}\, c \otimes \frac{b_n^{\dagger}}{\sqrt{\Delta t}} - \sqrt{\gamma}\, c^{\dagger} \otimes \frac{b_n}{\sqrt{\Delta t}}\right) \tag{4.16}$$

is the interaction Hamiltonian during the nth probe segment. It is this Hamiltonian that is used to generate the discrete unitaries in figure 4.
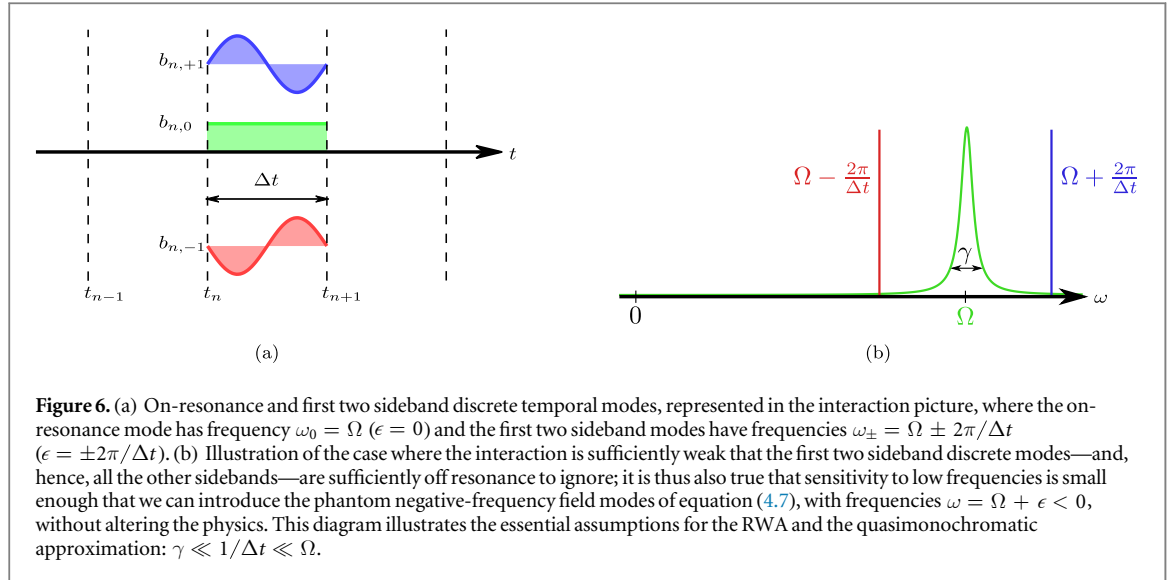
Figure 6. (a) On-resonance and first two sideband discrete temporal modes, represented in the interaction picture, where the on-resonance mode has frequency $\omega_0 = \Omega$ ($\epsilon = 0$) and the first two sideband modes have frequencies $\omega_\pm = \Omega \pm 2\pi/\Delta t$ ($\epsilon = \pm 2\pi/\Delta t$). (b) Illustration of the case where the interaction is sufficiently weak that the first two sideband discrete modes—and, hence, all the other sidebands—are sufficiently off resonance to ignore; it is thus also true that sensitivity to low frequencies is small enough that we can introduce the phantom negative-frequency field modes of equation (4.7), with frequencies $\omega = \Omega + \epsilon < 0$, without altering the physics. This diagram illustrates the essential assumptions for the RWA and the quasimonochromatic approximation: $\gamma \ll 1/\Delta t \ll \Omega$.

Before exploring the interaction unitary, however, it is good to pause to review, expand, and formalize the assumptions necessary to get to the discrete Hamiltonian (4.16) that applies to each time segment or, more generally, to get to the Markovian quantum circuit of figure 4. The restriction of the system-probe interaction to be a sequence of joint unitaries between the system and a single probe segment is often referred to as the *first Markov approximation*. This approximation is valid when the spatial extent Δx of the system is small with respect to the spatial extent $c\Delta t$ of the discretized probes. For many typical scenarios (e.g., atomic systems), the time interval Δt can be made quite small, often even smaller than the characteristic evolution time Ω^{-1}, before the spatial extent of the probes becomes comparable to the spatial extent of the system, which would force us to use a non-Markovian description like figure 5(b). The reason we did not encounter this assumption in the analysis above is that it is already incorporated in our starting point, the interaction Hamiltonian (4.2). A typical interaction Hamiltonian involves a spatial integral over the extent of the system. In writing the interaction Hamiltonian (4.2), we have already assumed that the system is small enough that the spatial integral can be replaced by a point interaction.

The initial product state of the probes is often referred to as the *second Markov approximation*. This approximation is valid when the correlation time τ_c in the bath is much shorter than the duration Δt of the discrete probe segments. This is often an excellent approximation, as baths with even very low temperatures have very small correlation times. For example, the thermal correlation time $\tau_c = \hbar/2\pi kT \simeq 10 \text{ ps} \cdot KT$ given by equation (3.3.20) in [73] is approximately 10 ns for a temperature of 1 mK. On the other hand, the vacuum correlation time $\tau_c \simeq 1/2\pi\Omega$ at the characteristic frequency means that if vacuum noise dominates, then the second Markov approximation requires that the probe segments be much longer than the system's dynamical time, i.e., $\Delta t \gg 1/\Omega$. For a treatment of the nonzero correlation time of the vacuum in an exactly solvable model, see [74].

The product measurements at the output of the circuit in figure 4(c) do not affect open-system dynamics, for which the bath is not monitored, but they do enter into a Markovian description of dynamics conditioned on measurement of the bath. The product measurements are a good approximation when the bandwidth of the detectors is sufficiently wide to give temporal resolution much finer than the duration of the probe segments we used to discretize the bath.

The remaining pair of closely related approximations, as we discussed previously, are the RWA, which has to do with simplifying the form of the interaction Hamiltonian, and the quasimonochromatic approximation, which has to do with simplifying the description of the field so that each Δt probe segment has only one relevant probe mode. The three important parameters in these two approximations are the characteristic system frequency Ω, the linewidth γ, and the duration of the time segments, Δt, and the approximations require that $\gamma \ll 1/\Delta t \ll \Omega$.

The approximations we make are summarized below:

$$\Delta x \ll c\Delta t \qquad\qquad \text{First Markov,} \qquad\qquad (4.17)$$

$$\tau_c \ll \Delta t \qquad\qquad \text{Second Markov,} \qquad\qquad (4.18)$$

$$\Omega^{-1} \ll \Delta t \ll \gamma^{-1} \qquad\qquad \text{RWA and quasimonochromatic.} \qquad\qquad (4.19)$$

We note that it is possible to model systems with several different, well-separated transition frequencies by introducing separate probe fields for each transition frequency, as long as it is possible to choose discrete probe

time segments in such a way that the above approximations are valid for all fields introduced. The several probe fields can actually be parts of a single probe field, with each part consisting of the probe frequencies that are close to resonance with a particular transition frequency.

The approximations now well in hand, we return to the Hamiltonian (4.16) for the nth probe segment. The associated interaction unitary between the system and the nth probe segment is given by

$$U_I^{(n)} = e^{-iH_I^{(n)}\Delta t} = \mathbf{1} \otimes \mathbf{1} + \sqrt{\Delta\tau}\,(c \otimes b_n^\dagger - c^\dagger \otimes b_n) + \frac{1}{2}\Delta\tau(c \otimes b_n^\dagger - c^\dagger \otimes b_n)^2 + \mathcal{O}(\Delta\tau^{3/2}), \quad (4.20)$$

where we define a dimensionless time interval,

$$\Delta\tau := \gamma\Delta t \ll 1, \tag{4.21}$$

suitable for series expansions. We only need to expand the unitary to second order because we are only interested in terms up to order $\Delta\tau$ for writing first-order differential equations. A comprehensive and related presentation of the issues discussed above can be found in the recent paper of Fischer *et al* [75].

Notice that we can account for an external Hamiltonian H_{ext} applied to the system, provided it changes slowly on the characteristic dynamical time scale $1/\Omega$ of the system and leads to slow evolution of the system on the characteristic time scale (if such a Hamiltonian is not slow, it should be included in the free system Hamiltonian H_{sys}). In the interaction picture, the external Hamiltonian acquires a time dependence and becomes part of the interaction Hamiltonian; since it is essentially constant in each time segment, its effect in each time segment can be captured by expanding its effect to linear order in Δt. It is easy to see that the interaction unitary (4.20) is then supplemented by an additional term $-i\Delta t\,H_{\text{ext}}$; when we convert to the final differential equation, this term introduces the standard commutator $-i\,dt\,[H_{\text{ext}}, \rho]$ for an external Hamiltonian.

5. Quantum trajectories for vacuum field and qubit probes

We are now prepared to discuss the quantum trajectories arising from the continuous measurement of a probe field coupled to a system as described in the previous section. In this context we often drop the explicit reference to which probe segment we are dealing with, since the Markovicity of figure 4(c) means we can consider each probe segment separately. Unconditional open-system evolution follows from averaging over the quantum trajectories or, equivalently, tracing out the probes.

Probe fields initially in the vacuum state are our concern in this section. Because the interaction between individual probes and the system is weak, the one-photon amplitude of the post-interaction probe segment is $\mathcal{O}(\sqrt{\Delta\tau})$, the two-photon amplitude is $\mathcal{O}(\Delta\tau)$, and so on. Since these amplitudes are squared in probability calculations, the probability of detecting a probe with more than one photon is $\mathcal{O}(\Delta\tau^2)$ and can be ignored. This suggests that it is sufficient to model the probe segments with qubits, with $|g\rangle$ corresponding to the vacuum state of the field and $|e\rangle$ corresponding to the single-photon state. We replace the discrete-field-mode annihilation operator b_n in equation (4.20) with the qubit lowering operator σ_- and $b_n^\dagger$ with σ_+:

$$U_I = \mathbf{1} \otimes \mathbf{1} + \sqrt{\Delta\tau}\,(c \otimes \sigma_+ - c^\dagger \otimes \sigma_-) + \frac{1}{2}\Delta\tau(c \otimes \sigma_+ - c^\dagger \otimes \sigma_-)^2 \tag{5.1a}$$

$$= \mathbf{1} \otimes \mathbf{1} + \sqrt{\Delta\tau}\,(c \otimes \sigma_+ - c^\dagger \otimes \sigma_-) - \frac{1}{2}\Delta\tau(c\,c^\dagger \otimes |e\rangle\langle e| + c^\dagger c \otimes |g\rangle\langle g|). \tag{5.1b}$$

With this replacement, the neglect of two-photon transitions in the probe-field segments is made exact by the fact that $\sigma_+^2 = \sigma_-^2 = 0$; these squared terms thus do not appear in equation (5.1b).

In sections 5.1–5.4 we establish the correspondence between this qubit model and *vacuum SMEs*, where vacuum refers to the state of the probe field. In particular, we present qubit analogues of three typical measurements performed on probe fields: photon counting, homodyne measurement, and heterodyne measurement.

We transcend the vacuum probe fields in section 6 to Gaussian probe fields and find that formulating a qubit model requires additional tricks beyond just noting that weak interactions with the probe do not lead to significant two-photon transitions. Nevertheless, we are able to find qubit models that yield all the essential features of these Gaussian stochastic evolutions.

While the qubit model we develop is meant to capture the behavior of a 'true' field-theoretic model, it is important to note that there are scenarios where qubits are the natural description. For example, in Haroche-style experiments [76] a cavity interacts with a beam of atoms, accurately described as a sequence of finite-dimensional quantum probes. Such scenarios have been analyzed for their non-Markovian behavior [77], section 9.2, and similar models are increasingly studied in the literatures of thermodynamics [78, 79] and collisional models [80–82].
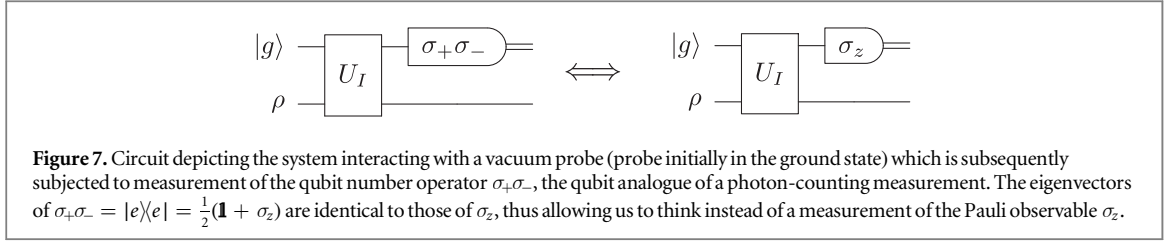
Figure 7. Circuit depicting the system interacting with a vacuum probe (probe initially in the ground state) which is subsequently subjected to measurement of the qubit number operator $\sigma_+\sigma_-$, the qubit analogue of a photon-counting measurement. The eigenvectors of $\sigma_+\sigma_- = |e\rangle\langle e| = \frac{1}{2}(\mathbf{1} + \sigma_z)$ are identical to those of σ_z, thus allowing us to think instead of a measurement of the Pauli observable σ_z.

5.1. Z basis measurement: Photon counting or direct detection

As a first example, we consider performing photon-counting measurements on the probe field after its interaction with the system. We calculate the quantum trajectory by first constructing the Kraus operators given by equation (3.15). For probes initially in the vacuum state we have $|\phi\rangle = |g\rangle$, and our interaction unitary is given by equations (5.1). What remains is to identify the measurement outcomes $\langle o_j|$. The qubit version of the number operator $b^\dagger b$ is $\sigma_+\sigma_- = |e\rangle\langle e| = \frac{1}{2}(\mathbf{1} + \sigma_z)$. Measuring this observable, as depicted in figure 7, is equivalent to measuring σ_z. The measurement outcomes are then $\langle g|$ and $\langle e|$ and give the Kraus operators

$$K_g = \langle g|U_I|g\rangle = \mathbf{1} - \tfrac{1}{2}\Delta\tau\; c^\dagger c, \tag{5.2a}$$

$$K_e = \langle e|U_I|g\rangle = \sqrt{\Delta\tau}\; c. \tag{5.2b}$$

The corresponding POVM elements (to linear order in $\Delta\tau$) are

$$E_g = K_g^\dagger K_g = \mathbf{1} - \Delta\tau\; c^\dagger c, \tag{5.3a}$$

$$E_e = K_e^\dagger K_e = \Delta\tau\; c^\dagger c, \tag{5.3b}$$

which trivially satisfy $E_g + E_e = \mathbf{1}$. We call the Kraus operators (5.2) the *photon-counting Kraus operators*. These operators are identical to those derived for photon counting with continuous field modes [66, equations (4.5) and (4.7)], as we expected from the vanishing multi-photon probability discussed earlier.

To calculate a quantum trajectory we need to describe the evolution of the system conditioned on the outcomes of repeated measurements of this kind. The state of the system after making a measurement and getting the result g during the $(n + 1)$th time interval, i.e., between t_n and t_{n+1}, is

$$\rho_{n+1|g} := \frac{K_g\rho_n K_g^\dagger}{\mathrm{Tr}\,[\rho_n E_g]} = \frac{\rho_n - \tfrac{1}{2}\Delta\tau(c^\dagger c\rho_n + \rho_n c^\dagger c)}{1 - \Delta\tau\;\mathrm{Tr}\,[\rho_n c^\dagger c]}. \tag{5.4}$$

The subscript $n + 1$ on $\rho_{n+1|g}$ indicates, as in equation (3.24), that this is the state at the end of this probe segment, after the measurement; the subscript g indicates that this is the state conditioned on the measurement outcome g. The state ρ_{n+1} is conditioned on all previous measurement outcomes as well, but we omit all of that conditioning, letting it be implicit in ρ_n. Expanding the denominator to first order in $\Delta\tau$ using the standard expansion $(1 + x\Delta\tau)^{-1} = 1 - x\Delta\tau + \mathcal{O}(\Delta\tau^2)$ allows us to calculate the difference equation (3.26) when the measurement result is g:

$$\Delta\rho_{n|g} := \rho_{n+1|g} - \rho_n = -\tfrac{1}{2}\Delta\tau(c^\dagger c\rho_n + \rho_n c^\dagger c - 2\rho_n\,\mathrm{Tr}\,[\rho_n c^\dagger c]) + \mathcal{O}(\Delta\tau^2) = -\tfrac{1}{2}\Delta\tau\,\mathcal{H}[c^\dagger c]\rho_n, \tag{5.5}$$

where we employ the shorthand

$$\mathcal{H}[X]\rho := X\rho + \rho X^\dagger - \rho\,\mathrm{Tr}\,[\rho(X + X^\dagger)]. \tag{5.6}$$

Repeating the analysis for the case when the measurement result is e gives

$$\rho_{n+1|e} := \frac{K_e\rho_n K_e^\dagger}{\mathrm{Tr}\,[\rho_n E_e]} = \frac{c\rho_n c^\dagger}{\mathrm{Tr}\,[\rho_n c^\dagger c]}. \tag{5.7}$$

The difference between the pre- and post-measurement system states when the measurement result is e is thus

$$\Delta\rho_{n|e} := \rho_{n+1|e} - \rho_n = \frac{c\rho_n c^\dagger}{\mathrm{Tr}\,[\rho_n c^\dagger c]} - \rho_n = \mathcal{G}[c]\rho_n, \tag{5.8}$$

where we define

$$\mathcal{G}[X]\rho := \frac{X\rho X^\dagger}{\mathrm{Tr}\,[\rho X^\dagger X]} - \rho. \tag{5.9}$$

Having separate equations for the two measurement outcomes is not at all convenient. Fortunately, we can combine the equations by introducing a random variable ΔN that represents the outcome of the measurement:

$$\Delta N : g \mapsto 0,\ e \mapsto 1. \tag{5.10}$$

Since this random variable is a bit (i.e., a Bernoulli random variable) its statistics are completely specified by its mean:

$$\mathbb{E}[\Delta N] = 0 \cdot \mathrm{Tr}[\rho E_g] + 1 \cdot \mathrm{Tr}[\rho E_e] = \Delta \tau\, \mathrm{Tr}[\rho c^\dagger c]. \tag{5.11}$$

We now combine the difference equations into a single stochastic equation using the random variable ΔN:

$$
\begin{aligned}
\Delta \rho_{n|\Delta N} &:= \rho_{n+1|\Delta N} - \rho_n \\
&= \Delta N \left(\frac{c \rho_n c^\dagger}{\mathrm{Tr}[\rho_n c^\dagger c]} - \rho_n \right) - (1 - \Delta N) \tfrac{1}{2} \Delta \tau (c^\dagger c \rho_n + \rho_n c^\dagger c - 2 \rho_n \mathrm{Tr}[\rho_n c^\dagger c]) \\
&= \Delta N \mathcal{G}[c] \rho_n - (1 - \Delta N) \tfrac{1}{2} \Delta \tau\, \mathcal{H}[c^\dagger c] \rho_n.
\end{aligned}
\tag{5.12}
$$

It quickly becomes unnecessarily tedious to keep timestep indices around explicitly, since everything in our equations now refers to the same timestep, so we drop those indices now. Discarding $\Delta N \Delta \tau$, since it is second order in $\Delta \tau$ (see equation (5.11) and [66, Chap. 4]), we simplify equation (5.12) to

$$
\begin{aligned}
\Delta \rho_{\Delta N} &= \Delta N \left(\frac{c \rho c^\dagger}{\mathrm{Tr}[\rho c^\dagger c]} - \rho \right) - \tfrac{1}{2} \Delta \tau (c^\dagger c \rho + \rho c^\dagger c - 2 \rho\, \mathrm{Tr}[\rho c^\dagger c]) \\
&= \Delta \tau\, \mathcal{D}[c] \rho + \Delta \mathcal{I}_D \mathcal{G}[c] \rho,
\end{aligned}
\tag{5.13}
$$

where we introduce the standard diffusion superoperator,

$$\mathcal{D}[X]\rho := X \rho X^\dagger - \tfrac{1}{2}(X^\dagger X \rho + \rho X^\dagger X), \tag{5.14}$$

and the *photon-counting innovation*,

$$\Delta \mathcal{I}_D := \Delta N - \mathbb{E}[\Delta N], \tag{5.15}$$

which is the difference between the measurement result and the mean result (i.e., it can be thought of as what is learned from the measurement). The subscript D here plays off the fact that photon counting is often called *direct detection* and is used in place of N because N has too many other uses in this paper.

By taking the limit $\Delta \tau \to \gamma dt$ we obtain a stochastic differential equation,

$$
\begin{aligned}
d\rho_D &= dN \left(\frac{c \rho c^\dagger}{\mathrm{Tr}[\rho c^\dagger c]} - \rho \right) - \tfrac{1}{2} \gamma dt (c^\dagger c \rho + \rho c^\dagger c - 2 \rho\, \mathrm{Tr}[\rho c^\dagger c]) \\
&= dt\, \mathcal{D}[\sqrt{\gamma}\, c] \rho + d\mathcal{I}_D \mathcal{G}[c] \rho,
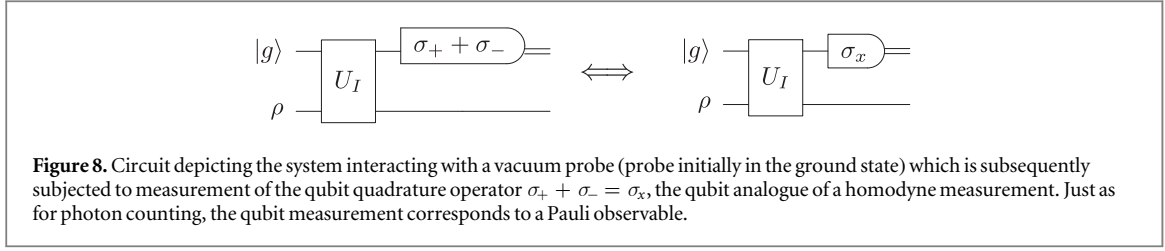\end{aligned}
\tag{5.16}
$$

where dN is a bit-valued random process, termed a point process, with mean $\mathbb{E}[dN] = \gamma dt\, \mathrm{Tr}[\rho c^\dagger c]$ and the innovation is given by $d\mathcal{I}_D = dN - \mathbb{E}[dN]$. This equation is called the *vacuum stochastic master equation (SME) for photon counting*; i.e., it is the stochastic differential equation that describes the conditional evolution of a system that interacts with vacuum probes that are subjected to photon-counting measurements.

Equation (5.16) has no explicit system-Hamiltonian term. Although this differs from other presentations our readers might be familiar with, it is merely an aesthetic distinction. Recall from the discussion at the end of section 4 that well-behaved system Hamiltonians can be introduced by including an additional commutator term in our differential equations. In this case, the modification yields

$$d\rho_D = -i\, dt\, [H_{\mathrm{ext}}, \rho] + dt\, \mathcal{D}[\sqrt{\gamma}\, c] \rho + d\mathcal{I}_D \mathcal{G}[c] \rho. \tag{5.17}$$

It is important to stress that in practice, for numerical integration of these equations, one uses the difference equation (5.13), not the differential equation (5.16); i.e., what one uses in practice is the difference equation that corresponds to the discrete-time quantum circuit in figure 4(c). One assigns to the system a prior state ρ_0 that combines with the initial probe states to make an initial product state on the full system/probe arrangement. This prior state describes the system at the moment coupling to the probes is turned on and measurements begin. Each time a new measurement result is sampled, equation (5.13) is used to update the description of the system. If we describe our system by ρ_n after collecting n samples from our measurement device, observing ΔN for sample $n + 1$ leads to the updated state $\rho_{n+1} = \rho_n + \Delta \rho_{\Delta N}$.

Another application of the difference equation is state/parameter inference. In the case of state inference, one has uncertainty regarding what initial state ρ_0 to assign to the system. General choices for ρ_0 will be incorrect, invalidating some of the properties described above. In particular, the innovation will deviate from a zero-mean random variable, and these deviations observed for a variety of guesses for ρ_0 will yield likelihood ratios that can be used to estimate the state, as was done in [33]. One can also keep track of the trace of the unnormalized state (3.19), which encodes the relative likelihood of the trajectory given the evolution parameters, allowing one to judge different parameter values against one another, as was implemented in [28].

Figure 8. Circuit depicting the system interacting with a vacuum probe (probe initially in the ground state) which is subsequently subjected to measurement of the qubit quadrature operator $\sigma_+ + \sigma_- = \sigma_x$, the qubit analogue of a homodyne measurement. Just as for photon counting, the qubit measurement corresponds to a Pauli observable.

The differential equation that describes the unconditional evolution corresponding to equation (5.16) is called the master equation. To obtain the master equation, we simply average over measurement results in equation (5.16). The only term that depends on the results is $d\mathcal{I}_D$, and its mean is zero, so the master equation is

$$d\rho = \mathbb{E}[d\rho_D] = dt \,\mathcal{D}[\sqrt{\gamma}\,c]\rho. \tag{5.18}$$

Just as was the case for the SME (5.16), equation (5.18) has no explicit system-Hamiltonian term. The same reasoning that allowed us to add such a term and arrive at equation (5.17) allows us to add the same term to equation (5.18):

$$d\rho = \mathbb{E}[d\rho_D] = -i \,dt \,[H_{\text{ext}}, \rho] + dt \,\mathcal{D}[\sqrt{\gamma}\,c]\rho. \tag{5.19}$$

For the remainder of our presentation, such system-Hamiltonian terms are generally left implicit.

5.2. X basis measurement: Homodyne detection

We can produce, as in Brun's model [34], a different system evolution simply by measuring the probes in a different basis. To be concrete, let us consider measuring the x-quadrature of the field, $b^\dagger + b$. In the qubit-probe approach, this means measuring $\sigma_+ + \sigma_- = \sigma_x$ as shown in figure 8.

This measurement projects onto the eigenstates

$$|\phi_\pm\rangle := (|g\rangle \pm |e\rangle)/\sqrt{2} \tag{5.20}$$

of σ_x. The Kraus operators are linear combinations of the photon-counting Kraus operators,

$$K_\pm = \langle\phi_\pm|U_I|g\rangle = \frac{1}{\sqrt{2}}(K_g \pm K_e) = \frac{1}{\sqrt{2}}\Big(\mathbf{1} \pm \sqrt{\Delta\tau}\,c - \tfrac{1}{2}\Delta\tau\,c^\dagger c\Big), \tag{5.21}$$

and the corresponding POVM elements (to linear order in $\Delta\tau$) are

$$E_\pm = K_\pm^\dagger K_\pm = \frac{1}{2}(\mathbf{1} \pm \sqrt{\Delta\tau}\,(c + c^\dagger)), \tag{5.22}$$

which clearly satisfy $E_+ + E_- = \mathbf{1}$. We write the difference equation as before, keeping terms up to order $\Delta\tau$,

$$\begin{aligned}\Delta\rho_\pm &:= \frac{K_\pm\rho K_\pm^\dagger}{\text{Tr}\,[\rho E_\pm]} - \rho = \frac{\rho \pm \sqrt{\Delta\tau}\,(c\rho + \rho c^\dagger) + \Delta\tau\,\mathcal{D}[c]\rho}{1 \pm \sqrt{\Delta\tau}\,\text{Tr}\,[\rho(c + c^\dagger)])} - \rho \\ &= \Big(\pm\sqrt{\Delta\tau}\, - \Delta\tau\,\text{Tr}[(c + c^\dagger)\rho]\Big)\mathcal{H}[c]\rho + \Delta\tau\,\mathcal{D}[c]\rho,\end{aligned} \tag{5.23}$$

where we have again expanded the denominator using a standard series,

$$\frac{1}{1 + x\sqrt{\Delta\tau}} = 1 - x\sqrt{\Delta\tau}\, + x^2\Delta\tau + \mathcal{O}(\Delta\tau^{3/2}). \tag{5.24}$$

The dependence on the measurement result $\pm$ is reduced now to the coefficient $\pm\sqrt{\Delta\tau}\,$ in equation (5.23). We rewrite this stochastic coefficient as a random variable, ΔR, again dependent on the measurement outcome such that $\Delta R : \pm \mapsto \pm\sqrt{\Delta\tau}\,$. The average of this random variable to order $\Delta\tau$ is

$$\mathbb{E}[\Delta R] = \sqrt{\Delta\tau}\,\text{Tr}\,[\rho E_+] - \sqrt{\Delta\tau}\,\text{Tr}\,[\rho E_-] = \Delta\tau\,\text{Tr}[(c + c^\dagger)\rho]. \tag{5.25}$$

This is exactly the term subtracted from ΔR in the coefficient of $\mathcal{H}[c]\rho$ in equation (5.23); thus, defining the homodyne version of the innovation as

$$\Delta\mathcal{I}_H := \Delta R - \mathbb{E}[\Delta R], \tag{5.26}$$

we bring the homodyne difference equation into the form,

$$\Delta\rho_\pm = \Delta\tau\,\mathcal{D}[c]\rho + \Delta\mathcal{I}_H\mathcal{H}[c]\rho, \tag{5.27}$$

which is the difference equation one uses for numerical integration in the presence of homodyne measurements.

Another simple calculation shows the second moment of ΔR to be

$$\mathbb{E}[(\Delta R)^2] = \Delta\tau \, \mathrm{Tr}[E_+ \rho] + \Delta\tau \, \mathrm{Tr}[E_- \rho] = \Delta\tau. \tag{5.28}$$

By definition the innovation has zero mean, and its second moment is the variance of ΔR,

$$\mathbb{E}[(\Delta\mathcal{I}_H)^2] = \mathbb{E}[(\Delta R)^2] - (\mathbb{E}[\Delta R])^2 = \Delta\tau, \tag{5.29}$$

where again we work to linear order in $\Delta\tau$. It is now trivial to write the continuous-time stochastic differential equation that goes with the difference equation (5.27):

$$d\rho_H = dt \, \mathcal{D}[\sqrt{\gamma} \, c]\rho + dW \, \mathcal{H}[\sqrt{\gamma} \, c]\rho. \tag{5.30}$$

In the continuous limit, the innovation $\Delta\mathcal{I}_H$ becomes $\sqrt{\gamma} \, dW$, where dW is the Weiner process, satisfying $\mathbb{E}[dW] = 0$ and $\mathbb{E}[dW^2] = dt$.

Changing the measurement performed on the probes does not alter the unconditional evolution of the system, so averaging over the homodyne measurement results gives again the master equation (5.18):

$$d\rho = \mathbb{E}[d\rho_H] = dt \, \mathcal{D}[\sqrt{\gamma} \, c]\rho = \mathbb{E}[d\rho_D]. \tag{5.31}$$

The results so far in this subsection are for homodyne detection of the probe quadrature component $X = \sigma_+ + \sigma_- = \sigma_x$, i.e., measurement in the basis (5.20). It is easy to generalize to measurement of an arbitrary field quadrature $e^{i\varphi}b + e^{-i\varphi}b^\dagger$, which for a qubit probe becomes a measurement of the spin component

$$X(\varphi) := e^{i\varphi}\sigma_- + e^{-i\varphi}\sigma_+ = \sigma_x \cos\varphi + \sigma_y \sin\varphi. \tag{5.32}$$

This means measurement in the probe basis [eigenstates of $X(\varphi)$],

$$|\phi_\pm(\varphi)\rangle := \frac{1}{\sqrt{2}}\big(|g\rangle \pm e^{-i\varphi}|e\rangle\big), \tag{5.33}$$

where we can also write

$$\begin{aligned}
|\phi_+(\varphi)\rangle &= e^{-i\varphi/2}\big[\cos(\varphi/2)|\phi_+\rangle + i\sin(\varphi/2)|\phi_-\rangle\big], \\
|\phi_-(\varphi)\rangle &= e^{-i\varphi/2}\big[i\sin(\varphi/2)|\phi_+\rangle + \cos(\varphi/2)|\phi_-\rangle\big].
\end{aligned} \tag{5.34}$$

The resulting Kraus operators are

$$\begin{aligned}
K_\pm(\varphi) &= \langle\phi_\pm(\varphi)|U_I|g\rangle \\
&= \frac{1}{\sqrt{2}}(K_g \pm e^{i\varphi}K_e) \\
&= \frac{1}{\sqrt{2}}\Big(\mathbf{1} \pm \sqrt{\Delta\tau} \, e^{i\varphi}c - \tfrac{1}{2}\Delta\tau \, c^\dagger c\Big),
\end{aligned} \tag{5.35}$$

with corresponding POVM elements

$$E_\pm(\varphi) = K_\pm^\dagger(\varphi)K_\pm(\varphi) = \frac{1}{2}\Big(\mathbf{1} \pm \sqrt{\Delta\tau} \, (e^{i\varphi}c + e^{-i\varphi}c^\dagger)\Big). \tag{5.36}$$

We see that the results for measuring X can be converted to those for measuring $X(\varphi)$ by replacing c with $c \, e^{i\varphi}$. Thus the conditional difference equation is

$$\Delta\rho_\pm = \Delta\tau \, \mathcal{D}[c]\rho + \Delta\mathcal{I}_H \mathcal{H}[c \, e^{i\varphi}]\rho, \tag{5.37}$$

and the vacuum SME becomes

$$d\rho_H = dt \, \mathcal{D}[\sqrt{\gamma} \, c]\rho + dW \, \mathcal{H}[\sqrt{\gamma} \, c \, e^{i\varphi}]\rho. \tag{5.38}$$

5.3. Generalized measurement of X and Y: Heterodyne detection

Heterodyne measurement can be thought of as simultaneous measurement of two orthogonal field quadrature components, e.g., $b + b^\dagger$ and $-i(b - b^\dagger)$. In our qubit model, this corresponds to simultaneously measuring along two orthogonal axes in the x-y plane of the Bloch sphere, e.g., $\sigma_- + \sigma_+ = \sigma_x = X$ and $i(\sigma_- - \sigma_+) = \sigma_y = Y = X(\pi/2)$. Obviously, it is not possible to measure these two-qubit observables simultaneously and perfectly, since they do not commute, but we can borrow a strategy employed in optical experiments to measure two quadrature components simultaneously. The optical strategy makes two 'copies' of the field mode to be measured, by combining the field mode with vacuum at a 50-50 beamsplitter; this is followed by orthogonal homodyne measurements on the two copies. This strategy works equally well for our qubit probes, once we define an appropriate beamsplitter unitary for two qubits,
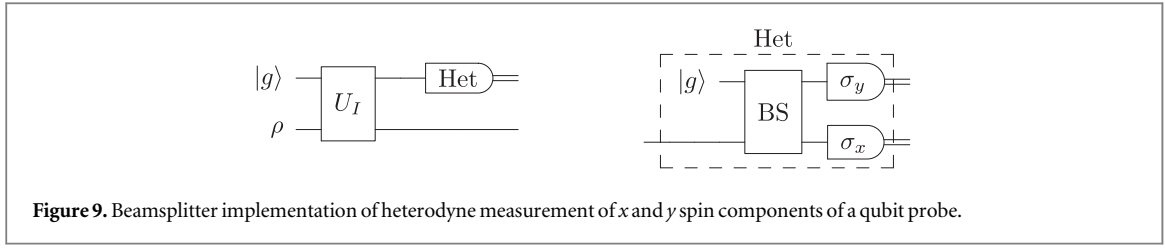
Figure 9. Beamsplitter implementation of heterodyne measurement of x and y spin components of a qubit probe.

$$BS(\eta) := \exp\left[i(\eta\sigma_- \otimes \sigma_+ + \eta^*\sigma_+ \otimes \sigma_-)\right]$$

$$= |gg\rangle\langle gg| + |ee\rangle\langle ee| + \cos|\eta|(|ge\rangle\langle ge| + |eg\rangle\langle eg|) + i\sin|\eta|(e^{i\delta}|ge\rangle\langle eg| + e^{-i\delta}|eg\rangle\langle ge|), \quad (5.39)$$

where $\eta = |\eta|e^{i\delta}$. Specializing to $\eta = -i\pi/4$ yields

$$BS := BS(-i\pi/4) = |gg\rangle\langle gg| + |ee\rangle\langle ee| + \frac{1}{\sqrt{2}}(|ge\rangle\langle ge| + |eg\rangle\langle eg| + |ge\rangle\langle eg| - |eg\rangle\langle ge|). \quad (5.40)$$

This 'beamsplitter' behaves rather strangely when excitations are fed to both input ports, but this is not an issue since the second (top) port of the beamsplitter is fed the ground state, as illustrated in figure 9.

It is useful to note here, for use a bit further on, that the beamsplitter unitary, when written in terms of Pauli operators, factors into two commuting unitaries,

$$BS = \exp\left(i\frac{\pi}{8}\sigma_x \otimes \sigma_y\right)\exp\left(-i\frac{\pi}{8}\sigma_y \otimes \sigma_x\right). \quad (5.41)$$

This factored form is easy to work with and leads to

$$BS = [\mathbf{1} \otimes \mathbf{1}\cos(\pi/8) + i\sigma_x \otimes \sigma_y \sin(\pi/8)][\mathbf{1} \otimes \mathbf{1}\cos(\pi/8) - i\sigma_y \otimes \sigma_x \sin(\pi/8)]$$

$$= \frac{1}{2}(\mathbf{1} \otimes \mathbf{1} + \sigma_z \otimes \sigma_z) + \frac{1}{2\sqrt{2}}(\mathbf{1} \otimes \mathbf{1} - \sigma_z \otimes \sigma_z + i\sigma_x \otimes \sigma_y - i\sigma_y \otimes \sigma_x), \quad (5.42)$$

which immediately confirms equation (5.40).

To calculate the Kraus operators for heterodyne measurement, we project the first probe qubit onto the eigenstates of the spin component $X = \sigma_x$ and second probe qubit onto the eigenstates of the spin component $Y = \sigma_y$. Before proceeding to that, we deal with a notational point for the eigenstates of $\sigma_y = Y = X(\pi/2)$, analogous to the notational convention for σ_x that is summarized in figure 1. The conventional quantum-information notation for the ± 1 eigenstates of σ_y is $|\pm i\rangle = (|0\rangle \pm i|1\rangle)/\sqrt{2}$, whereas as we introduced in equation (5.33), we are using eigenstates that differ by a phase factor of $\mp i$:

$$|\phi_{\pm i}\rangle := |\phi_\pm(\pi/2)\rangle = \frac{1}{\sqrt{2}}(|g\rangle \mp i|e\rangle) = \mp i\frac{1}{\sqrt{2}}(|0\rangle \pm i|1\rangle) = \mp i|\pm i\rangle. \quad (5.43)$$

When all this is accounted for, the Kraus operators come out to be

$$K_{\pm,\widetilde{\pm}} = (\langle\phi_\pm|\otimes\langle\phi_{\widetilde{\mp}i}|)(\mathbf{1} \otimes BS)(U_I \otimes \mathbf{1})|gg\rangle = \frac{1}{\sqrt{2}}\langle\phi_\pm\left(\pm\widetilde{\mp}\pi/4\right)|U_I|g\rangle$$

$$= \frac{1}{2}(K_g \pm e^{\pm\widetilde{\mp}i\pi/4}K_e) = \frac{1}{2}\left(\mathbf{1} \pm e^{\pm\widetilde{\mp}i\pi/4}\sqrt{\Delta\tau}c - \frac{1}{2}\Delta\tau\, c^\dagger c\right), \quad (5.44)$$

where we have introduced two binary variables, $\pm$ and $\widetilde{\pm}$, to account for the four measurement outcomes. The juxtaposition of these two variables, $\pm\widetilde{\pm}$, denotes their product, i.e., the parity of the two bits. We see this notation at work in
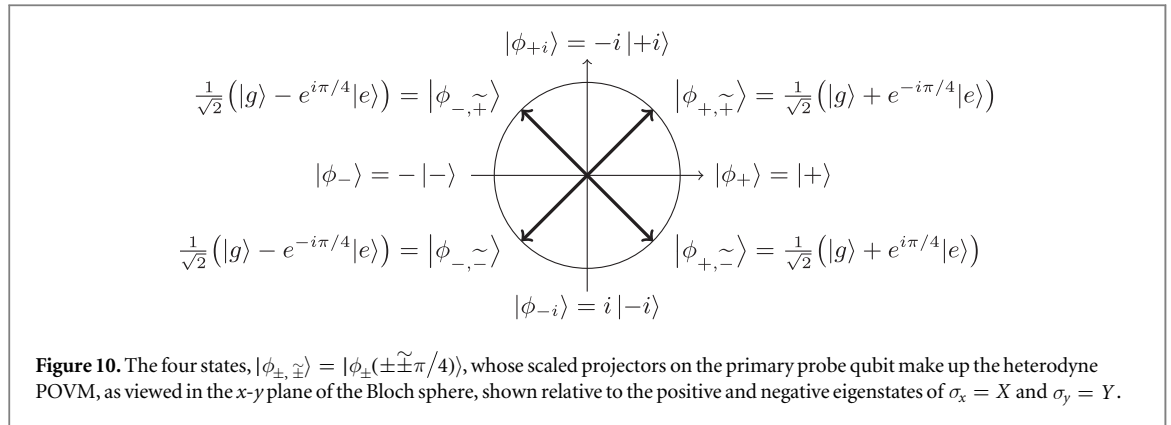
$$\pm e^{\pm\widetilde{\pm}i\pi/4} = \pm\frac{1}{\sqrt{2}}(1 \pm\widetilde{\pm} i) = \frac{1}{\sqrt{2}}(\pm 1 \widetilde{\mp} i). \quad (5.45)$$

The POVM elements that correspond to the Kraus operators (5.44) are

$$E_{\pm,\widetilde{\pm}} = \frac{1}{4}\left(\mathbf{1} \pm \sqrt{\Delta\tau}\left(e^{\mp\widetilde{\pm}i\pi/4}c^\dagger + e^{\pm\widetilde{\pm}i\pi/4}c\right)\right) \quad (5.46)$$

$$= \frac{1}{4}\left[\mathbf{1} + \sqrt{\Delta\tau}\left(\pm\frac{c + c^\dagger}{\sqrt{2}} \widetilde{\pm} \frac{i(c - c^\dagger)}{\sqrt{2}}\right)\right]. \quad (5.47)$$

The second form of the Kraus operators in equation (5.44) is equivalent to finding the Kraus operators of the primary probe qubit for the heterodyne measurement model on the left side of figure 9. One sees from this second form that the σ_x and σ_y measurements on the two probe qubits are equivalent to projecting the primary probe qubit onto one of the following four states:

Figure 10. The four states, $|\phi_{\pm,\stackrel{\sim}{\mp}}\rangle = |\phi_\pm(\pm\stackrel{\sim}{\mp}\pi/4)\rangle$, whose scaled projectors on the primary probe qubit make up the heterodyne POVM, as viewed in the x-y plane of the Bloch sphere, shown relative to the positive and negative eigenstates of $\sigma_x = X$ and $\sigma_y = Y$.

$$|\phi_{\pm,\stackrel{\sim}{\mp}}\rangle := |\phi_\pm(\pm\stackrel{\sim}{\mp}\pi/4)\rangle = \frac{1}{\sqrt{2}}(|g\rangle \pm e^{\mp\stackrel{\sim}{\mp}i\pi/4}|e\rangle) = \frac{1}{\sqrt{2}}\left(|g\rangle + \frac{1}{\sqrt{2}}(\pm 1 \stackrel{\sim}{\mp} i)|e\rangle\right). \tag{5.48}$$

These four states are depicted in figure 10; they carry two bits of information, which are the results of the σ_x and σ_y measurements in the beamsplitter measurement model. The four states not being orthogonal, they must be subnormalized by the factor of $\sqrt{2}$ that appears in equation (5.44) to obtain legitimate Kraus operators.

We conclude that as far as the primary probe qubit is concerned, the heterodyne measurement can be regarded as flipping a fair coin to determine whether one measures $X(\pi/4) = (\sigma_x + \sigma_y)/\sqrt{2}$ or $X(-\pi/4) = (\sigma_x - \sigma_y)/\sqrt{2}$. The ± 1 eigenstates of $X(\pi/4)$ are $|\phi_\pm(\pi/4)\rangle$; $|\phi_+(\pi/4)\rangle = |\phi_{+\stackrel{\sim}{+}}\rangle$ has eigenvalue $+1$, and $|\phi_-(\pi/4)\rangle = |\phi_{-\simeq}\rangle$ has eigenvalue -1. The ± 1 eigenstates of $X(-\pi/4)$ are $|\phi_\pm(-\pi/4)\rangle$; $|\phi_+(-\pi/4)\rangle = |\phi_{+\simeq}\rangle$ has eigenvalue $+1$, and $|\phi_-(-\pi/4)\rangle = |\phi_{-\stackrel{\sim}{+}}\rangle$ has eigenvalue -1. Notice that the fair coin that decides between these two measurements is the parity of the measurements of σ_x and σ_y in the heterodyne circuit of figure 9. Figure 11 goes through the circuit identities that convert the heterodyne circuit involving measurements on two probe qubits to one that is a coin flip that chooses between the two measurement bases on the primary probe qubit.

We now turn to deriving the explicit form of the conditional heterodyne difference equation,

$$\Delta\rho_{\pm,\stackrel{\sim}{\mp}} := \frac{K_{\pm,\stackrel{\sim}{\mp}} \rho \, K^\dagger_{\pm,\stackrel{\sim}{\mp}}}{\mathrm{Tr}[\rho E_{\pm,\stackrel{\sim}{\mp}}]} - \rho. \tag{5.49}$$

This time we need two binary random variables to account for the dependence on measurement outcome:

$$\Delta R_x : (\pm, \stackrel{\sim}{\mp}) \mapsto \pm\sqrt{\Delta\tau}, \tag{5.50}$$

$$\Delta R_y : (\pm, \stackrel{\sim}{\mp}) \mapsto \stackrel{\sim}{\mp}\sqrt{\Delta\tau}. \tag{5.51}$$

We want to write the equation in terms of innovations again, so we need the probability distribution of measurement outcomes in order to calculate $\mathbb{E}[\Delta R_x]$ and $\mathbb{E}[\Delta R_y]$:

$$\mathrm{Pr}(\pm,\stackrel{\sim}{\mp}) = \mathrm{Tr}[\rho E_{\pm,\stackrel{\sim}{\mp}}] = \frac{1}{4}\left(1 \pm \sqrt{\Delta\tau}\,\mathrm{Tr}\left[\rho\frac{c+c^\dagger}{\sqrt{2}}\right] \stackrel{\sim}{\mp} \sqrt{\Delta\tau}\,\mathrm{Tr}\left[\rho\frac{ic+(ic)^\dagger}{\sqrt{2}}\right]\right). \tag{5.52}$$

The marginal probabilities, given by

$$\mathrm{Pr}(\pm) = \sum_{\stackrel{\sim}{\mp}} \mathrm{Pr}(\pm,\stackrel{\sim}{\mp}) = \frac{1}{2}\left(1 \pm \sqrt{\Delta\tau}\,\mathrm{Tr}\left[\rho\frac{c+c^\dagger}{\sqrt{2}}\right]\right), \tag{5.53}$$

$$\mathrm{Pr}(\stackrel{\sim}{\mp}) = \sum_{\pm} \mathrm{Pr}(\pm,\stackrel{\sim}{\mp}) = \frac{1}{2}\left(1 \stackrel{\sim}{\mp} \sqrt{\Delta\tau}\,\mathrm{Tr}\left[\rho\frac{ic+(ic)^\dagger}{\sqrt{2}}\right]\right), \tag{5.54}$$

allow us to calculate expectation values,

$$\mathbb{E}[\Delta R_x] = \sum_{\pm} \pm\sqrt{\Delta\tau}\,\mathrm{Pr}(\pm) = \Delta\tau\,\mathrm{Tr}\left[\rho\frac{c+c^\dagger}{\sqrt{2}}\right], \tag{5.55}$$

$$\mathbb{E}[\Delta R_y] = \sum_{\stackrel{\sim}{\mp}} \stackrel{\sim}{\mp}\sqrt{\Delta\tau}\,\mathrm{Pr}(\stackrel{\sim}{\mp}) = \Delta\tau\,\mathrm{Tr}\left[\rho\frac{ic+(ic)^\dagger}{\sqrt{2}}\right]. \tag{5.56}$$

We can also find the correlation matrix,

$$\mathbb{E}[(\Delta R_x)^2] = \sum_{\pm} \Delta\tau\,\mathrm{Pr}(\pm) = \Delta\tau, \tag{5.57}$$
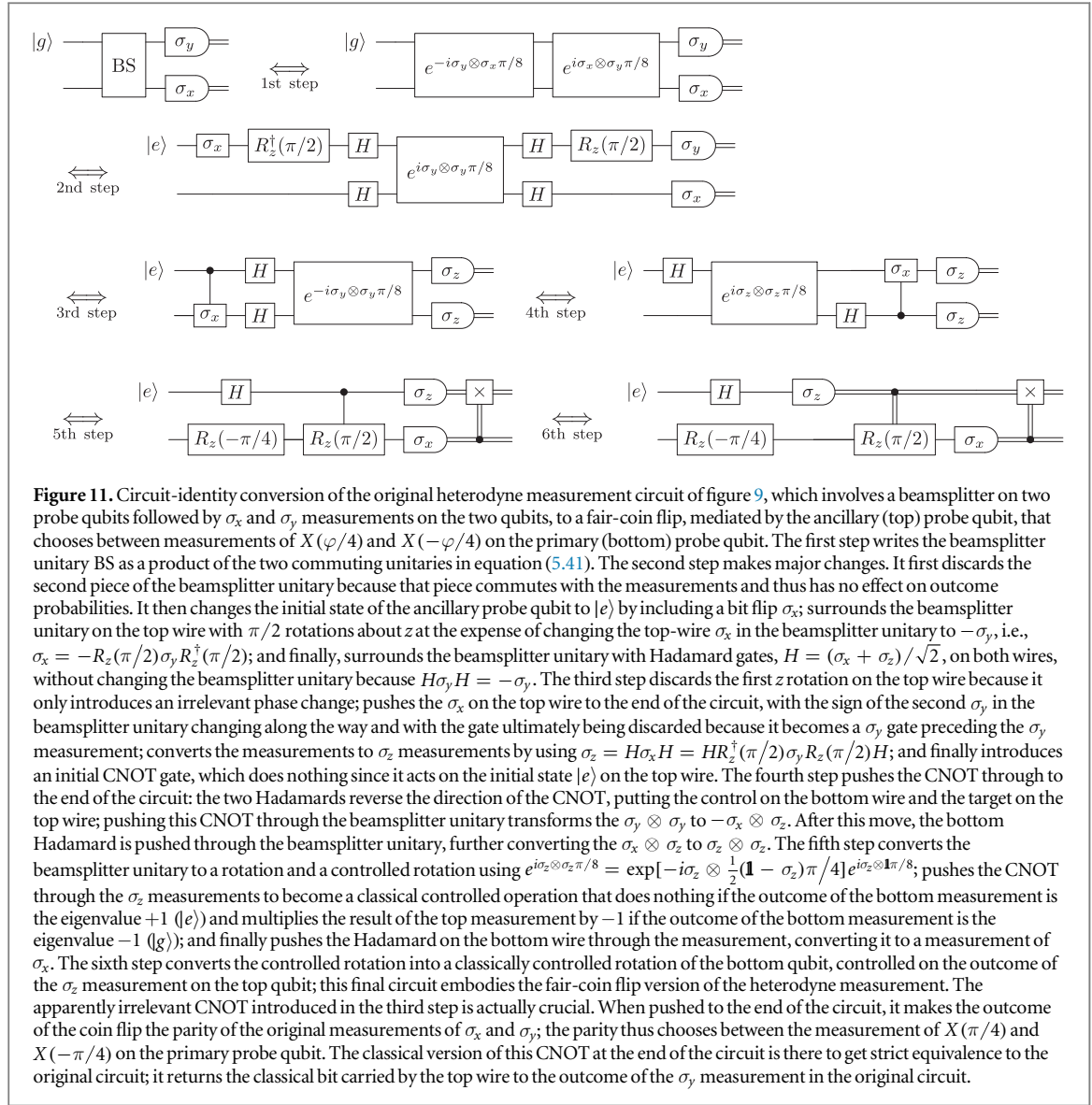
Figure 11. Circuit-identity conversion of the original heterodyne measurement circuit of figure 9, which involves a beamsplitter on two probe qubits followed by σ_x and σ_y measurements on the two qubits, to a fair-coin flip, mediated by the ancillary (top) probe qubit, that chooses between measurements of $X(\varphi/4)$ and $X(-\varphi/4)$ on the primary (bottom) probe qubit. The first step writes the beamsplitter unitary BS as a product of the two commuting unitaries in equation (5.41). The second step makes major changes. It first discards the second piece of the beamsplitter unitary because that piece commutes with the measurements and thus has no effect on outcome probabilities. It then changes the initial state of the ancillary probe qubit to $|e\rangle$ by including a bit flip σ_x; surrounds the beamsplitter unitary on the top wire with $\pi/2$ rotations about z at the expense of changing the top-wire σ_x in the beamsplitter unitary to $-\sigma_y$, i.e., $\sigma_x = -R_z(\pi/2)\sigma_y R_z^\dagger(\pi/2)$; and finally, surrounds the beamsplitter unitary with Hadamard gates, $H = (\sigma_x + \sigma_z)/\sqrt{2}$, on both wires, without changing the beamsplitter unitary because $H\sigma_y H = -\sigma_y$. The third step discards the first z rotation on the top wire because it only introduces an irrelevant phase change; pushes the σ_x on the top wire to the end of the circuit, with the sign of the second σ_y in the beamsplitter unitary changing along the way and with the gate ultimately being discarded because it becomes a σ_y gate preceding the σ_y measurement; converts the measurements to σ_z measurements by using $\sigma_z = H\sigma_x H = HR_z^\dagger(\pi/2)\sigma_y R_z(\pi/2)H$; and finally introduces an initial CNOT gate, which does nothing since it acts on the initial state $|e\rangle$ on the top wire. The fourth step pushes the CNOT through to the end of the circuit: the two Hadamards reverse the direction of the CNOT, putting the control on the bottom wire and the target on the top wire; pushing this CNOT through the beamsplitter unitary transforms the $\sigma_y \otimes \sigma_y$ to $-\sigma_x \otimes \sigma_z$. After this move, the bottom Hadamard is pushed through the beamsplitter unitary, further converting the $\sigma_x \otimes \sigma_z$ to $\sigma_z \otimes \sigma_z$. The fifth step converts the beamsplitter unitary to a rotation and a controlled rotation using $e^{i\sigma_z\otimes\sigma_z\pi/8} = \exp[-i\sigma_z \otimes \frac{1}{2}(\mathbf{1} - \sigma_z)\pi/4]e^{i\sigma_z\otimes\mathbf{1}\pi/8}$; pushes the CNOT through the σ_z measurements to become a classical controlled operation that does nothing if the outcome of the bottom measurement is the eigenvalue $+1$ ($|e\rangle$) and multiplies the result of the top measurement by -1 if the outcome of the bottom measurement is the eigenvalue -1 ($|g\rangle$); and finally pushes the Hadamard on the bottom wire through the measurement, converting it to a measurement of σ_x. The sixth step converts the controlled rotation into a classically controlled rotation of the bottom qubit, controlled on the outcome of the σ_z measurement on the top qubit; this final circuit embodies the fair-coin flip version of the heterodyne measurement. The apparently irrelevant CNOT introduced in the third step is actually crucial. When pushed to the end of the circuit, it makes the outcome of the coin flip the parity of the original measurements of σ_x and σ_y; the parity thus chooses between the measurement of $X(\pi/4)$ and $X(-\pi/4)$ on the primary probe qubit. The classical version of this CNOT at the end of the circuit is there to get strict equivalence to the original circuit; it returns the classical bit carried by the top wire to the outcome of the σ_y measurement in the original circuit.

$$\mathbb{E}[(\Delta R_y)^2] = \sum_{\widetilde{\pm}} \Delta\tau \Pr(\widetilde{\pm}) = \Delta\tau, \tag{5.58}$$

$$\mathbb{E}[\Delta R_x \Delta R_y] = \sum_{\pm,\widetilde{\pm}} \pm\widetilde{\pm}\Delta\tau \Pr(\pm, \widetilde{\pm}) = 0. \tag{5.59}$$

The first nonvanishing cross-moment of ΔR_x and ΔR_y is $\mathbb{E}[(\Delta R_x)^2(\Delta R_y)^2] = \Delta\tau^2$. This means that we should think of $\Delta R_x \Delta R_y = \pm\widetilde{\pm}\Delta\tau$ as a stochastic term of order $\Delta\tau$, and this is too small to survive the limit $\Delta\tau \to 0$ (only stochastic terms of order $\sqrt{\Delta\tau}$ survive this limit).

Returning now to the difference equation (5.49), we find, to linear order in $\Delta\tau$,

$$\Delta\rho_{\pm,\widetilde{\pm}} = \Delta\tau\, \mathcal{D}[c]\rho + \frac{1}{\sqrt{2}}(\Delta\mathcal{I}_x \mathcal{H}[c]\rho + \Delta\mathcal{I}_y \mathcal{H}[ic]\rho)$$

$$- \frac{1}{2}\Delta R_x \Delta R_y(\mathrm{Tr}[\rho(ic + (ic)^\dagger)]\mathcal{H}[c]\rho + \mathrm{Tr}[\rho(c + c^\dagger)]\mathcal{H}[ic]\rho), \tag{5.60}$$

where we introduce the innovations for the two random processes,

$$\Delta\mathcal{I}_x := \Delta R_x - \mathbb{E}[\Delta R_x], \tag{5.61}$$

$$\Delta\mathcal{I}_y := \Delta R_y - \mathbb{E}[\Delta R_y]. \tag{5.62}$$

The innovations are zero-mean random processes, with variance $\mathbb{E}[(\Delta\mathcal{I}_x)^2] = \mathbb{E}[(\Delta\mathcal{I}_x)^2] = \Delta\tau$. Since, as we discussed above, the term proportional to $\Delta R_x \Delta R_y$ is a zero-mean stochastic term of order $\Delta\tau$ (and thus vanishes in the continuous-time limit), we drop it, leaving us with the difference equation

Table 1. Input state, measurement basis, Kraus operators, and type of resulting stochastic master equation (SME); $X(\varphi)$ is the arbitrary probe quadrature defined in equation (5.32).

Initial state	Measurement basis	Kraus operators	SME
$\lvert g\rangle$	$\lvert e\rangle, \lvert g\rangle$	$K_e = \sqrt{\Delta\tau}\, c,\ K_g = \mathbf{1} - \frac{1}{2}\Delta\tau\, c^\dagger c$	Jump
$\lvert g\rangle$	$\lvert\phi_\pm\rangle = \frac{1}{\sqrt{2}}(\lvert g\rangle \pm \lvert e\rangle)$	$K_\pm = \frac{1}{\sqrt{2}}(\mathbf{1} \pm \sqrt{\Delta\tau}\, c - \frac{1}{2}\Delta\tau\, c^\dagger c)$	Homodyne X
$\lvert g\rangle$	$\lvert\phi_\pm(\varphi)\rangle = \frac{1}{\sqrt{2}}(\lvert g\rangle \pm e^{-i\varphi}\lvert e\rangle)$	$K_\pm(\varphi) = \frac{1}{\sqrt{2}}(\mathbf{1} \pm \sqrt{\Delta\tau}\, e^{i\varphi}c - \frac{1}{2}\Delta\tau\, c^\dagger c)$	Homodyne $X(\varphi)$
$\lvert g\rangle$	$\lvert\phi_{\pm,\widetilde{\pm}}\rangle = \frac{1}{\sqrt{2}}\big(\lvert g\rangle + \frac{1}{\sqrt{2}}(\pm 1 \overset{\sim}{\mp} i)\lvert e\rangle\big)$	$K_{\pm,\widetilde{\pm}} = \frac{1}{2}\big(\mathbf{1} + \sqrt{\Delta\tau}\,\frac{1}{\sqrt{2}}(\pm 1 \overset{\sim}{\mp} i)c - \frac{1}{2}\Delta\tau\, c^\dagger c\big)$	Heterodyne

$$\Delta\rho_{\pm,\widetilde{\pm}} = \Delta\tau\,\mathcal{D}[c]\rho + \frac{1}{\sqrt{2}}(\Delta\mathcal{I}_x\mathcal{H}[c]\rho + \Delta\mathcal{I}_y\mathcal{H}[ic]\rho). \tag{5.63}$$

When we take the continuous-time limit, the innovations $\Delta\mathcal{I}_{x,y}$ become $\sqrt{\gamma}\,dW_{x,y}$, where $dW_{x,y}$ are independent Weiner processes, i.e., $\mathbb{E}[dW_{x,y}] = 0$ and $\mathbb{E}[dW_j dW_k] = dt\,\delta_{jk}$. The resulting SME is

$$d\rho_{\mathrm{Het}} = dt\,\mathcal{D}[\sqrt{\gamma}\, c]\rho + \frac{1}{\sqrt{2}}(dW_x\,\mathcal{H}[\sqrt{\gamma}\, c]\rho + dW_y\,\mathcal{H}[i\sqrt{\gamma}\, c]\rho). \tag{5.64}$$

The unconditional master equation, obtained by averaging over the Weiner processes, is, of course, the vacuum master equation (5.18).

Notice that the heterodyne SME (5.64) has the same form as homodyne SME (5.30), except that the former has two Weiner processes acting independently in the place where the latter has just one. This is a consequence of the heterodyne measurement's having provided information about two quadrature components of the system, $c + c^\dagger$ and $i(c - c^\dagger)$. These two real-valued Wiener processes may be interpreted as a single complex-valued Wiener process, as in the original formulation of this unravelling by Gisin and Percival [83]. Their *quantum state diffusion equation* was conceived without reference to any measurement model, but Wiseman and Milburn soon demonstrated the correspondence to heterodyne measurement [84].

5.4. Summary of qubit-probe measurement schemes

To end this section, we briefly summarize the results. Throughout this section, we kept the probe initial state fixed as the ground state $\lvert g\rangle$, and we kept the interaction unitary fixed as that in equation (5.1). What changed from one subsection to the next was the kind of measurement on the probe qubits. Section 5.1 analyzed measurements of the probe qubits in Z basis, which is analogous to photon-counting measurements for probe fields; this resulted in a SME that is identical to the photon-counting SME. Section 5.2 considered measurement of the probes in the X basis, which is analogous to homodyne measurements on probe fields; this resulted in a stochastic master equation that is identical to the homodyne SME. Section 5.3 derived the stochastic master equation for a generalized measurement on the probe qubits that is analogous to heterodyne measurement on a probe field; the SME is identical to the heterodyne SME. The results for vacuum photon-counting, homodyne, and heterodyne measurements are summarized in table 1, as well as the comparable information for homodyne measurement of an arbitrary quadrature.

6. Quantum trajectories for Gaussian probe-qubit states

In this section, we generalize the results of the previous section by addressing the following question: Can we extend our qubit bath model, so successful in capturing the behavior of vacuum stochastic dynamics, to describe more general Gaussian stochastic dynamics? By Gaussian we mean that the probe field is in a state with a Gaussian Wigner function. Gaussian baths are capable of describing combinations of mean fields (probe field in a coherent state), thermal fluctuations (probe field in a thermal state), and quadrature correlation/anticorrelation (probe field in a squeezed state). These baths have been thoroughly studied in the literature. Wiseman and Milburn, who did much of the primary work in [57, 84, 85], summarize the results in Wiseman's thesis [63] and in their joint book [66]. Important related work exists on simulation methods [86, 87] and the mathematical formalism behind these descriptions [88–91].

To handle the case of a vacuum probe field in terms of qubit probes, it is sufficient, we found, to have a fixed initial probe state $\lvert g\rangle$ and the fixed interaction unitary (5.1). To handle the general Gaussian case in terms of qubit probes, we must allow a variety of initial probe states, including mixed states, as one does with fields, but we also find it necessary to allow modifications to the interaction unitary (5.1). The reason is that a qubit has nowhere near as much freedom in states as even the Gaussian states of a field mode; thus, for example, to handle a squeezed bath in terms of qubits, we have to modify the interaction unitary to handle the quadrature-dependent noise that for a field bath comes from putting the field in a squeezed state.

To guide our generalization procedure, we recall in section 6.1 some facts about the standard field-mode analysis; we also review how standard input-output formalism of quantum optics emerges from this analysis. We then proceed in section 6.2 to the translation to probe qubits. Throughout these discussions, we label field operators with the letters *b* and *B*, and we label the analogous operators for probe qubits with *a* and *A*.

6.1. Gaussian problem for probe fields and input-output formalism

For a probe field divided up into the discrete temporal modes of section 4, we can introduce the quantum noise increment,

$$\Delta B_n := \sqrt{\Delta\tau}\ b_n = \sqrt{\gamma}\int_{t_n}^{t_{n+1}} ds\ b(s). \tag{6.1}$$

Gaussian bath statistics of the field are captured by the first and second moments of these increments:

$$\langle \Delta B_n \rangle = \langle b_n \rangle \sqrt{\Delta\tau}\ = \alpha_n \Delta\tau, \quad \beta_n = \sqrt{\gamma}\ \alpha_n, \tag{6.2a}$$

$$\langle \Delta B_n^\dagger \Delta B_n \rangle = \langle b_n^\dagger b_n \rangle \Delta\tau = N\Delta\tau, \tag{6.2b}$$

$$\langle \Delta B_n^2 \rangle = \langle b_n^2 \rangle \Delta\tau = M\Delta\tau, \tag{6.2c}$$

$$\langle [\Delta B_n, \Delta B_n^\dagger] \rangle = \langle [b_n, b_n^\dagger] \rangle \Delta\tau = \Delta\tau, \tag{6.2d}$$

where β_n is the mean probe field, N is related to the mean number of thermal photons, and M is related to the amount of squeezing. These interpretations are made more precise in sections 6.3–6.5. The parameters N and M satisfy the inequality

$$|M|^2 \leqslant N(N+1), \tag{6.3}$$

which ensures that the field state is a valid Gaussian quantum state. Noise increments for different time segments are uncorrelated, in accordance with the Markovian nature of Gaussian noise.

Much of the quantum-optics literature works directly with the quantum Weiner process or infinitesimal quantum noise increment, $dB(t)$, which is defined as an appropriate limit of ΔB_n,

$$dB(t) := \int_t^{t+dt} b(s)ds = \lim_{\Delta t \to dt} \sqrt{\Delta t}\ b_n = \lim_{\Delta t \to dt} \Delta B_n/\sqrt{\gamma}, \tag{6.4}$$

where the limiting form assumes $t = t_n$. Equation (6.4) is analogous to the relationship between classical white noise $\xi(s)$ and the Weiner process $dW_t := \int_t^{t+dt} \xi(s)ds$. The Gaussian bath statistics of an instantaneous field mode are described by the first and second moments of $dB(t)$,

$$\langle dB(t) \rangle = \beta(t)dt, \quad \beta(t) = \sqrt{\gamma}\ \alpha(t), \tag{6.5a}$$

$$\langle dB^\dagger(t)dB(t) \rangle = N\ dt, \tag{6.5b}$$

$$\langle dB(t)^2 \rangle = M\ dt, \tag{6.5c}$$

$$\langle [dB(t), dB^\dagger(t)] \rangle = dt. \tag{6.5d}$$

As a first step in our generalization to qubits below, we consider the unconditional master equation for general Gaussian baths in the continuous limit (taken from equation (4.254) of [66]):

$$d\rho = dt\Big([\beta^*(t)\sqrt{\gamma}\ c - \beta(t)\sqrt{\gamma}\ c^\dagger, \rho] + (N+1)\mathcal{D}[\sqrt{\gamma}\ c]\rho + N\mathcal{D}[\sqrt{\gamma}\ c^\dagger]\rho$$
$$+ \tfrac{1}{2}M^*[\sqrt{\gamma}\ c, [\sqrt{\gamma}\ c, \rho]] + \tfrac{1}{2}M[\sqrt{\gamma}\ c^\dagger, [\sqrt{\gamma}\ c^\dagger, \rho]]\Big). \tag{6.6}$$

Notice that, as is well known, the terms linear in *c*, i.e., those proportional to β, are a commutator that corresponds to Hamiltonian evolution; indeed, this Hamiltonian is the system evolution one gets if one replaces the bath by its mean field, neglecting quantum effects entirely. Just as we discussed for an external Hamiltonian in section 4, these mean fields must vary much slower than $1/\Omega$. In comparing equation (6.6) and other results between our paper and [66], it is important to be aware of the distinction between our definitions of the *c* operators. We choose *c* to be a dimensionless system operator, whereas in Wiseman and Milburn, it contains an implicit factor of $\sqrt{\gamma}$, which is pointed out in the paragraph below their equation (3.155).

Stochastic master equations for a general Gaussian bath, conditioned on the sorts of measurements considered in section 5, are significantly more complicated than the unconditional master equation (6.6) and are the subject of sections 6.3–6.5.

Before getting to the qubit-probe model, however, we pause to review how this is related to the input-output formalism of quantum optics. From the interaction unitary (4.20), we can calculate how the probe-field operators for each time segment change in the Heisenberg picture. To make the distinction clear, we now label all the Heisenberg probe operators before the interaction as ΔB_n^{in}. The output operators are obtained by unitarily evolving the input operators

$$\Delta B_n^{\text{out}} = \sqrt{\Delta\tau}\, b_n^{\text{out}} = U_I^{(n)\dagger} \Delta B_n^{\text{in}} U_I^{(n)} = \left(\mathbf{1} - \frac{1}{2}\Delta\tau[c, c^\dagger]\right) \otimes \sqrt{\Delta\tau}\, b_n^{\text{in}} + c\,\Delta\tau + \mathcal{O}(\Delta\tau^2)$$

$$= \Delta B_n^{\text{in}} + c\,\Delta\tau + \mathcal{O}(\Delta\tau^{3/2}), \tag{6.7}$$

which shows that the output field is the scattered input field plus radiation from the system. We can calculate the number of quanta in the output probe field,

$$\Delta N^{\text{out}} = \frac{\Delta B_n^{\text{out}\dagger}\Delta B_n^{\text{out}}}{\Delta\tau} = b_n^{\text{out}\dagger} b_n^{\text{out}} = (\mathbf{1} - \Delta\tau[c, c^\dagger]) \otimes b_n^{\text{in}\dagger} b_n^{\text{in}}$$

$$+ (c \otimes \Delta B_n^{\text{in}\dagger} + c^\dagger \otimes \Delta B_n^{\text{in}}) + c^\dagger c\,\Delta\tau + \mathcal{O}(\Delta\tau^{3/2}). \tag{6.8}$$

In the literature these are known as input-output relations. Analyses using input-output relations were first used in quantum optics to analyze the noise added as a bosonic mode is amplified [92, 93] and, most importantly, in the pioneering description of linear damping by Yurke and Denker [94]. The input-output relations display clearly how the probe field is changed by scattering off the system. Although we work in the interaction picture in this paper, one can see the input-output relations at work indirectly in our results. Specifically, the conditional expectation of the measurement result at the current timestep [see, e.g., equations (5.11) and (5.25) and similar equations below] is the trace of the relevant output operator with the initial field state and a conditional system state.

Experienced practitioners of input-output theory might express concern about the term proportional to $[c, c^\dagger]$ in equation (6.8), but not to worry. When one takes the expectation of this equation in vacuum or a coherent state, the commutator term becomes too high an order in $\Delta\tau$ and thus can be ignored. For thermal and squeezed baths, equation (6.8) is irrelevant since we cannot sensibly perform photon counting on such fields due to the field's infinite photon flux (which can be identified in our model as the finite photon-detection probability in each infinitesimal time interval).

6.2. Gaussian problem for probe qubits

To make the correspondence to our qubit-probe model, we define a qubit quantum-noise increment analogous to the probe-field quantum noise increment (6.1):

$$\Delta A_n := \sqrt{\Delta\tau}\, a_n. \tag{6.9}$$

In section 5, we consistently chose a_n to be the qubit lowering operator, but in this section, we find it useful to allow more general possibilities. We remind the reader that in the picture of time increments Δt, we work with the dimensionless time interval $\Delta\tau = \gamma\Delta t$, not with Δt itself. The main way this might cause confusion is that if we introduce a continuous-time noise increment $dA = \sqrt{dt}\, a_n$ for a qubit probe—or use the continuous-time field increment $dB(t) = \sqrt{dt}\, b_n$—we have to remember the factor of $\sqrt{\gamma}$ in $\Delta A_n = \sqrt{\gamma}\sqrt{\Delta t}\, a_n$.

For probe qubits prepared in the (possibly mixed) state σ (distinguished from the similarly notated Pauli operators by subscripts or lack thereof), we write the qubit bath statistics as

$$\langle \Delta A_n \rangle_\sigma = \alpha_n \Delta\tau, \qquad \beta_n = \sqrt{\gamma}\,\alpha_n, \tag{6.10a}$$

$$\langle \Delta A_n^\dagger \Delta A_n \rangle_\sigma = N\Delta\tau, \tag{6.10b}$$

$$\langle \Delta A_n^2 \rangle_\sigma = M\Delta\tau, \tag{6.10c}$$

$$\langle [\Delta A_n, \Delta A_n^\dagger] \rangle_\sigma = \Delta\tau. \tag{6.10d}$$

For the choice $a_n := \sigma_-^{(n)}$ that we used in section 5, with vacuum probe state $\sigma = |g\rangle\langle g|$, these relations are satisfied with $\alpha = N = M = 0$. Notice that with a slight abuse of notation, which we have already used and which can be excused because we only want to get the scaling with γ right, we have
$\beta\,dt = \langle dA \rangle = \langle \Delta A \rangle / \sqrt{\gamma} = \alpha\Delta\tau / \sqrt{\gamma} = \sqrt{\gamma}\,\alpha dt$, which implies that $\beta_n = \sqrt{\gamma}\,\alpha_n$, as displayed above.

Replacing the explicit σ_- in the interaction unitary (5.1a) with the more general qubit operator a (and thus σ_+ with $a^\dagger$), we get a new interaction unitary,

$$U_I = \mathbf{1} \otimes \mathbf{1} + \sqrt{\Delta\tau}\,(c \otimes a_n^\dagger - c^\dagger \otimes a_n) + \frac{1}{2}\Delta\tau(c \otimes a_n^\dagger - c^\dagger \otimes a_n)^2$$

$$= \mathbf{1} \otimes \mathbf{1} + (c \otimes \Delta A_n^\dagger - c^\dagger \otimes \Delta A_n) + \frac{1}{2}(c \otimes \Delta A_n^\dagger - c^\dagger \otimes \Delta A_n)^2, \tag{6.11}$$

which we use throughout the remainder of this section, specifying the operator a_n appropriately for each case we consider. Using this new interaction unitary, we find that the expectation values (6.10) are the only properties of the bath that influence the unconditional master equation,

$$
\begin{aligned}
\Delta\rho_n &:= \mathrm{Tr}_{\mathrm{pr}}[U_I(\rho_n \otimes \sigma_n)U_I^\dagger] - \rho_n \\
&= [\langle \Delta A_n \rangle_\sigma^* c - \langle \Delta A_n \rangle_\sigma c^\dagger, \rho_n] + (\langle \Delta A_n^\dagger \Delta A_n \rangle_\sigma + \langle [\Delta A_n, \Delta A_n^\dagger] \rangle_\sigma)\mathcal{D}[c]\rho_n + \langle \Delta A_n^\dagger \Delta A_n \rangle_\sigma \mathcal{D}[c^\dagger]\rho_n \\
&\quad + \tfrac{1}{2}\langle \Delta A_n^2 \rangle_\sigma^* [c, [c, \rho_n]] + \tfrac{1}{2}\langle \Delta A_n^2 \rangle_\sigma [c^\dagger, [c^\dagger, \rho_n]].
\end{aligned}
\tag{6.12}
$$

Here $\mathrm{Tr}_{\mathrm{pr}}$ denotes a trace over the nth probe qubit; in the interaction unitary and the master equation, we only keep terms to linear order in $\Delta\tau$ or, equivalently, quadratic order in ΔA_n. This tells us that satisfying equations (6.10) is a necessary and sufficient condition for reproducing the Gaussian master equation with our qubit model. Since a SME implies a master equation, (6.10) is also a necessary condition for reproducing the corresponding conditional evolution, i.e., the Gaussian SMEs, with our qubit model. This serves as a guiding principle for exploring nonvacuum probes in the qubit model.

Notice that we could develop an input-output formalism for probe qubits, analogous to that for fields in equations (6.7) and (6.8). Since a_n and $a_n^\dagger$ do not satisfy the canonical bosonic commutation relations, however, the qubit input-output relation will not have the same form as the field relations (6.7) and (6.8). Another complication in the qubit input-output formalism is the dependence of a_n on the Gaussian field state we want to model, which results in a state-dependent input-output relation. This complication shows up in the field input-output relations as well, and so is not unique to our qubit model. Everything would work out right once we included the probe initial state and the appropriate measurement, but these complications mean that the qubit input-output formalism does not have the simple interpretation we can attach to the vacuum field version, so we do not develop it here.

6.3. Coherent states and mean-field stochastic master equation

One way to extend the qubit model presented so far is to to generalize to nonvacuum Gaussian pure states, the simplest of which is a coherent state. For a field probe, we create a coherent state with a wavepacket mean field $\beta(t)$ by applying to the vacuum the continuous-time displacement operator [95],

$$
D[\beta(t)] := \exp\left(\int dt \, [\beta(t)b^\dagger(t) - \beta^*(t)b(t)]\right).
\tag{6.13}
$$

To use this continuous-time displacement operator, it is often convenient to write it as a product of displacement operators for the field modes b_n of the time increments, during each of which the mean field is assumed to be essentially constant, yielding

$$
D[\beta(t)] = \prod_n D(\alpha_n),
\tag{6.14}
$$

where

$$
D(\alpha_n) := e^{\sqrt{\Delta t}(\beta_n b_n^\dagger - \beta_n^* b_n)} = e^{\sqrt{\Delta\tau}(\alpha_n b_n^\dagger - \alpha_n^* b_n)} = e^{\alpha_n \Delta B_n^\dagger - \alpha_n^* \Delta B_n},
\tag{6.15}
$$

is the displacement operator for the nth field mode b_n and $\beta_n = \beta(t_n) = \sqrt{\gamma}\,\alpha_n$. Applying this displacement operator to vacuum creates a product coherent state, in which the field mode b_n for the nth time increment is a coherent state with mean number of photons $|\beta_n|^2 \Delta t = \gamma\,|\alpha_n|^2 \Delta\tau$. Thus, in the continuous-time limit, the mean rate at which photons encounter the system is $|\beta(t)|^2 = \gamma\,|\alpha(t)|^2$.

Up till this point in this section, we have retained the subscript n that labels each time increment, but from here on, as in section 5, we omit this label because it is just a nuisance when dealing with the time increments one at a time. We only note that the omitted n dependence is necessary to describe a time-changing mean field $\alpha(t) = \beta(t)/\sqrt{\gamma}$.

To translate from field modes to qubits, we let $a = \sigma_-$, as in section 5, and we introduce a qubit analogue of a displacement operator for a probe qubit,

$$
D(\alpha) := e^{\sqrt{\Delta\tau}(\alpha\sigma_+ - \alpha^*\sigma_-)} = e^{\alpha\Delta A^\dagger - \alpha^*\Delta A}.
\tag{6.16}
$$

This operator does not act much like the field displacement operator for large displacements, but because we are working with small time increments, we can assume that $\alpha\sqrt{\Delta\tau}$ is small and expand the displacement operator as

$$
\begin{aligned}
D(\alpha) &= \mathbf{1} + \alpha\Delta A^\dagger - \alpha^*\Delta A + \tfrac{1}{2}(\alpha\Delta A^\dagger - \alpha^*\Delta A)^2 + \mathcal{O}(\Delta\tau^{3/2}) \\
&= \mathbf{1} + \alpha\Delta A^\dagger - \alpha^*\Delta A - \tfrac{1}{2}|\alpha|^2(\Delta A\Delta A^\dagger + \Delta A^\dagger\Delta A) + \mathcal{O}(\Delta\tau^{3/2}),
\end{aligned}
\tag{6.17}
$$

where the final form uses $\Delta A^2 = 0 = (\Delta A^\dagger)^2$ since $a = \sigma_-$. Throughout we work to linear order in $\Delta\tau$, without bothering to indicate explicitly that the next-order terms are $\mathcal{O}(\Delta\tau^{3/2})$. The aficionado might notice equation (6.17) is related to the quantum stochastic differential equation for the displacement (or 'Weyl') operator; see equation (4.11) of [64].

Applying the displacement operator to the ground state $|g\rangle$ gives the normalized probe coherent states,

$$
\begin{aligned}
|\alpha\rangle &:= D(\alpha)|g\rangle \\
&= (1 - \tfrac{1}{2}|\alpha|^2 \Delta\tau)|g\rangle + \alpha\sqrt{\Delta\tau}\,|e\rangle \\
&= (1 - \tfrac{1}{2}|\alpha|^2 \Delta\tau)(|g\rangle + \alpha\sqrt{\Delta\tau}\,|e\rangle).
\end{aligned}
\tag{6.18}
$$

The state (6.18) is analogous to a field-mode coherent state because it reproduces the mean-field bath statistics (and therefore the unconditional master equation):

$$
\langle \Delta A \rangle_\alpha = \alpha\,\Delta\tau,
\tag{6.19a}
$$

$$
\langle \Delta A^\dagger \Delta A \rangle_\alpha = 0,
\tag{6.19b}
$$

$$
\langle \Delta A^2 \rangle_\alpha = 0,
\tag{6.19c}
$$

$$
\langle [\Delta A,\, \Delta A^\dagger] \rangle_\alpha = \Delta\tau.
\tag{6.19d}
$$

In calculating the difference equation for any kind of measurement on the probe qubits, we necessarily use normalized post-measurement system states. Since we normalize the post-measurement state we can work with an unnormalized probe initial state, because the magnitude of the probe initial state cancels out when the post-measurement state is normalized. In particular, it is convenient to work here with an unnormalized version of the coherent states,

$$
|\alpha\rangle = |g\rangle + \alpha\sqrt{\Delta\tau}\,|e\rangle,
\tag{6.20}
$$

keeping in mind that the resulting Kraus operators are off by a factor of $1 - \tfrac{1}{2}|\alpha|^2\Delta\tau$ and POVM elements and probabilities of measurement outcomes are off by a factor of $1 - |\alpha|^2\Delta\tau$.

We focus now on the case of performing photon counting on the probes, i.e., a measurement in the basis $\{|g\rangle, |e\rangle\}$. This results in Kraus operators,

$$
K_g = \langle g|U_I|\alpha\rangle = \mathbf{1} - \Delta\tau(\alpha c^\dagger + \tfrac{1}{2}c^\dagger c),
\tag{6.21a}
$$

$$
K_e = \langle e|U_I|\alpha\rangle = \sqrt{\Delta\tau}\,(\alpha\mathbf{1} + c),
\tag{6.21b}
$$

which are analogous to equations 4.53 and 4.55 in [66] (in comparing, recall that a Hamiltonian term can be added in trivially). As we observed for the vacuum case in equations (5.21) and (5.44), both the homodyne and heterodyne Kraus operators are linear combinations of the photon-counting Kraus operators.

Following our treatment of the vacuum case for photon counting in section 5.1, we now find a difference equation

$$
\begin{aligned}
\Delta\rho_{\Delta N} &= \Delta N\,\mathcal{G}[\alpha\mathbf{1} + c]\rho - \Delta\tau\,\mathcal{H}\Big[\alpha c^\dagger + \tfrac{1}{2}c^\dagger c\Big]\rho \\
&= \Delta\tau([\alpha^* c - \alpha c^\dagger,\, \rho] + \mathcal{D}[c]\rho) + \Delta\mathcal{I}_D\,\mathcal{G}[\alpha\mathbf{1} + c]\rho,
\end{aligned}
\tag{6.22}
$$

where ΔN is the bit-valued random variable introduced in section 5.1, i.e., $\Delta N = 0$ for outcome g and $\Delta N = 1$ for outcome e, and $\Delta\mathcal{I}_D = \Delta N - \mathbb{E}[\Delta N]$ is the photon-counting innovation (5.15). Taking the continuous-time limit gives the Gaussian SME with a mean field for the case of direct detection,

$$
\begin{aligned}
d\rho_D &= dN\,\mathcal{G}[\beta\mathbf{1} + \sqrt{\gamma}\,c]\rho - dt\,\mathcal{H}\Big[\beta\sqrt{\gamma}\,c^\dagger + \tfrac{1}{2}\gamma c^\dagger c\Big]\rho \\
&= dt([\beta^*\sqrt{\gamma}\,c - \beta\sqrt{\gamma}\,c^\dagger,\, \rho] + \mathcal{D}[\sqrt{\gamma}\,c]\rho) + d\mathcal{I}_D\,\mathcal{G}[\beta\mathbf{1} + \sqrt{\gamma}\,c]\rho,
\end{aligned}
\tag{6.23}
$$

where $\beta = \sqrt{\gamma}\,\alpha$; this result is also found in [66]. The driving terms due to the mean field are those of a Hamiltonian $i\sqrt{\gamma}(\beta^* c - \beta c^\dagger)$, as we would get if we replaced the probe operators with their mean values. The unconditional master equation for a mean-field probe follows from retaining only the deterministic part of equation (6.23) and agrees with equation (6.6) when we set $N = M = 0$.

An equivalent method for dealing with a bath with a mean field, more attuned to the approach we use later in this section, is discussed at the end of section 6.5 and is sketched in figure 15.

6.4. Thermal states

Having dealt with a pure state that carries a mean field, we turn now to Gaussian states that have more noise than vacuum, i.e., thermal baths. A thermal state at temperature T is defined by

$$
\sigma_{\mathrm{th}} := \frac{e^{-H/k_B T}}{\mathrm{Tr}\,[e^{-H/k_B T}]}.
\tag{6.24}
$$

For a field mode at frequency ω, the Hamiltonian is $H = \hbar\omega(a^\dagger a + \frac{1}{2})$, and the corresponding thermal state is given by

$$\sigma_{\text{th}} = \frac{1}{N+1} \sum_{m=0}^{\infty} \left(\frac{N}{N+1}\right)^m |m\rangle\langle m|, \tag{6.25}$$

where

$$N := \frac{1}{e^{\hbar\omega/k_B T} - 1} \tag{6.26}$$

is the mean number of photons.

The thermal state for a qubit probe is diagonal in the basis $\{|g\rangle, |e\rangle\}$ with the ratio of excited-state population to ground-state population being $N/(N+1)$:

$$\sigma_{\text{th}} = \frac{N+1}{2N+1} |g\rangle\langle g| + \frac{N}{2N+1} |e\rangle\langle e|. \tag{6.27}$$

This state has an obvious problem, however, since if we choose $a = \sigma_-$ ($\Delta A = \sqrt{\Delta\tau}\, \sigma_-$), we find that $\langle \Delta A^\dagger \Delta A \rangle_{\text{th}} / \Delta\tau = \sigma_+ \sigma_- = \langle e | \sigma_{\text{th}} | e \rangle = N/(2N+1)$. Indeed, no qubit state has more than one excitation in it, and the thermal state (6.27) has at most half an excitation. It is easy to deal with this problem, however, by introducing an *effective* qubit field operator,

$$a_{\text{th}} = \sqrt{2N+1}\, \sigma_-, \tag{6.28}$$

which goes into the qubit increment $\Delta A = \sqrt{\Delta\tau}\, a_{\text{th}}$. This increases the strength of the coupling of the qubit probes to the system in a way that yields the desired bath statistics,

$$\langle \Delta A \rangle_{\text{th}} = 0, \tag{6.29a}$$

$$\langle \Delta A^\dagger \Delta A \rangle_{\text{th}} = N\, \Delta\tau, \tag{6.29b}$$

$$\langle \Delta A^2 \rangle_{\text{th}} = 0, \tag{6.29c}$$

$$\langle [\Delta A, \Delta A^\dagger] \rangle_{\text{th}} = \Delta\tau. \tag{6.29d}$$

A glance at the interaction unitary (6.11) shows that the rescaled coupling strength is $\gamma_N = (2N+1)\gamma$, i.e.,

$$U_{\text{th},I} = \mathbf{1} \otimes \mathbf{1} + \sqrt{2N+1}\, \sqrt{\Delta\tau}\, (c \otimes \sigma_+ - c^\dagger \otimes \sigma_-) + \frac{1}{2}(2N+1)\Delta\tau(c \otimes \sigma_+ - c^\dagger \otimes \sigma_-)^2. \tag{6.30}$$

The power delivered by this idealized broadband thermal bath is infinite, so photon counting yields nonsensical results. Instead, we consider homodyne detection on the bath, i.e., measurement in the basis (5.20), which avoids the infinite-power problem. Because the probe state is a mixture of two pure states, $|g\rangle\langle g|$ and $|e\rangle\langle e|$, we need Kraus operators corresponding to each combination of probe pure state and measurement outcome in order to calculate the unnormalized updated state (see equation (3.29)):

$$K_{\pm g} = \sqrt{\frac{N+1}{2N+1}} \langle \phi_\pm | U_{\text{th},I} | g \rangle = \frac{1}{\sqrt{2}} \sqrt{\frac{N+1}{2N+1}} \left(\mathbf{1} \pm \sqrt{\Delta\tau}\, \sqrt{2N+1}\, c - \frac{1}{2}\Delta\tau(2N+1)c^\dagger c \right), \tag{6.31}$$

$$K_{\pm e} = \sqrt{\frac{N}{2N+1}} \langle \phi_\pm | U_{\text{th},I} | e \rangle = \pm \frac{1}{\sqrt{2}} \sqrt{\frac{N}{2N+1}} \left(\mathbf{1} \mp \sqrt{\Delta\tau}\, \sqrt{2N+1}\, c^\dagger - \frac{1}{2}\Delta\tau(2N+1)cc^\dagger \right). \tag{6.32}$$

The $\pm$ at the head of the expression for $K_{\pm e}$ can be ignored, since Kraus operators always appear in a quadratic combination involving the Kraus operator and its adjoint. We are interested in the state after a measurement that yields the result $\pm$, and this means summing over the two possibilities for the initial state of the probe,

$$\rho_\pm = \frac{K_{\pm g} \rho K_{\pm g}^\dagger + K_{\pm e} \rho K_{\pm e}^\dagger}{\text{Tr}[\rho] E_\pm}, \tag{6.33}$$

where

$$E_\pm := K_{\pm g}^\dagger K_{\pm g} + K_{\pm e}^\dagger K_{\pm e} = \frac{1}{2}\left(\mathbf{1} \pm \sqrt{\Delta\tau}\, \frac{c + c^\dagger}{\sqrt{2N+1}} \right). \tag{6.34}$$

is the POVM element for the outcome $\pm$.

The resulting difference equation for the system state is

$$\Delta\rho_{\pm} = \left(\pm\sqrt{\Delta\tau} - \Delta\tau \frac{\mathrm{Tr}\left[\rho(c + c^{\dagger})\right]}{\sqrt{2N+1}}\right)\left((N+1)\frac{\mathcal{H}[c]\rho}{\sqrt{2N+1}} - N\frac{\mathcal{H}[c^{\dagger}]\rho}{\sqrt{2N+1}}\right)$$
$$+ \Delta\tau(N+1)\mathcal{D}[c]\rho + \Delta\tau N \mathcal{D}[c^{\dagger}]\rho$$
$$= \Delta\tau((N+1)\mathcal{D}[c]\rho + N\mathcal{D}[c^{\dagger}]\rho) + \frac{\Delta\mathcal{I}_{H}}{\sqrt{2N+1}}\mathcal{H}[(N+1)c - Nc^{\dagger}]\rho, \qquad (6.35)$$

where we use the same random process $\Delta R = \pm\sqrt{\Delta\tau}$ and innovation $\Delta\mathcal{I}_{H} = \Delta R - \mathbb{E}[\Delta R]$ as for the vacuum SME for homodyning. In the continuous-time limit, the difference equation becomes

$$d\rho = dt\left((N+1)\mathcal{D}[\sqrt{\gamma}\,c]\rho + N\mathcal{D}[\sqrt{\gamma}\,c^{\dagger}]\rho\right) + \frac{dW}{\sqrt{2N+1}}\mathcal{H}[(N+1)\sqrt{\gamma}\,c - N\sqrt{\gamma}\,c^{\dagger}]\rho, \qquad (6.36)$$

where dW is the Weiner process that is the limit of the innovation. This result agrees with equations 4.253 and 4.254 of [66] when we set $M = 0$ in those equations. The unconditional thermal master equation retains only the deterministic part of equation (6.36) and agrees with equation (6.6) when we set $\beta = 0$ and $M = 0$.

The strategy of increasing the coupling strength clearly allows us to handle the thermal-state SME, but it is worth spelling out in a little more detail how that works, i.e., how we are able to mimic a field mode that has all energy levels occupied in a thermal state with a qubit that has only two levels. Because the thermal state for a field mode is diagonal in the number basis, the terms from $U_{I}(\rho \otimes \sigma_{\mathrm{th}})U_{I}^{\dagger}$ that survive tracing out the probe field are those balanced in b_{m} and $b_{m}^{\dagger}$:

$$-\frac{1}{2}\Delta t\, c^{\dagger}c\, \gamma\, \mathrm{Tr}\left[\sigma_{\mathrm{th}}b_{n}^{\dagger}b_{n}\right] - \frac{1}{2}\Delta t\, cc^{\dagger}\, \gamma\, \mathrm{Tr}\left[\sigma_{\mathrm{th}}b_{n}b_{n}^{\dagger}\right]. \qquad (6.37)$$

The normally ordered expression with $b_{n}^{\dagger}b_{n}$ corresponds to the system absorbing an excitation from the bath, while the antinormally ordered expression with $b_{n}b_{n}^{\dagger}$ corresponds to the system emitting an excitation into the bath.

Focusing just on the coupling strength for these two processes, the relevant expressions are

$$\gamma\,\mathrm{Tr}\left[\sigma_{\mathrm{th}}b_{n}^{\dagger}b_{n}\right] = \gamma\sum_{m=0}^{\infty}\mathrm{Pr}(m|N)m = \frac{N}{2N+1}\sum_{m=0}^{\infty}\mathrm{Pr}(m|N)\frac{\gamma(2N+1)m}{N}$$
$$= \frac{N}{2N+1}\gamma_{N}, \qquad (6.38)$$

$$\gamma\,\mathrm{Tr}\left[\sigma_{\mathrm{th}}b_{n}b_{n}^{\dagger}\right] = \gamma\sum_{m=0}^{\infty}\mathrm{Pr}(m|N)(m+1) = \frac{N+1}{2N+1}\sum_{m=0}^{\infty}\mathrm{Pr}(m|N)\frac{\gamma(2N+1)(m+1)}{N+1}$$
$$= \frac{N+1}{2N+1}\gamma_{N}, \qquad (6.39)$$

where

$$\mathrm{Pr}(m|N) = \frac{1}{N+1}\left(\frac{N}{N+1}\right)^{m} \qquad (6.40)$$

is the thermal probability for m photons given mean number N and

$$\gamma_{N} := (2N+1)\gamma \qquad (6.41)$$

is a rescaled interaction strength. The terms have been written so as to suggest the following: absorption occurs with overall probability $N/(2N+1)$ and effective interaction strength $\gamma(2N+1)m/N$, which depends on the number of photons m in the field mode, and emission occurs with probability $(N+1)/(2N+1)$ and effective interaction strength $\gamma(2N+1)(m+1)/(N+1)$. The absorption and emission probabilities are, respectively, proportional to the absorption and total (spontaneous plus stimulated) emission rates given by the Einstein A and B coefficients for a collection of two-level atoms in thermal equilibrium with an optical cavity at temperature T [96, section 1.2.2]. Since $\langle m \rangle = N$, both of the effective interaction strengths average to the rescaled interaction strength γ_{N}. This is what allows us to replace the effective interaction strengths by their average and pretend that only two bath levels undergo absorption and emission.

It is worth noting here what happens if we measure the rotated quadrature component $X(\varphi)$ of equation (5.32) instead of $X = \sigma_{x}$, i.e., if we measure in the basis of equation (5.33). The Kraus operators become

$$K_{\pm g} = \sqrt{\frac{N+1}{2N+1}}\langle\phi_{\pm}(\varphi)|U_{\mathrm{th},I}|g\rangle = \frac{1}{\sqrt{2}}\sqrt{\frac{N+1}{2N+1}}\left(\mathbf{1} \pm \sqrt{\Delta\tau}\,\sqrt{2N+1}\,e^{i\varphi}c - \frac{1}{2}\Delta\tau(2N+1)c^{\dagger}c\right), \quad (6.42)$$

$$K_{\pm e} = \sqrt{\frac{N}{2N+1}} \langle \phi_{\pm}(\varphi)|U_{\mathrm{th},I}|e\rangle = \pm \frac{e^{i\varphi}}{\sqrt{2}} \sqrt{\frac{N}{2N+1}} \left(\mathbf{1} \mp \sqrt{\Delta\tau} \ \sqrt{2N+1} \ e^{-i\varphi}c^{\dagger} - \frac{1}{2}\Delta\tau(2N+1)cc^{\dagger} \right).$$
(6.43)

The $\pm e^{i\varphi}$ at the head of the expression for $K_{\pm e}$ can be ignored, since a Kraus operator always appears in combination with its adjoint. Thus all the results for homodyne measurement of $X(\varphi)$ follow from those for homodyne measurement of σ_x by replacing c by $e^{i\varphi}c$. In particular, the difference equation and the limiting SME are given by

$$\Delta\rho_{\pm} = \Delta\tau\big((N+1)\mathcal{D}[c]\rho + N\mathcal{D}[c^{\dagger}]\rho\big) + \frac{\Delta\mathcal{I}_H}{\sqrt{2N+1}}\mathcal{H}[(N+1)e^{i\varphi}c - Ne^{-i\varphi}c^{\dagger}]\rho,$$
(6.44)

$$d\rho = dt\big((N+1)\mathcal{D}[\sqrt{\gamma}\,c]\rho + N\mathcal{D}[\sqrt{\gamma}\,c^{\dagger}]\rho\big) + \frac{dW}{\sqrt{2N+1}}\mathcal{H}[(N+1)\sqrt{\gamma}\,e^{i\varphi}c - N\sqrt{\gamma}\,e^{-i\varphi}c^{\dagger}]\rho.$$
(6.45)

6.5. Pure and thermal squeezed states

When we turn our attention to squeezed baths, the use of qubit probes immediately presents a new challenge. This comes from the obvious fact that if we choose $a \propto \sigma_-$, as in all previous work in this paper, the second moment that quantifies squeezing, $\langle \Delta A_n^2 \rangle_{\mathrm{sq}} = M\Delta\tau$, cannot be nonzero for any choice of qubit-probe state since $\sigma_-^2 = 0$. To surmount this obstacle, it is clear that we should make a different choice for a; fortunately, once one has formulated the problem properly, the right choice becomes obvious, although it has not been considered previously.

To see how to proceed, consider first the case of field modes in pure squeezed vacuum,

$$|\phi_{\mathrm{sq}}\rangle := S(r, \mu)|\mathrm{vac}\rangle,$$
(6.46)

which is generated from vacuum by the *squeeze operator*,

$$S(r, \mu) := \exp\left[\frac{1}{2}r(e^{-2i\mu}b^2 - e^{2i\mu}b^{\dagger 2})\right].$$
(6.47)

The squeeze operator conjugates the field annihilation operator b according to

$$S^{\dagger}(r, \mu)\,b\,S(r, \mu) = b\cosh r - e^{2i\mu}b^{\dagger}\sinh r =: b_{\mathrm{sq}},$$
(6.48)

yielding new field operators b_{sq}. Using this transformation, it is easy to see that $\langle b\rangle_{\mathrm{sq}} = \langle b_{\mathrm{sq}}\rangle_{\mathrm{vac}} = 0$ and

$$N = \langle b^{\dagger}b\rangle_{\mathrm{sq}} = \langle b_{\mathrm{sq}}^{\dagger}b_{\mathrm{sq}}\rangle_{\mathrm{vac}} = \sinh^2 r,$$
(6.49)

$$M = \langle b^2\rangle_{\mathrm{sq}} = \langle b_{\mathrm{sq}}^2\rangle_{\mathrm{vac}} = -e^{2i\mu}\sinh r\cosh r.$$
(6.50)

We stress that for all our results on a pure squeezed bath, equations (6.49) and (6.50) are the expressions we use to relate the squeezing parameters r and μ to the bath parameters N and M of (6.5). Notice that for this case of pure squeezed bath, the inequality (6.3) is saturated. In this subsection, we find it useful to let $M_R = (M + M^*)/2$ and $M_I = -i(M - M^*)/2$ denote the real and imaginary parts of M.

The transformation (6.48) is the key to translating from field modes to qubits. What the transformation allows us to do is to model squeezed noise in terms of vacuum noise that has a quadrature-dependent coupling to the system. In this section, we again focus on homodyne measurements of the probe; just as for thermal states, this is because of the infinite photon intensity of the infinitely broadband squeezed states we are considering. As part of the overall transformation, the homodyne measurement is also transformed to measurement of another observable. The transformation and the translation from field modes to qubits are depicted and described in detail in terms of circuits in figure 12.

The conclusion is that we can model squeezed noise in terms of qubits by starting the probe in the ground state $|g\rangle$ and having it interact with the system via an interaction unitary obtained from equation (6.11) by substituting

$$a_{\mathrm{sq}} := \sigma_-\cosh r - e^{2i\mu}\sigma_+\sinh r$$
$$= \frac{\cosh r - e^{2i\mu}\sinh r}{2}\sigma_x - i\frac{\cosh r + e^{2i\mu}\sinh r}{2}\sigma_y$$
(6.51)

in place of a. The resulting interaction unitary is

$$U_{\mathrm{sq},I} = \mathbf{1}\otimes\mathbf{1} + \sqrt{\Delta\tau}\,(c\otimes a_{\mathrm{sq}}^{\dagger} - c^{\dagger}\otimes a_{\mathrm{sq}}) + \frac{1}{2}\Delta\tau(c\otimes a_{\mathrm{sq}}^{\dagger} - c^{\dagger}\otimes a_{\mathrm{sq}})^2$$
$$= \mathbf{1}\otimes\mathbf{1} + \sqrt{\Delta\tau}\,(c_{\mathrm{sq}}\otimes\sigma_+ - c_{\mathrm{sq}}^{\dagger}\otimes\sigma_-) + \frac{1}{2}\Delta\tau(c_{\mathrm{sq}}\otimes\sigma_+ - c_{\mathrm{sq}}^{\dagger}\otimes\sigma_-)^2,$$
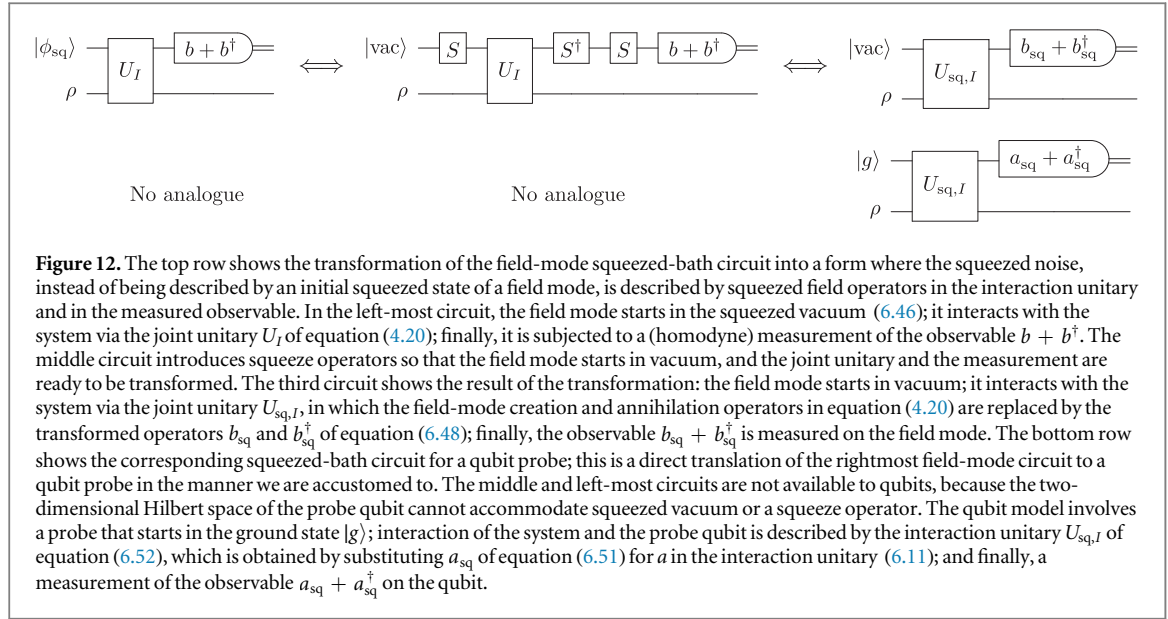(6.52)

Figure 12. The top row shows the transformation of the field-mode squeezed-bath circuit into a form where the squeezed noise, instead of being described by an initial squeezed state of a field mode, is described by squeezed field operators in the interaction unitary and in the measured observable. In the left-most circuit, the field mode starts in the squeezed vacuum (6.46); it interacts with the system via the joint unitary U_I of equation (4.20); finally, it is subjected to a (homodyne) measurement of the observable $b + b^\dagger$. The middle circuit introduces squeeze operators so that the field mode starts in vacuum, and the joint unitary and the measurement are ready to be transformed. The third circuit shows the result of the transformation: the field mode starts in vacuum; it interacts with the system via the joint unitary $U_{\mathrm{sq},I}$, in which the field-mode creation and annihilation operators in equation (4.20) are replaced by the transformed operators b_{sq} and $b_{\mathrm{sq}}^\dagger$ of equation (6.48); finally, the observable $b_{\mathrm{sq}} + b_{\mathrm{sq}}^\dagger$ is measured on the field mode. The bottom row shows the corresponding squeezed-bath circuit for a qubit probe; this is a direct translation of the rightmost field-mode circuit to a qubit probe in the manner we are accustomed to. The middle and left-most circuits are not available to qubits, because the two-dimensional Hilbert space of the probe qubit cannot accommodate squeezed vacuum or a squeeze operator. The qubit model involves a probe that starts in the ground state $|g\rangle$; interaction of the system and the probe qubit is described by the interaction unitary $U_{\mathrm{sq},I}$ of equation (6.52), which is obtained by substituting a_{sq} of equation (6.51) for a in the interaction unitary (6.11); and finally, a measurement of the observable $a_{\mathrm{sq}} + a_{\mathrm{sq}}^\dagger$ on the qubit.

where

$$c_{\mathrm{sq}} := c \cosh r + e^{2i\mu} c^\dagger \sinh r \qquad (6.53)$$

is a species of squeezed system operator.

The qubit operators reproduce the general pure state, but zero-mean-field Gaussian bath statistics for $\Delta A_{\mathrm{sq}} = \sqrt{\Delta \tau}\, a_{\mathrm{sq}}$:

$$\langle \Delta A_{\mathrm{sq}} \rangle_g = 0, \qquad (6.54a)$$

$$\langle \Delta A_{\mathrm{sq}}^\dagger \Delta A_{\mathrm{sq}} \rangle_g = \sinh^2 r\, \Delta \tau = N\, \Delta \tau, \qquad (6.54b)$$

$$\langle \Delta A_{\mathrm{sq}}^2 \rangle_g = -e^{2i\mu} \sinh r \cosh r\, \Delta \tau = M\, \Delta \tau, \qquad (6.54c)$$

$$\langle [\Delta A_{\mathrm{sq}}, \Delta A_{\mathrm{sq}}^\dagger] \rangle_g = \Delta \tau. \qquad (6.54d)$$

Thus we know that the qubit model generates the desired unconditional system evolution.

A helpful way to think about this transformation is as a modification of the coupling of the system to the bath. Just as for thermal states, where we were able to make up for a limited number of excitations in the bath by increasing the interaction strength, here we compensate for the limitation that the qubit ground state has equal uncertainties in σ_x and σ_y by modifying the originally symmetric coupling to $a = \sigma_- = (\sigma_x - i\sigma_y)/2$ to the asymmetric 'squeezed' coupling embodied in the operator a_{sq} of equation (6.51). One sees the effect of the coupling strengths most plainly when $\mu = 0$, in which case $a_{\mathrm{sq}} = (\sigma_x e^{-r} - i\sigma_y e^r)/2$; i.e., the coupling of σ_x to the system is reduced by the squeeze factor e^{-r}, and the coupling of σ_y is increased by the same factor. The change in coupling strengths is not the only twist, however. The Pauli operators $\sigma_x = X$ and $\sigma_y = Y$ are transformed under the squeezing transformation into

$$X_{\mathrm{sq}} := a_{\mathrm{sq}} + a_{\mathrm{sq}}^\dagger = \sigma_x(\cosh r - \cos 2\mu \sinh r) + \sigma_y \sin 2\mu \sinh r, \qquad (6.55)$$

$$Y_{\mathrm{sq}} := i a_{\mathrm{sq}} - i a_{\mathrm{sq}}^\dagger = \sigma_x \sin 2\mu \sinh r + \sigma_y(\cosh r + \cos 2\mu \sinh r). \qquad (6.56)$$

These operators have the same commutator as σ_x and σ_y, i.e., $[X_{\mathrm{sq}}, Y_{\mathrm{sq}}] = [\sigma_x, \sigma_y] = 2i\sigma_z$, but unlike σ_x and σ_y, they are correlated in vacuum when $\sin 2\mu \neq 0$:

$$\left\langle \tfrac{1}{2}(X_{\mathrm{sq}} Y_{\mathrm{sq}} + Y_{\mathrm{sq}} X_{\mathrm{sq}}) \right\rangle_{\mathrm{vac}} = 2 \sin 2\mu \sinh r \cosh r = -2M_I. \qquad (6.57)$$

This vacuum correlation is how our qubit model captures the correlation between quadrature components in the squeezed state of a field mode.

As mentioned above, we focus on homodyne detection, which in our transformed and translated scheme, corresponds to measuring the observable X_{sq} of equation (6.55), but X_{sq} is not a normalized spin component. We can, however, write X_{sq} as

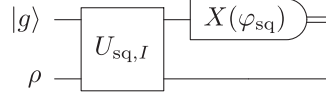$$X_{\mathrm{sq}} = \sqrt{L}\, X(\varphi_{\mathrm{sq}}), \qquad (6.58)$$

Figure 13. Final qubit circuit for pure squeezed noise and a homodyne measurement of σ_x. In our model of this situation, the probe, initially in the ground state $|g\rangle$, interacts with the system via the unitary $U_{\mathrm{sq},I}$ of equation (6.52) and then is subjected to a measurement of the spin component $X(\varphi_{\mathrm{sq}})$. This model is identical to that of figure 12 except that the measurement of $a_{\mathrm{sq}} + a_{\mathrm{sq}}^\dagger = \sqrt{L}\, X(\varphi_{\mathrm{sq}})$ is replaced by the equivalent measurement of $X(\varphi_{\mathrm{sq}})$.

where

$$L := 1 + 2\sinh^2 r - 2\cos 2\mu\, \sinh r \cosh r \tag{6.59}$$

and $X(\varphi_{\mathrm{sq}})$ is the normalized spin component of equation (5.32), with the phase angle defined by

$$e^{i\varphi_{\mathrm{sq}}} := \frac{\cosh r - e^{-2i\mu}\sinh r}{\sqrt{L}}. \tag{6.60}$$

Since the factor $\sqrt{L}$ in X_{sq} changes only the eigenvalues, not the eigenvectors of the measured observable, we can say that we are measuring the spin component $X(\varphi_{\mathrm{sq}})$, instead of $a_{\mathrm{sq}} + a_{\mathrm{sq}}^\dagger$; either way, we are measuring in the basis $|\phi_\pm(\varphi_{\mathrm{sq}})\rangle$. Making this change brings our qubit model for homodyne measurement on pure squeezed noise into its final form, depicted in figure 13.

The qubit model is now identical to the vacuum qubit model for measurement of an arbitrary spin component, so we can obtain the results for the present case by appropriating the results for vacuum homodyning, replacing c with c_{sq} of equation (6.53) and choosing the homodyne angle to be φ_{sq} of equation (6.60). Formulas helpful in making this replacement are given in appendix A. The resulting Kraus operators are

$$
\begin{aligned}
K_\pm &= \langle\phi_\pm(\varphi_{\mathrm{sq}})|U_{\mathrm{sq},I}|g\rangle \\
&= \frac{1}{\sqrt{2}}\Big(\mathbf{1} \pm \sqrt{\Delta\tau}\, e^{i\varphi_{\mathrm{sq}}} c_{\mathrm{sq}} - \tfrac{1}{2}\Delta\tau\, c_{\mathrm{sq}}^\dagger c_{\mathrm{sq}}\Big) \\
&= \frac{1}{\sqrt{2}}\Big(\mathbf{1} \pm \frac{\sqrt{\Delta\tau}}{\sqrt{L}}((N + M^* + 1)c - (N + M)c^\dagger) - \tfrac{1}{2}\Delta\tau((N+1)c^\dagger c + Ncc^\dagger - M^*c^2 - Mc^{\dagger\,2})\Big),
\end{aligned}
\tag{6.61}
$$

with corresponding POVM elements

$$E_\pm = K_\pm^\dagger K_\pm = \frac{1}{2}\Big(\mathbf{1} \pm \frac{\sqrt{\Delta\tau}}{\sqrt{L}}(c + c^\dagger)\Big). \tag{6.62}$$

Likewise, the conditional difference equation is

$$
\begin{aligned}
\Delta\rho_\pm &= \Delta\tau\, \mathcal{D}[c_{\mathrm{sq}}]\rho + \Delta\mathcal{I}_H\mathcal{H}[e^{i\varphi_{\mathrm{sq}}}c_{\mathrm{sq}}]\rho \\
&= \Delta\tau\Big((N+1)\mathcal{D}[c]\rho + N\mathcal{D}[c^\dagger]\rho + \tfrac{1}{2}M^*[c,[c,\rho]] + \tfrac{1}{2}M[c^\dagger,[c^\dagger,\rho]]\Big) \\
&\quad + \frac{\Delta\mathcal{I}_H}{\sqrt{L}}\mathcal{H}[(N+M^*+1)c - (N+M)c^\dagger]\rho,
\end{aligned}
\tag{6.63}
$$

and the SME is

$$d\rho = dt\,\mathcal{D}[\sqrt{\gamma}\, c_{\mathrm{sq}}]\rho + dW\,\mathcal{H}[\sqrt{\gamma}\, c_{\mathrm{sq}}\, e^{i\varphi_{\mathrm{sq}}}]\rho, \tag{6.64}$$

which becomes

$$
\begin{aligned}
d\rho &= dt\Big((N+1)\mathcal{D}[\sqrt{\gamma}\, c]\rho + N\mathcal{D}[\sqrt{\gamma}\, c^\dagger]\rho + \tfrac{1}{2}M^*[\sqrt{\gamma}\, c,[\sqrt{\gamma}\, c,\rho]] + \tfrac{1}{2}M[\sqrt{\gamma}\, c^\dagger,[\sqrt{\gamma}\, c^\dagger,\rho]]\Big) \\
&\quad + \frac{dW}{\sqrt{L}}\mathcal{H}[(N+M^*+1)\sqrt{\gamma}\, c - (N+M)\sqrt{\gamma}\, c^\dagger]\rho.
\end{aligned}
\tag{6.65}
$$

This SME is presented as equations 4.253 and 4.254 in [66]; see also section 4.4.1 of Wiseman's thesis [63].

Generalizing to a squeezed thermal bath for a field mode, for which the inequality (6.3) is not saturated, proceeds by representing a squeezed thermal bath as a thermal state (6.25) to which the squeeze operator (6.47) has been applied:
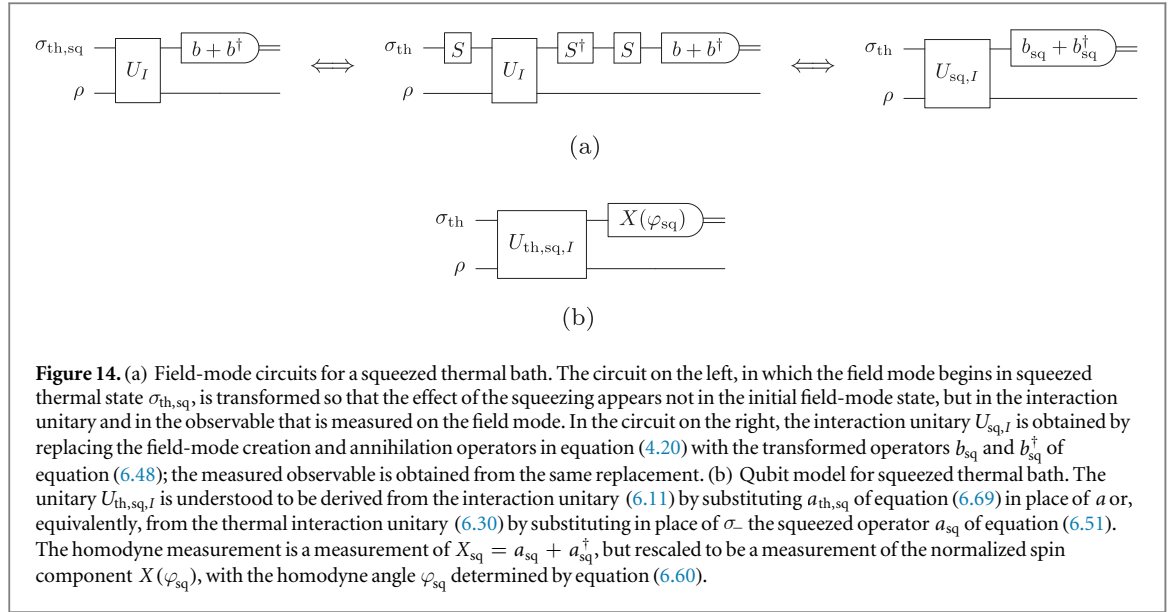
Figure 14. (a) Field-mode circuits for a squeezed thermal bath. The circuit on the left, in which the field mode begins in squeezed thermal state $\sigma_{\text{th,sq}}$, is transformed so that the effect of the squeezing appears not in the initial field-mode state, but in the interaction unitary and in the observable that is measured on the field mode. In the circuit on the right, the interaction unitary $U_{\text{sq},I}$ is obtained by replacing the field-mode creation and annihilation operators in equation (4.20) with the transformed operators b_{sq} and $b_{\text{sq}}^\dagger$ of equation (6.48); the measured observable is obtained from the same replacement. (b) Qubit model for squeezed thermal bath. The unitary $U_{\text{th,sq},I}$ is understood to be derived from the interaction unitary (6.11) by substituting $a_{\text{th,sq}}$ of equation (6.69) in place of a or, equivalently, from the thermal interaction unitary (6.30) by substituting in place of σ_- the squeezed operator a_{sq} of equation (6.51). The homodyne measurement is a measurement of $X_{\text{sq}} = a_{\text{sq}} + a_{\text{sq}}^\dagger$, but rescaled to be a measurement of the normalized spin component $X(\varphi_{\text{sq}})$, with the homodyne angle φ_{sq} determined by equation (6.60).

$$\sigma_{\text{th,sq}} = S(r, \mu)\sigma_{\text{th}}S^\dagger(r, \mu). \tag{6.66}$$

For this squeezed thermal state, the bath parameters N and M are functions both of the squeezing parameters r and μ and of the 'thermal excitation number' N_{th}:

$$N_{\text{th}} := \langle b_n^\dagger b_n \rangle_{\text{th}}, \tag{6.67a}$$

$$N = \langle b^\dagger b \rangle_{\text{th,sq}} = \langle b_{\text{sq}}^\dagger b_{\text{sq}} \rangle_{\text{th}} = (2N_{\text{th}} + 1)\sinh^2 r + N_{\text{th}}, \tag{6.67b}$$

$$M = \langle b^2 \rangle_{\text{th,sq}} = \langle b_{\text{sq}}^2 \rangle_{\text{th}} = -(2N_{\text{th}} + 1)e^{2i\mu}\sinh r \cosh r. \tag{6.67c}$$

Making this squeezed thermal state the initial state of the field mode gives the circuit for a squeezed thermal bath. Transforming the squeezing to appear not in the initial state, but in the interaction unitary and the homodyne measurement, is the same as for a squeezed-vacuum input and is depicted in figure 14(a). We emphasize that for the case of squeezed thermal bath, equations (6.67) are the expressions we use to derive the bath parameters N and M from the thermal parameter N_{th} and squeezing parameters r and μ.

We need only to combine our work on thermal baths and pure squeezed baths to translate the rightmost circuit in figure 14(a) to a qubit probe. The result of the translation is depicted in figure 14(b). The initial state of the probe qubit is the thermal state (6.27), now written as

$$\sigma_{\text{th}} = \frac{N_{\text{th}} + 1}{2N_{\text{th}} + 1}|g\rangle\langle g| + \frac{N_{\text{th}}}{2N_{\text{th}} + 1}|e\rangle\langle e|. \tag{6.68}$$

The interaction unitary U_I is translated by letting a in equation (6.11) be the squeezed annihilation operator (6.51), further modified by being rescaled by the thermal coupling factor $\sqrt{2N_{\text{th}} + 1}$, i.e., $\Delta A_{\text{th,sq}} = \sqrt{\Delta\tau}\, a_{\text{th,sq}}$, where

$$a_{\text{th,sq}} := \sqrt{2N_{\text{th}} + 1}\, a_{\text{sq}} = \sqrt{2N_{\text{th}} + 1}\,(\sigma_-\cosh r - e^{2i\mu}\sigma_+\sinh r). \tag{6.69}$$

The resulting interaction unitary is

$$
\begin{aligned}
U_{\text{th,sq},I} &= \mathbf{1} \otimes \mathbf{1} + \sqrt{2N_{\text{th}} + 1}\sqrt{\Delta\tau}\,(c \otimes a_{\text{sq}}^\dagger - c^\dagger \otimes a_{\text{sq}}) + \frac{1}{2}(2N_{\text{th}} + 1)\Delta\tau(c \otimes a_{\text{sq}}^\dagger - c^\dagger \otimes a_{\text{sq}})^2 \\
&= \mathbf{1} \otimes \mathbf{1} + \sqrt{2N_{\text{th}} + 1}\sqrt{\Delta\tau}\,(c_{\text{sq}} \otimes \sigma_+ - c_{\text{sq}}^\dagger \otimes \sigma_-) + \frac{1}{2}(2N_{\text{th}} + 1)\Delta\tau(c_{\text{sq}} \otimes \sigma_+ - c_{\text{sq}}^\dagger \otimes \sigma_-)^2,
\end{aligned}
\tag{6.70}
$$

where c_{sq} is the squeezed system operator of equation (6.53). The homodyne measurement of σ_x is transformed to a measurement of $a_{\text{sq}} + a_{\text{sq}}^\dagger = \sqrt{L}X(\varphi_{\text{sq}})$; as we discussed previously for a pure squeezed bath, we can regard this as a measurement of the normalized spin component $X(\varphi_{\text{sq}})$, with the phase angle defined by equation (6.60).

The qubit operators $\Delta A_{\text{th,sq}} = \sqrt{\Delta\tau}\, a_{\text{th,sq}}$ reproduce the general, but zero-mean-field Gaussian bath statistics:

$$\langle \Delta A_{\text{th,sq}} \rangle_{\text{th}} = 0, \tag{6.71a}$$

$$\langle \Delta A_{\mathrm{th,sq}}^{\dagger} \Delta A_{\mathrm{th,sq}} \rangle_{\mathrm{th}} = [(2N_{\mathrm{th}} + 1)\sinh^2 r + N_{\mathrm{th}}]\Delta\tau = N\,\Delta\tau, \tag{6.71b}$$

$$\langle \Delta A_{\mathrm{sq}}^{2} \rangle_{\mathrm{th}} = -(2N_{\mathrm{th}} + 1)e^{2i\mu}\sinh r \cosh r\,\Delta\tau = M\,\Delta\tau, \tag{6.71c}$$

$$\langle [\Delta A_{\mathrm{sq}}, \Delta A_{\mathrm{sq}}^{\dagger}] \rangle_{\mathrm{th}} = \Delta\tau. \tag{6.71d}$$

For the conditional evolution we note that the circuit in figure 14(b) is the same as that for a thermal probe with no squeezing, subjected to a homodyne measurement specified by the angle φ_{sq} of equation (6.60), and with the system operator c replaced by the squeezed system operator c_{sq} of equation (6.53). In particular, just as the thermal bath with no squeezing has the two pairs of Kraus operators in equation (6.42), the squeezed thermal bath gives the two pairs of Kraus operators,

$$\begin{aligned}
K_{\pm g} &= \sqrt{\frac{N_{\mathrm{th}} + 1}{2N_{\mathrm{th}} + 1}}\,\langle\phi_{\pm}(\varphi_{\mathrm{sq}})|U_{\mathrm{th,sq},I}|g\rangle \\
&= \frac{1}{\sqrt{2}}\sqrt{\frac{N_{\mathrm{th}} + 1}{2N_{\mathrm{th}} + 1}}\left(\mathbf{1} \pm \sqrt{\Delta\tau}\,\sqrt{2N_{\mathrm{th}} + 1}\,e^{i\varphi_{\mathrm{sq}}}c_{\mathrm{sq}} - \frac{1}{2}\Delta\tau(2N_{\mathrm{th}} + 1)c_{\mathrm{sq}}^{\dagger}c_{\mathrm{sq}}\right) \\
&= \frac{1}{\sqrt{2}}\sqrt{\frac{N_{\mathrm{th}} + 1}{2N_{\mathrm{th}} + 1}}\left(\mathbf{1} \pm \frac{\sqrt{\Delta\tau}}{\sqrt{L'}}\left((N + N_{\mathrm{th}} + M^* + 1)c - (N - N_{\mathrm{th}} + M)c^{\dagger}\right)\right. \\
&\qquad\qquad \left. - \frac{1}{2}\Delta\tau\left((N + N_{\mathrm{th}} + 1)c^{\dagger}c + (N - N_{\mathrm{th}})cc^{\dagger} - M^*c^2 - Mc^{\dagger 2}\right)\right),
\end{aligned} \tag{6.72}$$

$$\begin{aligned}
K_{\pm e} &= \sqrt{\frac{N_{\mathrm{th}}}{2N_{\mathrm{th}} + 1}}\,\langle\phi_{\pm}(\varphi_{\mathrm{sq}})|U_{\mathrm{th,sq},I}|e\rangle \\
&= \pm\frac{e^{i\varphi_{\mathrm{sq}}}}{\sqrt{2}}\sqrt{\frac{N_{\mathrm{th}}}{2N_{\mathrm{th}} + 1}}\left(\mathbf{1} \mp \sqrt{\Delta\tau}\,\sqrt{2N_{\mathrm{th}} + 1}\,e^{-i\varphi_{\mathrm{sq}}}c_{\mathrm{sq}}^{\dagger} - \frac{1}{2}\Delta\tau(2N_{\mathrm{th}} + 1)c_{\mathrm{sq}}c_{\mathrm{sq}}^{\dagger}\right) \\
&= \pm\frac{e^{i\varphi_{\mathrm{sq}}}}{\sqrt{2}}\sqrt{\frac{N_{\mathrm{th}}}{2N_{\mathrm{th}} + 1}}\left(\mathbf{1} \pm \frac{\sqrt{\Delta\tau}}{\sqrt{L'}}\left((N - N_{\mathrm{th}} + M^*)c - (N + N_{\mathrm{th}} + M + 1)c^{\dagger}\right)\right. \\
&\qquad\qquad \left. - \frac{1}{2}\Delta\tau\left((N + N_{\mathrm{th}} + 1)cc^{\dagger} + (N - N_{\mathrm{th}})c^{\dagger}c - M^*c^2 - Mc^{\dagger 2}\right)\right).
\end{aligned} \tag{6.73}$$

The corresponding POVM elements for the measurement outcomes $\pm$ are

$$E_{\pm} := K_{\pm g}^{\dagger}K_{\pm g} + K_{\pm e}^{\dagger}K_{\pm e} = \frac{1}{2}\left(\mathbf{1} \pm \frac{\sqrt{\Delta\tau}}{\sqrt{L'}}(c + c^{\dagger})\right). \tag{6.74}$$

In these results we introduce

$$L' := (2N_{\mathrm{th}} + 1)L = (2N_{\mathrm{th}} + 1)(1 + 2\sinh^2 r - 2\cos 2\mu\,\sinh r \cosh r) = 2N + 2M_R + 1 \tag{6.75}$$
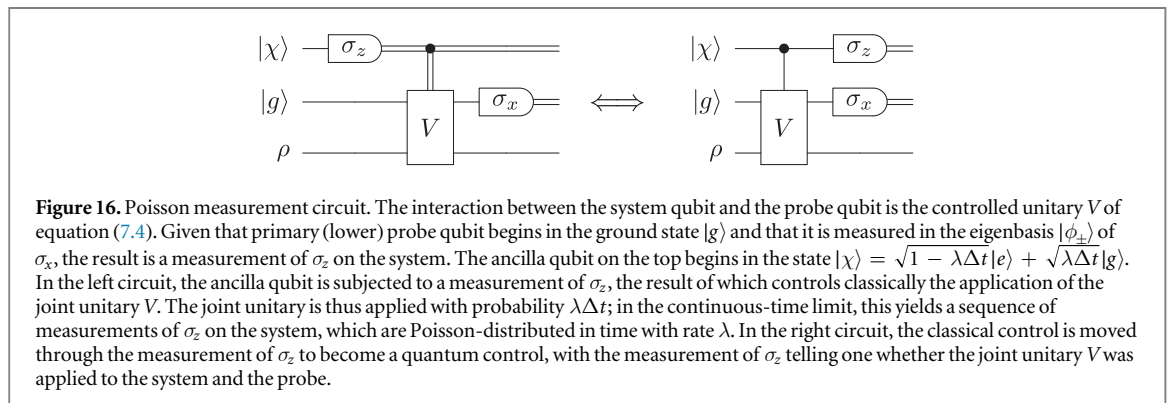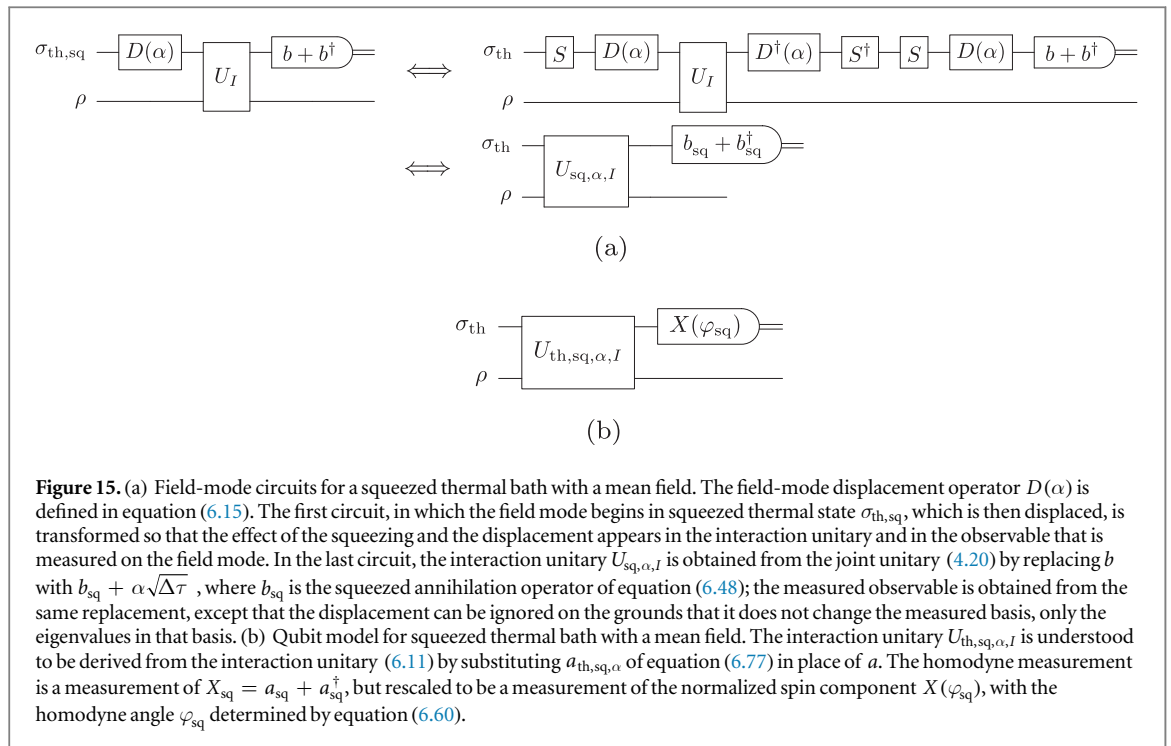
(see equations (A4) and (A5)).

Updating the system state to find the conditional difference equation is done using equation (6.33), with the result

$$\begin{aligned}
\Delta\rho_{\pm} &= \Delta\tau\left((N_{\mathrm{th}} + 1)\mathcal{D}[c_{\mathrm{sq}}]\rho + N_{\mathrm{th}}\mathcal{D}[c_{\mathrm{sq}}^{\dagger}]\rho\right) + \frac{\Delta\mathcal{I}_H}{\sqrt{2N_{\mathrm{th}} + 1}}\mathcal{H}[(N_{\mathrm{th}} + 1)e^{i\varphi_{\mathrm{sq}}}c_{\mathrm{sq}} - N_{\mathrm{th}}e^{-i\varphi_{\mathrm{sq}}}c_{\mathrm{sq}}^{\dagger}]\rho \\
&= \Delta\tau\left((N + 1)\mathcal{D}[c]\rho + N\mathcal{D}[c^{\dagger}]\rho + \frac{1}{2}M^*[c, [c, \rho]] + \frac{1}{2}M[c^{\dagger}, [c^{\dagger}, \rho]]\right) \\
&\quad + \frac{\Delta\mathcal{I}_H}{\sqrt{L'}}\mathcal{H}[(N + M^* + 1)c - (N + M)c^{\dagger}]\rho.
\end{aligned} \tag{6.76}$$

The final result is identical to that given in equation (6.63) for the case of a pure squeezed bath (since $L' = 2N + M_R + 1$, which is what L is in the case of pure squeezed bath), except that now N and M need only satisfy the inequality (6.3), rather than saturating it. This means that the corresponding SME has the form of equation (6.65), but with L replaced by L'. Notice that in the final form of the difference equation and the SME, all explicit reference to N_{th} disappears, whereas the Kraus operators do depend explicitly on N_{th}; this is because the Kraus operators involve projections onto the two possible initial states, $|g\rangle$ and $|e\rangle$, of the probe qubit, whereas the difference equation and the SME only involve appropriate averages over these two possibilities.

The case of a squeezed thermal bath is nearly the most general case of a Gaussian bath, with pure-squeezed and unsqueezed-thermal baths emerging as special cases. The only thing unaccounted for in the squeezed-thermal case is a mean field. It is easy to add a mean field to the current paradigm; the procedure for doing so is sketched in figure 15. The key point is to modify the interaction unitary (6.11) by replacing a with the operator

Figure 15. (a) Field-mode circuits for a squeezed thermal bath with a mean field. The field-mode displacement operator $D(\alpha)$ is defined in equation (6.15). The first circuit, in which the field mode begins in squeezed thermal state $\sigma_{th,sq}$, which is then displaced, is transformed so that the effect of the squeezing and the displacement appears in the interaction unitary and in the observable that is measured on the field mode. In the last circuit, the interaction unitary $U_{sq,\alpha,I}$ is obtained from the joint unitary (4.20) by replacing b with $b_{sq} + \alpha\sqrt{\Delta\tau}$, where b_{sq} is the squeezed annihilation operator of equation (6.48); the measured observable is obtained from the same replacement, except that the displacement can be ignored on the grounds that it does not change the measured basis, only the eigenvalues in that basis. (b) Qubit model for squeezed thermal bath with a mean field. The interaction unitary $U_{th,sq,\alpha,I}$ is understood to be derived from the interaction unitary (6.11) by substituting $a_{th,sq,\alpha}$ of equation (6.77) in place of a. The homodyne measurement is a measurement of $X_{sq} = a_{sq} + a_{sq}^{\dagger}$, but rescaled to be a measurement of the normalized spin component $X(\varphi_{sq})$, with the homodyne angle φ_{sq} determined by equation (6.60).

Figure 16. Poisson measurement circuit. The interaction between the system qubit and the probe qubit is the controlled unitary V of equation (7.4). Given that primary (lower) probe qubit begins in the ground state $|g\rangle$ and that it is measured in the eigenbasis $|\phi_\pm\rangle$ of σ_x, the result is a measurement of σ_z on the system. The ancilla qubit on the top begins in the state $|\chi\rangle = \sqrt{1 - \lambda\Delta t}|e\rangle + \sqrt{\lambda\Delta t}|g\rangle$. In the left circuit, the ancilla qubit is subjected to a measurement of σ_z, the result of which controls classically the application of the joint unitary V. The joint unitary is thus applied with probability $\lambda\Delta t$; in the continuous-time limit, this yields a sequence of measurements of σ_z on the system, which are Poisson-distributed in time with rate λ. In the right circuit, the classical control is moved through the measurement of σ_z to become a quantum control, with the measurement of σ_z telling one whether the joint unitary V was applied to the system and the probe.

$$a_{th,sq,\alpha} := a_{th,sq} + \alpha\sqrt{\Delta\tau}\ \mathbb{1} = \sqrt{2N_{th} + 1}\,(\sigma_- \cosh r - e^{2i\mu}\sigma_+ \sinh r) + \alpha\sqrt{\Delta\tau}\ \mathbb{1}. \qquad (6.77)$$

The effect of this is to add to the interaction unitary (6.70) the additional term $\Delta\tau(\alpha^* c - \alpha c^\dagger)$. When this interaction unitary evolves a density operator ρ, the additional term leads to a commutator, $\Delta\tau[\alpha^* c - \alpha c^\dagger, \rho]$, which is, of course, just the commutator that describes the mean-field evolution in the difference equation; it becomes the mean-field commutator $dt\,[\beta^*\sqrt{\gamma}\,c - \beta\sqrt{\gamma}\,c^\dagger, \rho]$ in the SME. The mean-field terms appear only in the deterministic part of the SME and do not affect the conditional evolution.

Perhaps as interesting as the success of the qubit technique we develop here is the failure of a variety of other techniques, which generally are unable to capture the conditional SME correctly. A sampling of these other techniques, which typically involve either more than one probe qubit in each time segment or probes with more than two levels, is discussed in appendix B.

7. Strong interactions at random times

In this section, we consider a different variety of continuous measurement. Instead of probing the system with a continuous stream of weakly interacting probes, we take inspiration from [97] and send a sequence of strongly interacting probes distributed randomly in time. We show that this technique for 'diluting' sequential interactions, i.e., by making the interactions occur less frequently as opposed to more weakly, bears some resemblance to the cases discussed before, but ultimately yields an inequivalent trajectory picture. A slight

variation on the dilution scheme is seen, however, to provide an interpretation of inefficient detection equivalent to the commonly employed model of attenuating the field incident on a photodetector with a beamsplitter.

Probe dilution generalizes section 5 by considering a qualitatively different interaction, while fixing an initial probe state, and thus complements the generalization carried out in section 6, where the focus was on varying the initial probe state. The probabilistic interaction of a single qubit probe during a time interval Δt can be modeled as a joint unitary interaction (not necessarily weak) between the system and the probe that is controlled off an ancilla qubit; this interaction is followed by strong measurements of the primary probe and the ancilla, as illustrated in figure 16. Measurement of the ancilla determines if the interaction between the system and the probe occurred or not; thus, depending on the result of the ancilla measurement, the probe measurement might or might not reveal information about the system. By choosing the state of the ancilla so that the probability of the interaction occurring is $\lambda \Delta t$, the continuous limit can be thought of as a long sequence of single-shot measurements occurring at Poisson-distributed times with constant rate λ.

The probe/system interaction we consider is generated by an interaction Hamiltonian of the form (4.16), except that we convert to qubit probes by making the standard replacement $b_n \rightarrow \sigma_-$. To achieve strong interactions, we now allow Δt to be as large as or even larger than $1/\gamma$. A glance at the derivation of the interaction Hamiltonian (4.16) in section 4 shows that for such strong interactions, we cannot neglect the sideband modes in each time segment. Thus we cannot consistently use such a strong interaction in the case of a probe field, but instead should think of the interaction as coming directly from the interaction with a sequence of qubit probes, perhaps two-level atoms. That said, the interaction Hamiltonian we assume for each probe time segment is

$$H := i\sqrt{\frac{\gamma}{\Delta t}}\,(c \otimes \sigma_+ - c^\dagger \otimes \sigma_-), \tag{7.1}$$

with corresponding joint unitary for the time segment,

$$V(\theta) = e^{-iH\Delta t} = \exp\left[\tfrac{1}{2}\theta(c \otimes \sigma_+ - c^\dagger \otimes \sigma_-)\right], \tag{7.2}$$

where we define $\theta := 2\sqrt{\gamma \Delta t}$. To ensure a strong interaction, we hold θ constant in the limit $\Delta t \rightarrow 0$.

When dealing with these strongly interacting probes, we are not justified in truncating the Taylor expansion of the exponential. This makes it difficult to draw general conclusions for all kinds of systems and all coupling operators c, so we retreat to investigating a particular example to illustrate what happens. We assume the system is a qubit that is coupled to the probe through the operator $c = \sigma_z$. Thus the strong probe/system interaction and subsequent measurement on the probe yield a measurement of σ_z on the system. The interaction unitary (7.2) becomes

$$\begin{aligned}
V(\theta) &= e^{\sigma_z \otimes (\sigma_+ - \sigma_-)\theta/2} \\
&= e^{i\sigma_z \otimes \sigma_y \theta/2} \\
&= \mathbf{1} \otimes \mathbf{1}\cos(\theta/2) + i\sigma_z \otimes \sigma_y \sin(\theta/2) \\
&= |e\rangle\langle e| \otimes R_y(-\theta) + |g\rangle\langle g| \otimes R_y(\theta),
\end{aligned} \tag{7.3}$$

where $R_y(\theta) := e^{-i\sigma_y\theta/2}$ is a rotation of the probe qubit by angle θ about the y axis of the Bloch sphere. This interaction is conveniently thought of as a controlled operation, with the system qubit as control and the probe qubit as target. If the system is in the excited state $|e\rangle$, the probe qubit is rotated by $-\theta$ about y; if the system is in the ground state $|g\rangle$, the probe qubit is rotated by θ about y.

We assume that the probe starts in the ground state and that after the interaction with the system, it is subjected to a measurement of σ_x, i.e., a measurement in the basis $|\phi_\pm\rangle$ of equation (5.20). Under these circumstances, it is easy to see that the measurement on the probe yields information about the z component of the system's spin. Indeed, it becomes an ideal measurement of σ_z if we choose $\theta = \pi/2$, so that the interaction unitary is

$$V := V(\pi/2) = \frac{1}{\sqrt{2}}(\mathbf{1} \otimes \mathbf{1} + i\sigma_z \otimes \sigma_y) = |e\rangle\langle e| \otimes R_y(-\pi/2) + |g\rangle\langle g| \otimes R_y(\pi/2). \tag{7.4}$$

This leaves us in the *good-measurement limit* defined by [97]. One sees the perfect correlation between system and probe after the interaction in

$$V(\alpha|g\rangle + \beta|e\rangle) \otimes |g\rangle = \frac{1}{\sqrt{2}}(\alpha|g\rangle \otimes |\phi_-\rangle + \beta|e\rangle \otimes |\phi_+\rangle). \tag{7.5}$$

To make the strong measurement events correspond to a Poisson process, we control the unitary V off an additional ancillary probe qubit that is initialized in the state

$$|\chi\rangle = \sqrt{1 - \lambda\Delta t}\,|e\rangle + \sqrt{\lambda\Delta t}\,|g\rangle. \tag{7.6}$$

The controlled unitary is defined in the same way as the previously encountered CNOT as

$$CV := \mathbf{1} \otimes \mathbf{1} \otimes |e\rangle\langle e| + V \otimes |g\rangle\langle g|. \tag{7.7}$$

The ancilla qubit is measured in the eigenbasis of σ_z. The unitary V is applied to the system and the primary probe qubit when the result is $|g\rangle$, which occurs with probability $\lambda\Delta t$. The protocol for a single time segment is summarized in the circuit diagrams of figure 16.

The Kraus operators for obtaining result $\pm$ on the probe qubit and result g or e on the ancilla qubit are

$$K_{\pm,e} = (\langle\phi_\pm| \otimes \langle e|)CV(|g\rangle \otimes |\chi\rangle) = \sqrt{1 - \lambda\Delta t}\,\langle\phi_\pm|\mathbf{1} \otimes \mathbf{1}|g\rangle = \sqrt{\frac{1 - \lambda\Delta t}{2}}\,\mathbf{1}, \tag{7.8a}$$

$$K_{\pm,g} = (\langle\phi_\pm| \otimes \langle g|)CV(|g\rangle \otimes |\chi\rangle) = \sqrt{\lambda\Delta t}\,\langle\phi_\pm|V|g\rangle = \sqrt{\lambda\Delta t}\,\frac{\mathbf{1} \pm \sigma_z}{2}. \tag{7.8b}$$

The ancilla outcome, g or e, is not something for which we actually record a measurement outcome, its purpose being merely to mock up a Poisson process, so we coarse-grain over those measurement outcomes to find the unnormalized conditional-state updates:

$$K_{\pm,e}\rho K_{\pm,e}^\dagger + K_{\pm,g}\rho K_{\pm,g}^\dagger = \frac{1}{2}(1 - \lambda\Delta t)\rho + \lambda\Delta t\frac{\mathbf{1} \pm \sigma_z}{2}\rho\frac{\mathbf{1} \pm \sigma_z}{2}$$

$$= \frac{1}{2}\Big(\rho \pm \tfrac{1}{2}\lambda\Delta t(\rho\sigma_z + \sigma_z\rho) + \tfrac{1}{2}\lambda\Delta t(\sigma_z\rho\sigma_z - \rho)\Big). \tag{7.9}$$

It is informative to compare this model of occasional strong measurements with our previously discussed model of continuous weak measurements. To do so, notice that if we remove the ancilla qubit from the circuit in figure 16 and replace the strong interaction unitary V with the analogous weak interaction unitary U_I of (5.1), letting $c = \sigma_z$, we are left with the homodyne measurement model analyzed in section 5.2. The Kraus operators for this model are given by equation (5.21) with $c = \sigma_z$, i.e.,

$$K_\pm = \frac{1}{\sqrt{2}}\Big(\mathbf{1} \pm \sqrt{\gamma\Delta t}\,\sigma_z - \tfrac{1}{2}\gamma\Delta t\,\mathbf{1}\Big); \tag{7.10}$$

The corresponding unnormalized conditional-state updates are

$$K_\pm\rho K_\pm^\dagger = \frac{1}{2}(\rho \pm \sqrt{\gamma\Delta t}\,(\rho\sigma_z + \sigma_z\rho) + \gamma\Delta t(\sigma_z\rho\sigma_z - \rho)). \tag{7.11}$$

The unnormalized conditional state-update rules equations (7.9), (7.11) reveal an important distinction between infrequent strong interactions and constant weak interactions. The $\pm(\rho\sigma_z + \sigma_z\rho)$ terms correspond to conditional stochastic evolution, while the $\sigma_z\rho\sigma_z - \rho$ terms correspond to the unconditional average evolution. In the case of infrequent strong interactions, the conditional and unconditional terms have the same scaling with respect to the time interval Δt, in contrast to the different scalings of these two terms in the case of continuous weak interactions. This means, in particular, that no matter what the Poisson rate λ is, the stochastic steps corresponding to the conditional evolution are of order Δt, not the $\sqrt{\Delta t}$ of a continuous weak interaction, and thus have vanishing effect on the trajectory in the continuum limit. The strong measurements, which project the system onto an eigenstate of σ_z, occur too infrequently to have any effect on the conditional evolution. The $\pm$ measurement outcomes are pure noise, providing no information about the system, and the conditional and unconditional evolutions are identical.

Something more interesting happens when we combine weak interaction strength with measurements that does not always happen. If we assume that $\theta = 2\sqrt{\gamma\Delta t} = 2\sqrt{\Delta\tau}$ is small, then we are back in the domain of weak interactions. If we also define $\eta := \lambda\Delta t$ to be a finite number between 0 and 1, then we are in a situation where ancilla outcome g, which occurs with probability η, leads to the weak interaction, and ancilla outcome e, which occurs with probability $1 - \eta$, leads to no interaction. This corresponds to an inefficient weak measurement. It is easy to see that the Kraus operators are

$$K_{\pm,e} = \sqrt{\frac{1 - \eta}{2}}\,\mathbf{1}, \tag{7.12a}$$

$$K_{\pm,g} = \sqrt{\frac{\eta}{2}}\Big(\mathbf{1} \pm \sqrt{\Delta\tau}\,\sigma_z - \tfrac{1}{2}\Delta\tau\mathbf{1}\Big). \tag{7.12b}$$

For the unnormalized conditional updates, we have

$$K_{\pm,e}\rho K_{\pm,e}^\dagger + K_{\pm,g}\rho K_{\pm,g}^\dagger = \frac{1}{2}(\rho \pm \eta\sqrt{\Delta\tau}\,(\rho\sigma_z + \sigma_z\rho) + \eta\Delta\tau(\sigma_z\rho\sigma_z - \rho)). \tag{7.13}$$

Not surprisingly, these are the same as the updates (7.11), except for the additional factors of η in front of both the conditional and unconditional parts of the evolution. This means that we can read the SME directly off the vacuum homodyne SME (5.30), by incorporating a factor of η on the right-hand side:
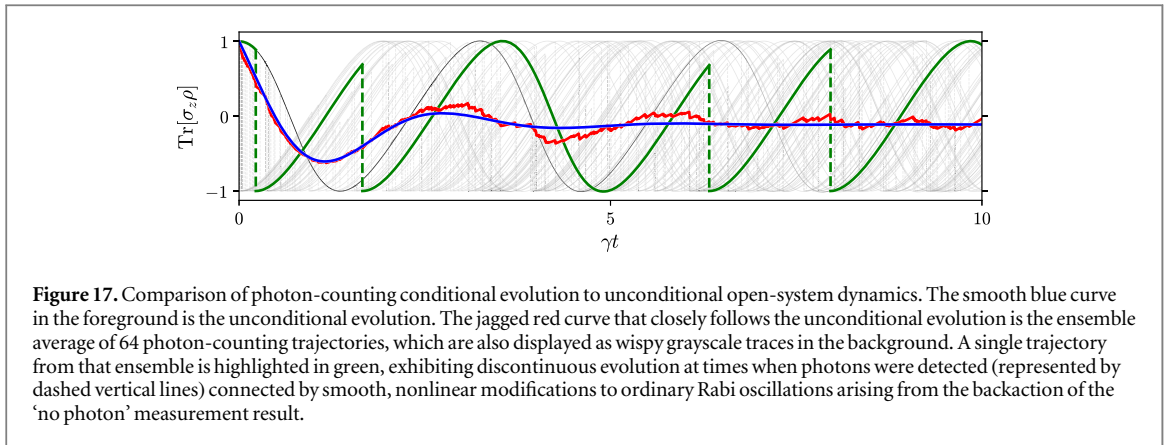
Figure 17. Comparison of photon-counting conditional evolution to unconditional open-system dynamics. The smooth blue curve in the foreground is the unconditional evolution. The jagged red curve that closely follows the unconditional evolution is the ensemble average of 64 photon-counting trajectories, which are also displayed as wispy grayscale traces in the background. A single trajectory from that ensemble is highlighted in green, exhibiting discontinuous evolution at times when photons were detected (represented by dashed vertical lines) connected by smooth, nonlinear modifications to ordinary Rabi oscillations arising from the backaction of the 'no photon' measurement result.

$$d\rho = dt\ \eta\ \mathcal{D}[\sqrt{\gamma}\,\sigma_z]\rho + dW\ \eta\ \mathcal{H}[\sqrt{\gamma}\,\sigma_z]\rho. \tag{7.14}$$

By defining a renormalized coupling strength $\bar{\gamma} := \eta\gamma$, we can put the SME (7.14) in the form

$$d\rho = dt\ \mathcal{D}[\sqrt{\bar{\gamma}}\,\sigma_z]\rho + dW\ \sqrt{\eta}\ \mathcal{H}[\sqrt{\bar{\gamma}}\,\sigma_z]\rho. \tag{7.15}$$

This equation is in the form of a homodyne measurement using detectors with efficiency η [66, see equation (4).238], where the efficiency is the probability of the detector's recording a count in the presence of an excitation. Relative to the model in [66], the additional renormalization of the coupling strength in equation (7.15) is because our model has a probabilistic interaction followed by a perfect measurement instead of a deterministic interaction followed by a measurement with sub-unity efficiency.
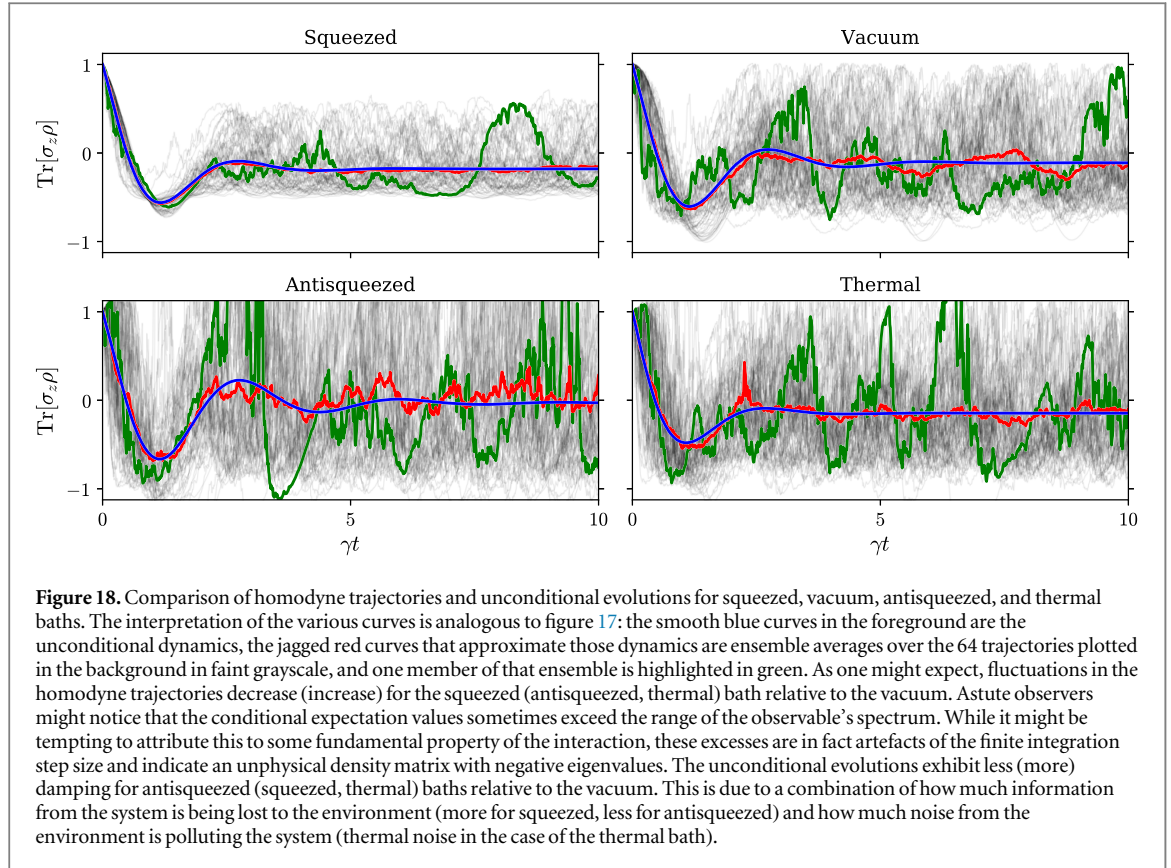
8. Examples: simulation and code

A helpful strategy for gaining intuition about the unconditional master equations and SMEs discussed above is to visualize the kinds of evolution they describe. The authors have published a software package in Python [98] designed to make such visualizations easy to produce. This package has been used to create many of the visualizations below and includes documentation that walks through formulating the quantum problem in a way that facilitates application of known stochastic-integration techniques [99].

We begin by considering a photon-counting measurement described by equation (5.16). Our example system is a two-level atom, coupled to some one-dimensional continuum of modes of the electromagnetic field (perhaps a waveguide) that are initially in the vacuum state, with coupling described by the operator $c = \sigma_-$. We additionally include a classical field driving Rabi oscillations between the two energy levels of the atom, as described by a system Hamiltonian $H_{\text{ext}} = \gamma\sigma_x$. The coupling to the waveguide induces decoherence, so we expect the evolution of the system, ignorant of the state of the waveguide, to exhibit damped Rabi oscillations. This unconditional evolution is given by equation (5.18), and when we solve for the evolution, as shown by the smooth blue curve in the foreground of figure 17, that is exactly what we see.

If we put a photon detector at the end of the waveguide, we maintain full information about the two-level atom. Therefore, we do not expect to see decoherence, but rather jumps in the system evolution when we detect photons in the waveguide. When we solve for a particular instance of the stochastic evolution, as highlighted by the discontinuous green curve in figure 17, we see the jumps corresponding to photon detection, as well as a deformation of pure Rabi oscillations that arises from the backaction of the 'no photon' result from our photon detector.

If we instead monitor the waveguide with homodyne measurements, the system undergoes qualitatively different evolution. The system state never jumps, but vacuum fluctuations appear as jagged white-noise effects in the trajectory. One instance of a stochastic homodyne trajectory is highlighted in green in the upper-right-hand corner of figure 18. The other plots in figure 18 provide some intuition regarding what effects the squeezing and thermalization of the bath have on the system.

The expression that various SMEs are 'unravelings' of the unconditional master equation is meant to communicate that averages of larger and larger ensembles of trajectories converge to the unconditional evolution. These ensemble averages are presented in figures 17 and 18 as the jagged red curves closely hugging the smooth, blue curves of the unconditional evolution. For finite ensembles of trajectories, one still sees vestigial qualities of the underlying stochastic evolution, although the average trajectories are visibly converging to the unconditional evolution.

Figure 18. Comparison of homodyne trajectories and unconditional evolutions for squeezed, vacuum, antisqueezed, and thermal baths. The interpretation of the various curves is analogous to figure 17: the smooth blue curves in the foreground are the unconditional dynamics, the jagged red curves that approximate those dynamics are ensemble averages over the 64 trajectories plotted in the background in faint grayscale, and one member of that ensemble is highlighted in green. As one might expect, fluctuations in the homodyne trajectories decrease (increase) for the squeezed (antisqueezed, thermal) bath relative to the vacuum. Astute observers might notice that the conditional expectation values sometimes exceed the range of the observable's spectrum. While it might be tempting to attribute this to some fundamental property of the interaction, these excesses are in fact artefacts of the finite integration step size and indicate an unphysical density matrix with negative eigenvalues. The unconditional evolutions exhibit less (more) damping for antisqueezed (squeezed, thermal) baths relative to the vacuum. This is due to a combination of how much information from the system is being lost to the environment (more for squeezed, less for antisqueezed) and how much noise from the environment is polluting the system (thermal noise in the case of the thermal bath).

9. Discussion and conclusion

We have now completed our introduction to trajectory theory, using only a minimal understanding of quantum optics to construct an interaction unitary and iterated quantum circuit. From that starting point, we built up the Gaussian theory using tools from finite-dimensional quantum information and computation. We found quantum circuits to illuminate the variety of conditions required to make the Markov approximations. We also found that all the relevant qualities of Gaussian bath modes can be compressed into the single transition of a qubit probe, capturing the effects of mean fields with infinitesimal rotations, thermal excitations with enhanced coupling, and squeezing with modified correlations between system operators c and $c^\dagger$ in the interaction. We also explored an alternative means of producing weak interactions with an environment, noting that stretches of isolation punctuated by strong probe interactions can yield unconditional open-system dynamics similar to that of continuous weak interactions, but the conditional stochastic dynamics remain irreconcilably distinct.

Our program of qubit-izing continuous quantum measurements could be extended in several ways. For instance, one could imagine changing the state of the probe and deriving quantum trajectories for single-photon [100, 101] or N-photon Fock states [102] or Schrödinger-cat states [100]. Recently Dąbrowska *et al.* have worked out the Schrödinger-cat-state version [103] and the single-photon version [104]. In the case of a single photon they define a wavepacket creation operator over N qubits of the form

$$B^\dagger(\xi) = \sum_{n=1}^{N} \xi_n \sqrt{\Delta\tau}\, \sigma_+^{(n)}, \qquad \sum_{n=1}^{N} \Delta\tau\, |\xi_n|^2 = 1. \qquad (9.1)$$

Applying this to the multiqubit 'vacuum' yields the single-photon state

$$|1_\xi\rangle = B^\dagger(\xi)|ggg \ldots g\rangle = \xi_1 \sqrt{\Delta\tau}\, |egg \ldots g\rangle + \xi_2 \sqrt{\Delta\tau}\, |geg \ldots g\rangle$$
$$+ \xi_3 \sqrt{\Delta\tau}\, |gge \ldots g\rangle + \cdots + \xi_N \sqrt{\Delta\tau}\, |ggg \ldots e\rangle. \qquad (9.2)$$

In addition to investigating different kinds of states, interactions, and measurements, we could also imagine trying to reproduce Carmichael's [105] and Gardiner's [106] cascaded quantum systems formalism (and its generalization [107, 108]). In the Markov approximation and the limit of zero delay between successive systems, we could imagine using an input-output formalism for probe qubits, of the sort alluded to at the end of section 6.2, to connect successive systems, or we could work directly in the interaction picture as we have done throughout this paper.

Such extensions hold the promise of identifying parsimonious descriptions of the associated theory, but ultimately, we believe our approach can produce fruit beyond economy of description. The tools we emphasized encourage a particular way of thinking about continuous measurements, trajectories, and feedback that we believe is conducive to the development of improved forms of quantum control.

Acknowledgments

Appendix A. Pure and thermal squeezed baths

In this appendix we list relations that are useful for deriving the results for pure and thermal squeezed baths. The expressions involve the squeezed system operator c_{sq} of equation (6.53) and the homodyne angle φ_{sq} of equation (6.60). When written in terms of the squeezing parameters, r and μ, the expressions are indifferent to whether the bath is pure or thermal; when written in terms of the bath parameters, N, M, and N_{th}, the expressions use equations (6.67b) and (6.67c), applicable for a squeezed thermal bath, to convert from the squeezing parameters to the bath parameters. To specialize the same expressions to a pure squeezed bath, one sets $N_{th} = 0$.

Now the formulas:

$$\cosh^2 r = \frac{N + N_{th} + 1}{2N_{th} + 1}, \tag{A1}$$

$$\sinh^2 r = \frac{N - N_{th}}{2N_{th} + 1}, \tag{A2}$$

$$e^{2i\mu} \sinh r \cosh r = -\frac{M}{2N_{th} + 1}, \tag{A3}$$

$$L = 1 + 2\sinh^2 r - 2\cos 2\mu \sinh r \cosh r = \frac{2N + 2M_R + 1}{2N_{th} + 1} = \frac{L'}{2N_{th} + 1}, \tag{A4}$$

$$L' = (2N_{th} + 1)L = 2N + 2M_R + 1, \tag{A5}$$

$$\begin{aligned} e^{i\varphi_{sq}}c_{sq} &= \frac{c(\cosh^2 r - e^{-2i\mu}\sinh r \cosh r) + c^\dagger(e^{2i\mu}\sinh r \cosh r - \sinh^2 r)}{\sqrt{L}} \\ &= \frac{c(N + N_{th} + M^* + 1) - c^\dagger(N - N_{th} + M)}{\sqrt{2N_{th} + 1}\sqrt{L'}}, \end{aligned} \tag{A6}$$

$$\begin{aligned} c_{sq}\rho c_{sq}^\dagger &= c\rho c^\dagger \cosh^2 r + c^\dagger\rho c \sinh^2 r + c\rho c\, e^{-2i\mu}\sinh r \cosh r + c^\dagger\rho c^\dagger e^{2i\mu}\sinh r \cosh r \\ &= \frac{c\rho c^\dagger(N + N_{th} + 1) + c^\dagger\rho c(N - N_{th}) - c\rho c\, M^* - c^\dagger\rho c^\dagger M}{2N_{th} + 1}, \end{aligned} \tag{A7}$$

$$\begin{aligned} c_{sq}^\dagger c_{sq} &= c^\dagger c \cosh^2 r + cc^\dagger \sinh^2 r + c^2 e^{-2i\mu}\sinh r \cosh r + c^{\dagger 2}e^{2i\mu}\sinh r \cosh r \\ &= \frac{c^\dagger c(N + N_{th} + 1) + cc^\dagger(N - N_{th}) - c^2 M^* - c^{\dagger 2}M}{2N_{th} + 1}, \end{aligned} \tag{A8}$$

$$\mathcal{D}[c_{sq}]\rho = \frac{1}{2N_{th} + 1}\left((N + N_{th} + 1)\mathcal{D}[c]\rho + (N - N_{th})\mathcal{D}[c^\dagger]\rho + \frac{1}{2}M^*[c, [c, \rho]] + \frac{1}{2}M[c^\dagger, [c^\dagger, \rho]]\right), \tag{A9}$$

$$\begin{aligned} c_{sq}^\dagger\rho c_{sq} &= c^\dagger\rho c \cosh^2 r + c\rho c^\dagger \sinh^2 r + c\rho c\, e^{-2i\mu}\sinh r \cosh r + c^\dagger\rho c^\dagger e^{2i\mu}\sinh r \cosh r \\ &= \frac{c^\dagger\rho c(N + N_{th} + 1) + c\rho c^\dagger(N - N_{th}) - c\rho c\, M^* - c^\dagger\rho c^\dagger M}{2N_{th} + 1}, \end{aligned} \tag{A10}$$

$$c_{sq} c_{sq}^\dagger = cc^\dagger \cosh^2 r + c^\dagger c \sinh^2 r + c^2 e^{-2i\mu} \sinh r \cosh r + c^{\dagger 2} e^{2i\mu} \sinh r \cosh r$$

$$= \frac{cc^\dagger (N + N_{th} + 1) + c^\dagger c(N - N_{th}) - c^2 M^* - c^{\dagger 2} M}{2N_{th} + 1}, \tag{A11}$$

$$\mathcal{D}[c_{sq}^\dagger]\rho = \frac{1}{2N_{th} + 1}\left((N + N_{th} + 1)\mathcal{D}[c^\dagger]\rho + (N - N_{th})\mathcal{D}[c]\rho + \frac{1}{2}M^*[c, [c, \rho]] + \frac{1}{2}M[c^\dagger, [c^\dagger, \rho]] \right). \tag{A12}$$

Appendix B. Mixed squeezed states

To evaluate potential qubit models for mixed squeezed states, it is convenient to derive necessary and sufficient conditions on the combination of bath state σ, probe operator a, and measured observable for reproducing the stochastic evolution for homodyne detection, much as equations (6.10) provide necessary and sufficient conditions on the bath state and probe operator for reproducing the unconditional evolution. Since the mixed nature of the bath generally introduces mixing into the system even when the bath is monitored, it is necessary to have at least four Kraus operators; this allows for two measurement outcomes and a conditional evolution for each of those outcomes, which is coarse-grained over two different Kraus evolutions corresponding to the other two outcomes. These Kraus operators can arise from a four-level probe in a pure initial state $|\Phi\rangle$ and observable eigenvectors $|\pm\tilde{\pm}\rangle$ (where the $\tilde{\pm}$ degree of freedom is coarse-grained over to reflect incomplete information) or from a pair of two-level probes in a mixed initial state $\lambda_{\tilde{\mp}}|\psi_{\tilde{\mp}}\rangle\langle\psi_{\tilde{\mp}}| + \lambda_{\simeq}|\psi_{\simeq}\rangle\langle\psi_{\simeq}|$ and observable eigenvectors $|\pm\rangle$. When we use these arrangements with the interaction unitary

$$U_I(a) := \exp\left[\sqrt{\Delta\tau} \left(c \otimes a^\dagger - c^\dagger \otimes a \right) \right], \tag{B1}$$

where a is a finite-dimensional operator analogous to the field annihilation operator b, we parametrize the resulting Kraus operators up to $\mathcal{O}(\Delta\tau)$ as

$$\begin{aligned} K_{\pm\tilde{\pm}} &= \langle U_I \rangle_{\pm\tilde{\pm}} \\ &= \alpha_{\pm\tilde{\pm}} + \sqrt{\Delta\tau}\,(\beta_{0\pm\tilde{\pm}}\, c + \beta_{1\pm\tilde{\pm}}\, c^\dagger) + \Delta\tau\,(\gamma_{0\pm\tilde{\pm}}\, c^2 + \gamma_{1\pm\tilde{\pm}}\, cc^\dagger + \gamma_{2\pm\tilde{\pm}}\, c^\dagger c + \gamma_{3\pm\tilde{\pm}}\, c^{\dagger 2}). \end{aligned} \tag{B2}$$

Here we introduce the notation that for any operator A, $\langle A \rangle_{\pm\tilde{\pm}} := \langle \pm\tilde{\pm}|A|\Phi\rangle$ for the case of a pure bath with four measurement outcomes and $\langle A \rangle_{\pm\tilde{\pm}} := \sqrt{\lambda_{\tilde{\pm}}}\,\langle \pm|A|\psi_{\tilde{\pm}}\rangle$ for a mixed bath with two measurement outcomes. With this notation, the various parameters become

$$\alpha_{\pm\tilde{\pm}} = \langle \mathbf{1} \rangle_{\pm\tilde{\pm}}, \tag{B3a}$$

$$\beta_{0\pm\tilde{\pm}} = \langle a^\dagger \rangle_{\pm\tilde{\pm}}, \qquad\qquad \beta_{1\pm\tilde{\pm}} = -\langle a \rangle_{\pm\tilde{\pm}}, \tag{B3b}$$

$$\gamma_{1\pm\tilde{\pm}} = -\frac{1}{2}\langle a^\dagger a \rangle_{\pm\tilde{\pm}}, \qquad\qquad \gamma_{2\pm\tilde{\pm}} = -\frac{1}{2}\langle aa^\dagger \rangle_{\pm\tilde{\pm}}, \tag{B3c}$$

$$\gamma_{0\pm\tilde{\pm}} = \frac{1}{2}\langle a^{\dagger 2} \rangle_{\pm\tilde{\pm}}, \qquad\qquad \gamma_{3\pm\tilde{\pm}} = \frac{1}{2}\langle a^2 \rangle_{\pm\tilde{\pm}}. \tag{B3d}$$

Just like the case of a thermal bath, the updated state is calculated by coarse-graining over one of the two binary variables in the measurement outcome, giving

$$\rho_\pm = \frac{K_{\pm\tilde{\mp}}\rho K_{\pm\tilde{\mp}}^\dagger + K_{\pm\simeq}\rho K_{\pm\simeq}^\dagger}{\text{Tr}[(E_\pm\rho)]}, \tag{B4}$$

where $E_\pm = K_{\pm\tilde{\mp}}^\dagger K_{\pm\tilde{\mp}} + K_{\pm\simeq}^\dagger \rho K_{\pm\simeq}$.

If we calculate the conditional difference equation from the parametrized Kraus operators (B2), we can match terms to the squeezed-bath conditional difference equation (6.76) and come up with a set of constraints on the Kraus parameters. For the α parameters, we get

$$\alpha_{\pm\tilde{\mp}} = \frac{1}{\sqrt{2}}\cos\phi_\pm, \tag{B5a}$$

$$\alpha_{\pm\simeq} = \frac{1}{\sqrt{2}}\sin\phi_\pm, \tag{B5b}$$

where we use the phase freedom inherent in the Kraus operators to make $\alpha_{\pm\tilde{\pm}} \geqslant 0$, i.e., $0 \leqslant \phi_\pm \leqslant \pi/2$. The constraints for the β parameters are

$$|\beta_{0\pm\widetilde{\mp}}|^2 + |\beta_{0\pm\simeq}|^2 = \frac{N+1}{2}, \tag{B6a}$$

$$|\beta_{1\pm\widetilde{\mp}}|^2 + |\beta_{1\pm\simeq}|^2 = \frac{N}{2}, \tag{B6b}$$

$$\beta_{1\pm\widetilde{\mp}}\beta^*_{0\pm\widetilde{\mp}} + \beta_{1\pm\simeq}\beta^*_{0\pm\simeq} = -\frac{M}{2}, \tag{B6c}$$

$$\beta_{0\pm\widetilde{\mp}}\cos\phi_\pm + \beta_{0\pm\simeq}\sin\phi_\pm = \pm\frac{N+M^*+1}{\sqrt{2L'}}, \tag{B6d}$$

$$\beta_{1\pm\widetilde{\mp}}\cos\phi_\pm + \beta_{1\pm\simeq}\sin\phi_\pm = \mp\frac{N+M}{\sqrt{2L'}}, \tag{B6e}$$

where $L' = 2N + M + M^* + 1$ as in equation (6.75). The nature of the constraints on the γ variables always allows appropriate values to be found, given any solution of the above equations:

$$\gamma_{1\pm\widetilde{\mp}} = -\frac{N}{4\sin(\phi_\pm + \pi/4)}, \tag{B7a}$$

$$\gamma_{2\pm\widetilde{\mp}} = -\frac{N+1}{4\sin(\phi_\pm + \pi/4)}, \tag{B7b}$$

$$\gamma_{3\pm\widetilde{\mp}} = -\frac{M}{4\sin(\phi_\pm + \pi/4)}, \tag{B7c}$$

$$\gamma_{0\pm\widetilde{\mp}} = -\frac{M^*}{4\sin(\phi_\pm + \pi/4)}. \tag{B7d}$$

B.1. Araki-Woods

One technique that presents itself for the squeezed thermal case is the Araki-Woods construction, employed in [88] to treat general Gaussian states with a vacuum-based technique. This construction transforms the bath statistics from the probe state to the field operator in a slightly different manner than the successful technique and puts the probe into a two-mode vacuum. The form of the updated field operators is

$$b_{\mathrm{AW}} := x(\mathbf{1} \otimes b) + y(b^\dagger \otimes \mathbf{1}) + z(b \otimes \mathbf{1}), \tag{B8}$$

corresponding to a qubit model with probe initial state $|gg\rangle$ and updated qubit field operators

$$a_{\mathrm{AW}} := x(\mathbf{1} \otimes \sigma_-) + y(\sigma_+ \otimes \mathbf{1}) + z(\sigma_- \otimes \mathbf{1}), \tag{B9}$$

where the constants x, y, and z are defined as

$$x := \sqrt{N + 1 - |M|^2/N}, \tag{B10a}$$

$$y := \sqrt{N}, \tag{B10b}$$

$$z := M/\sqrt{N}. \tag{B10c}$$

The above definitions are slightly different from those presented in [88], as we have suppressed the mean field term, it being trivial to include such a term, as is described at the end of section 6.5, and changed the ordering of the subsystems to reflect our notational conventions.

When the bath is in a pure state, $|M|^2 = N(N+1)$ and thus $x = 0$. Since the only term in a_{AW} that involves the second is proportional to x, for a pure bath we only need to consider the first field mode. In this case, using a_{AW} in the interaction unitary and measuring $a_{\mathrm{AW}} + a^\dagger_{\mathrm{AW}}$ gives the Kraus operators equation (6.61) and therefore produces the correct stochastic evolution.

Unfortunately, even though the Araki-Woods discrete field operators give the appropriate bath statistics and thus the correct unconditional evolution even for $|M|^2 < N(N+1)$, they do not satisfy the constraints given above to produce the correct conditional evolution. In particular, the Araki-Woods Kraus operators give us

$$\cos\phi_\pm = \sin\phi_\pm = \frac{1}{\sqrt{2}}, \tag{B11a}$$

$$\beta_{0\pm\widetilde{\mp}} + \beta_{0\pm\simeq} = \pm\frac{N+M^*+1}{\sqrt{L'}}\sqrt{\frac{N+2M_R+|M|^2/N}{2N+2M_R+1}}. \tag{B11b}$$

This only satisfies the SME constraints when $|M|^2 = N(N+1)$, i.e., when the bath is in a pure state.

One indication that something might break in the mixed case is that the field homodyne observable, $b_{\mathrm{AW}} + b^\dagger_{\mathrm{AW}}$, ought to have degeneracy in eigenvalues, since in the field picture the thermalization of the field can be interpreted as entanglement with an auxiliary mode that is not measured (i.e., we measure $(b + b^\dagger) \otimes \mathbf{1}$),

leading to degenerate subspaces for each eigenvalue of $b + b^\dagger$. In the qubit picture, the homodyne observable $a_{\mathrm{AW}} + a_{\mathrm{AW}}^\dagger$ has the spectrum

$$\lambda_{\pm\widetilde{\mp}} = \widetilde{\mp}x \pm |y + z|, \tag{B12}$$

which is degenerate only in the case $x = 0$, since $|z| \leqslant \sqrt{y^2 + 1} \leqslant y$ from equation (6.3). This condition is met only when the bath is pure.

B.2. Two-qubit setup analogous to two-mode squeezing

To manufacture thermal statistics, we might think to consider the thermal state of a bath mode as the marginal state of a two-mode squeezed state. Then, much as we did in the pure-state case, we could transfer all squeezing from the bath state to the field operators and on to analogous qubit operators. Using the two-mode squeeze operator,

$$S^{(1,2)}(r_{\mathrm{th}}) := \exp\left[r_{\mathrm{th}}(b \otimes b - b^\dagger \otimes b^\dagger)\right], \tag{B13}$$

gives us the squeezed field operator

$$b_{\mathrm{sq}} = S^{(12)\,\dagger}(r_{\mathrm{th}})S^{(1)\,\dagger}(r, \phi)(b \otimes \mathbb{1})S^{(1)}(r, \phi)S^{(12)}(r_{\mathrm{th}}) \tag{B14}$$

$$= \cosh r \cosh r_{\mathrm{th}}(b \otimes \mathbb{1}) - e^{2i\phi} \cosh r \sinh r_{\mathrm{th}}(\mathbb{1} \otimes b^\dagger) - e^{2i\phi} \sinh r \cosh r_{\mathrm{th}}(b^\dagger \otimes \mathbb{1}) + \sinh r \sinh r_{\mathrm{th}}(\mathbb{1} \otimes b), \tag{B15}$$

which translates to the squeezed qubit operators

$$a_{\mathrm{sq}} = \cosh r \cosh r_{\mathrm{th}}(\sigma_- \otimes \mathbb{1}) - e^{2i\phi} \cosh r \sinh r_{\mathrm{th}}(\mathbb{1} \otimes \sigma_+) - e^{2i\phi} \sinh r \cosh r_{\mathrm{th}}(\sigma_+ \otimes \mathbb{1})$$
$$+ \sinh r \sinh r_{\mathrm{th}}(\mathbb{1} \otimes \sigma_-). \tag{B16}$$

The quadrature operator for homodyne measurement, $a_{\mathrm{sq}} + a_{\mathrm{sq}}^\dagger$, has a problem similar to that of the Araki-Woods quadrature operator in that its eigenvalues are nondegenerate:

$$\lambda_{1\pm} = \pm\frac{1}{\sqrt{2}\,e^r}\sqrt{-e^{4r}e^{2r_{\mathrm{th}}}\cos 2\phi + e^{4r}e^{2r_{\mathrm{th}}} + e^{2r_{\mathrm{th}}}\cos 2\phi + e^{2r_{\mathrm{th}}}}, \tag{B17}$$

$$\lambda_{2\pm} = \pm\frac{1}{\sqrt{2}\,e^r e^{r_{\mathrm{th}}}}\sqrt{-e^{4r}\cos 2\phi + e^{4r} + 1 + \cos 2\phi}. \tag{B18}$$

This construction fails to satisfy the Kraus-operator constraints on thermal stochastic evolution even in the absence of squeezing ($N > 0$, $M = 0$), confirming our suspicion based on the nondegeneracy of the observable eigenvalues.

B.3. Two-qubit squeezed-thermal state

Another simple two-qubit setup uses the probe annihilation operator

$$a_{\mathrm{sq}} = \sqrt{\frac{2N + 1}{2}}(\mathbb{1} \otimes \sigma_- + \sigma_- \otimes \mathbb{1}) \tag{B19}$$

in conjunction with the interaction unitary $U(a_{\mathrm{sq}})$ from equation (B1) and the initial probe state

$$\sigma_{\mathrm{sq}} = \frac{1}{2N + 1}\begin{pmatrix} N & 0 & 0 & M \\ 0 & 0 & 0 & 0 \\ 0 & 0 & 0 & 0 \\ M^* & 0 & 0 & N + 1 \end{pmatrix}, \tag{B20}$$

which we consider as it is a positive state precisely when the parameters M and N satisfy the usual constraint $|M|^2 \leqslant (N + 1)N$ (obtaining purity only when $|M|^2 = (N + 1)N$). By observation or by calculation, we see that the bath density operator has rank two, i.e., has support only on a qubit subspace.

The consequences of this model are analogous to those of the Araki-Woods construction: unconditional statistics are reproduced, but the stochastic evolution is incorrect when measuring $a_{\mathrm{sq}} + a_{\mathrm{sq}}^\dagger$. The difficulty again appears to be a lack of degeneracy in the eigenvalues of the $a_{\mathrm{sq}} + a_{\mathrm{sq}}^\dagger$. Specifically, this setup reproduces the correct bath statistics, but the observable $a_{\mathrm{sq}} + a_{\mathrm{sq}}^\dagger$ has three distinct eigenvalues (unique positive and negative eigenvalues with a twofold degeneracy corresponding to an eigenvalue of 0) instead of degenerate positive and negative subspaces as we expect from the field case.

Naïvely pairing half of the zero subspace with both the positive and negative outcomes yields a SME in the pure case very close to the correct result, except that the Wiener process dW is divided by $\sqrt{2(2N + 1)}$ instead of $\sqrt{L'}$; this corresponds to doing homodyne detection on a pure squeezed bath with detectors having sub-unity efficiency. Likewise, setting $M = 0$ for a thermal bath with no squeezing yields a thermal SME with an extra factor of $1/\sqrt{2}$ in the stochastic term, again analogous to sub-unity detection efficiency.

This inefficiency makes sense given that we naïvely lumped distinguishable measurement outcomes together. Unfortunately, this model does not provide clear alternative recipes with which to construct a SME, so we do not consider this model any further.

B.4. Qutrit

One can also mock up a bath with three-level probes and field operators that give the correct unconditional evolution. We define the qutrit probe annihilation operator to be

$$a := \sqrt{2N+1}\left(|0\rangle\langle 1| + |1\rangle\langle 2|\right). \tag{B21}$$

The thermal and squeezed qutrit probe state we choose, following the reasoning by which we arrived at equation (B20), is

$$\sigma_{\mathrm{sq}} := \frac{1}{2N+1}\begin{pmatrix} N & 0 & M \\ 0 & 0 & 0 \\ M^* & 0 & N+1 \end{pmatrix}. \tag{B22}$$

In our matrix representations we have ordered the rows and columns starting from the top and left with $|2\rangle$ and decreasing to $|0\rangle$ as we move to the bottom and right.

The combination of the above lowering operator and state gives the correct unconditional master equation. Three-level systems present even more difficulty in understanding what to do with the conditional evolution, however, as the restriction to three Kraus operators means only one of the measurement results can be coarse-grained over multiple (two) Kraus operators, leaving the other measurement result only associated with a single Kraus operator and therefore producing no statistical mixing of the system state.

ORCID iDs

Jonathan A Gross ● https://orcid.org/0000-0001-7049-6206
Joshua Combes ● https://orcid.org/0000-0003-3199-5744

References

[1] Hood C J, Chapman M S, Lynn T W and Kimble H J 1998 Real-time cavity QED with single atoms *Phys. Rev. Lett.* **80** 4157
[2] Gambetta J, Blais A, Boissonneault M, Houck A A, Schuster D I and Girvin S M 2008 Quantum trajectory approach to circuit QED: quantum jumps and the Zeno effect *Phys. Rev.* A **77** 012112
[3] Boissonneault M, Gambetta J M and Blais A 2008 Nonlinear dispersive regime of cavity QED: the dressed dephasing model *Phys. Rev.* A **77** 060305
[4] Murch K W, Weber S J, Macklin C and Siddiqi I 2013 Observing single quantum trajectories of a superconducting quantum bit *Nature* **502** 211
[5] Goan H-S and Milburn G J 2001 Dynamics of a mesoscopic charge quantum bit under continuous quantum measurement *Phys. Rev.* B **64** 235307
[6] Oxtoby N P, Warszawski P, Wiseman H M, Sun H-B and Polkinghorne R E S 2005 Quantum trajectories for the realistic measurement of a solid-state charge qubit *Phys. Rev.* B **71** 165317
[7] Oxtoby N P, Gambetta J and Wiseman H M 2008 Model for monitoring of a charge qubit using a radio-frequency quantum point contact including experimental imperfections *Phys. Rev.* B **77** 125304
[8] Milburn G J, Jacobs K and Walls D F 1994 Quantum-limited measurements with the atomic force microscope *Phys. Rev.* A **50** 5256
[9] Hopkins A, Jacobs K, Habib S and Schwab K 2003 Feedback cooling of a nanomechanical resonator *Phys. Rev.* B **68** 235328
[10] Ruskov R, Schwab K and Korotkov A N 2005 Squeezing of a nanomechanical resonator by quantum nondemolition measurement and feedback *Phys. Rev.* B **71** 235407
[11] Jacobs K, Lougovski P and Blencowe M 2007 Continuous measurement of the energy eigenstates of a nanomechanical resonator without a nondemolition probe *Phys. Rev. Lett.* **98** 147201
[12] Ahn C, Doherty A C and Landahl A J 2002 Continuous quantum error correction via quantum feedback control *Phys. Rev.* A **65** 042301
[13] Sarovar M, Ahn C, Jacobs K and Milburn G J 2004 Practical scheme for error control using feedback *Phys. Rev.* A **69** 052324
[14] Ahn C, Wiseman H and Jacobs K 2004 Quantum error correction for continuously detected errors with any number of error channels per qubit *Phys. Rev.* A **70** 024302
[15] Gregoratti M and Werner R F 2004 On quantum error-correction by classical feedback in discrete time *J. Math. Phys.* **45** 2600
[16] van Handel R and Mabuchi H 2005 Optimal error tracking via quantum coding and continuous syndrome measurement arXiv:quant-ph/0511221
[17] Chase B A, Landahl A J and Geremia J 2008 Efficient feedback controllers for continuous-time quantum error correction *Phys. Rev.* A **77** 032304
[18] Mabuchi H 2009 Continuous quantum error correction as classical hybrid control *New J. Phys.* **11** 105044
[19] Lidar D A and Brun T A (ed) 2013 *Quantum Error Correction* (Cambridge: Cambridge University Press) (https://doi.org/10.1017/CBO9781139034807)
[20] Nguyen T, Hill C D, Hollenberg L C L and James M R 2015 Surface code continuous quantum error correction using feedback *2015 LIV IEEE Conf. on Decision and Control (CDC)* pp 7101–6
[21] Hsu K-C and Brun T A 2016 Method for quantum-jump continuous-time quantum error correction *Phys. Rev.* A **93** 022321
[22] Oreshkov O and Brun T A 2005 Weak measurements are universal *Phys. Rev. Lett.* **95** 110409

[23] Varbanov M and Brun T A 2007 Decomposing generalized measurements into continuous stochastic processes *Phys. Rev.* A **76** 032104

[24] Florjanczyk J and Brun T A 2015 Continuous decomposition of quantum measurements via Hamiltonian feedback *Phys. Rev.* A **92** 062113

[25] Florjanczyk J and Brun T A 2014 Continuous decomposition of quantum measurements via qubit-probe feedback *Phys. Rev.* A **90** 032102

[26] Mabuchi H 1996 Dynamical identification of open quantum systems *Quantum Semiclass. Opt.* **8** 1103

[27] Gambetta J and Wiseman H M 2001 State and dynamical parameter estimation for open quantum systems *Phys. Rev.* A **64** 042105

[28] Chase B A and Geremia J M 2009 Single-shot parameter estimation via continuous quantum measurement *Phys. Rev.* A **79** 022314

[29] Gammelmark S and Mølmer K 2013 Bayesian parameter inference from continuously monitored quantum systems *Phys. Rev.* A **87** 032115

[30] Kiilerich A H and Mølmer K 2014 Estimation of atomic interaction parameters by photon counting *Phys. Rev.* A **89** 052110

[31] Kiilerich A H and Mølmer K 2016 Bayesian parameter estimation by continuous homodyne detection *Phys. Rev.* A **94** 032103

[32] Gong B and Cui W 2017 On the calculation of Fisher information for quantum parameter estimation based on the stochastic master equation arXiv:1702.08089 [quant-ph]

[33] Cook R L, Riofrío C A and Deutsch I H 2014 Single-shot quantum state estimation via a continuous measurement in the strong backaction regime *Phys. Rev.* A **90** 032113

[34] Brun T A 2002 A simple model of quantum trajectories *Am. J. Phys.* **70** 719

[35] Scully M O and Lamb W E 1967 Quantum theory of an optical maser. I. General theory *Phys. Rev.* **159** 208

[36] Meyer P 1986 A finite approximation to boson Fock space *in Stochastic Processes in Classical and Quantum Systems* (Berlin: Springer) pp 405–10

[37] Attal S 2002 Approximating the Fock space with the toy Fock space *Séminaire de Probabilités de Strasbourg* **36** 477

[38] Gough J and Sobolev A 2004 Stochastic Schrödinger equations as limit of discrete filtering *Open Systems & Information Dynamics* **11** 235

[39] Gough J 2004 Holevo-ordering and the continuous-time limit for open Floquet dynamics *Lett. Math. Phys.* **67** 207

[40] Attal S and Pautrat Y 2005 From $(n + 1)$-level atom chains to n-dimensional noises *in Annales de l'Institut Henri Poincare (B) Probability and Statistics* vol 41 (Amsterdam: Elsevier) pp 391–407

[41] Attal S and Pautrat Y 2006 From repeated to continuous quantum interactions *Annales Henri Poincaré* **7** 59

[42] Belton A C R 2008 Approximation via toy Fock space—the vacuum-adapted viewpoint *in Quantum Stochastics and Information* (Singapore: World Scientific) pp 3–22

[43] Bouten L, van Handel R and James M R 2009 A discrete invitation to quantum filtering and feedback control *SIAM Rev.* **51** 239

[44] Attal S and Nechita I 2011 Discrete approximation of the free Fock space *in Séminaire de Probabilités XLIII* ed C Donati-Martin, A Lejay and A Rouault (Berlin, Heidelberg: Springer Berlin Heidelberg) pp 379–94

[45] Mensky M B 1979 Quantum restrictions for continuous observation of an oscillator *Phys. Rev.* D **20** 384

[46] Mensky M B 1993 *Continuous Quantum Measurements and Path Integrals* (Boca Raton, FL: CRC Press)

[47] Belavkin V P 1980 Quantum filtering of Markov signals with white quantum noise *Radiotechnika i Electronika* **25** 1445

[48] Srinivas M and Davies E 1981 Photon counting probabilities in quantum optics *Optica Acta: International Journal of Optics* **28** 981

[49] Braginskiĭ V B and Khalili F Y 1995 *Quantum Measurement* (Cambridge: Cambridge University Press) (https://doi.org/10.1017/CBO9780511622748)

[50] Barchielli A, Lanz L and Prosperi G M 1982 A model for the macroscopic description and continual observations in quantum mechanics *Il Nuovo Cimento B (1971-1996)* **72** 79

[51] Gisin N 1984 Quantum measurements and stochastic processes *Phys. Rev. Lett.* **52** 1657

[52] Diósi L 1986 Stochastic pure state representation for open quantum systems *Phys. Lett.* A **114** 451

[53] Diósi L 1988 Continuous quantum measurement and Itô formalism *Phys. Lett.* A **129** 419

[54] Caves C M 1986 Quantum mechanics of measurements distributed in time. A path-integral formulation *Phys. Rev.* D **33** 1643

[55] Caves C M 1987 Quantum mechanics of measurements distributed in time. II. Connections among formulations *Phys. Rev.* D **35** 1815

[56] Caves C M and Milburn G J 1987 Quantum-mechanical model for continuous position measurements *Phys. Rev.* A **36** 5543

[57] Wiseman H M and Milburn G J 1993a Quantum theory of field-quadrature measurements *Phys. Rev.* A **47** 642

[58] Carmichael H J 1993 An Open Systems Approach to Quantum Optics *Lecture Notes in Physics Monographs* vol 18 (Berlin Heidelberg: Springer-Verlag) (https://doi.org/10.1007/978-3-540-47620-7)

[59] Dalibard J, Castin Y and Mølmer K 1992 Wave-function approach to dissipative processes in quantum optics *Phys. Rev. Lett.* **68** 580

[60] Korotkov A N 1999 Continuous quantum measurement of a double dot *Phys. Rev.* B **60** 5737

[61] Korotkov A N 2001 Selective quantum evolution of a qubit state due to continuous measurement *Phys. Rev.* B **63** 115403

[62] Jacobs K and Steck D A 2006 A straightforward introduction to continuous quantum measurement *Contemp. Phys.* **47** 279

[63] Wiseman H M 1994a Quantum trajectories and feedback *Ph.D. Thesis* University of Queensland

[64] Bouten L, Handel R V and James M R 2007 An introduction to quantum filtering *SIAM J. Control Optim.* **46** 2199

[65] Carmichael H J 2008 Statistical Methods in Quantum Optics 2: Non-Classical Fields *Theoretical and Mathematical Physics* (Berlin Heidelberg: Springer-Verlag) (https://doi.org/10.1007/978-3-540-71320-3)

[66] Wiseman H M and Milburn G J 2010 *Quantum Measurement and Control* (Cambridge: Cambridge University Press) (https://doi.org/10.1017/CBO9780511813948)

[67] Jacobs K 2014 *Quantum Measurement Theory and Its Applications* (Cambridge: Cambridge University Press) (https://doi.org/10.1017/CBO9781139179027)

[68] Aharonov Y, Albert D Z and Vaidman L 1988 How the result of a measurement of a component of the spin of a spin-1/2 particle can turn out to be 100 *Phys. Rev. Lett.* **60** 1351

[69] Duck I M, Stevenson P M and Sudarshan E C G 1989 The sense in which a 'weak measurement' of a spin-$\frac{1}{2}$ particle's spin component yields a value 100 *Phys. Rev.* D **40** 2112

[70] Zoller P, Marte M and Walls D F 1987 Quantum jumps in atomic systems *Phys. Rev.* A **35** 198

[71] Nielsen M A and Chuang I L 2010 *Quantum Computation and Quantum Information* (Cambridge: Cambridge University Press) (https://doi.org/10.1017/CBO9780511976667)

[72] Doherty A C and Jacobs K 1999 Feedback control of quantum systems using continuous state estimation *Phys. Rev.* A **60** 2700

[73] Gardiner C W and Zoller P 2004 *Quantum Noise* (Berlin: Springer)

[74] Unruh W G and Zurek W H 1989 Reduction of a wave packet in quantum Brownian motion *Phys. Rev.* D **40** 1071

[75] Fischer K A, Trivedi R, Ramasesh V, Siddiqi I and Vučković J 2017 Scattering of coherent pulses from quantum-optical systems arXiv:1710.02875

[76] Sayrin C *et al* 2011 Real-time quantum feedback prepares and stabilizes photon number states *Nature* **477** 73

[77] Scully M O and Zubairy M S 1997 *Quantum Optics* (Cambridge: Cambridge University Press) (https://doi.org/10.1017/CBO9780511813993)

[78] Horowitz J M 2012 Quantum-trajectory approach to the stochastic thermodynamics of a forced harmonic oscillator *Phys. Rev.* E **85** 031110

[79] Strasberg P, Schaller G, Brandes T and Esposito M 2017 Quantum and information thermodynamics: a unifying framework based on repeated interactions *Phys. Rev.* X **7** 021003

[80] Giovannetti V and Palma G M 2012 Master equations for correlated quantum channels *Phys. Rev. Lett.* **108** 040401

[81] Rybár T, Filippov S N, Ziman M and Bužek V 2012 Simulation of indivisible qubit channels in collision models *J. Phys. B: At. Mol. Opt. Phys.* **45** 154006

[82] Ciccarello F 2017 Collision models in quantum optics *Quantum Measurements and Quantum Metrology* **4** 53–63

[83] Gisin N and Percival I C 1992 Wave-function approach to dissipative processes: are there quantum jumps? *Phys. Lett.* A **167** 315

[84] Wiseman H M and Milburn G J 1993b Interpretation of quantum jump and diffusion processes illustrated on the Bloch sphere *Phys. Rev.* A **47** 1652

[85] Wiseman H M 1994b Quantum theory of continuous feedback *Phys. Rev.* A **49** 2133

[86] Gardiner C W, Parkins A S and Zoller P 1992 Wave-function quantum stochastic differential equations and quantum-jump simulation methods *Phys. Rev.* A **46** 4363

[87] Dum R, Parkins A S, Zoller P and Gardiner C W 1992 Monte Carlo simulation of master equations in quantum optics for vacuum, thermal, and squeezed reservoirs *Phys. Rev.* A **46** 4382

[88] Gough J 2003 Quantum white noises and the master equation for Gaussian reference states *Russian Journal of Mathematical Physics* **10** 142 (http://irep.ntu.ac.uk/id/eprint/20037)

[89] Nechita I and Pellegrini C 2009 Quantum trajectories in random environment: the statistical model for a heat bath *Confluentes Mathematici* **01** 249

[90] Attal S and Pellegrini C 2010 Stochastic master equations in thermal environment *Open Systems & Information Dynamics* **17** 389

[91] Hellmich J, Honegger R, Köstler C, Kümmerer B and Rieckers A 2002 Couplings to classical and non-classical squeezed white noise as stationary Markov processes *Publications of the Research Institute for Mathematical Sciences* **38** 1

[92] Haus H A and Mullen J A 1962 Quantum noise in linear amplifiers *Phys. Rev.* **128** 2407

[93] Caves C M 1982 Quantum limits on noise in linear amplifiers *Phys. Rev.* D **26** 1817

[94] Yurke B and Denker J S 1984 Quantum network theory *Phys. Rev.* A **29** 1419

[95] Blow K J, Loudon R, Phoenix S J D and Shepherd T J 1990 Continuum fields in quantum optics *Phys. Rev.* A **42** 4102

[96] Chiao R Y and Garrison J C 2008 *Quantum Optics* (Oxford: Oxford University Press) (https://doi.org/10.1093/acprof:oso/9780198508861.001.0001)

[97] Milburn G J 2014 Quantum control based on measurement *in Quantum Information and Coherence* ed E Andersson and P Öhberg (Berlin: Springer) pp 147–58

[98] Gross J 2017 Pysme: a package for simulating stochastic master equations in python *github.com* 10.5281/zenodo.1034811

[99] Kloeden P E and Platen E 1992 *Numerical Solution of Stochastic Differential equations* (Berlin, Heidelberg: Springer Berlin Heidelberg) (https://doi.org/10.1007/978-3-662-12616-5)

[100] Gough J E, James M R and Nurdin H I 2011 Quantum master equation and filter for systems driven by fields in a single photon state *Proc. of the Joint L IEEE Conf. on Decision and Control and European Control Conf. (CDC-ECC)* pp 5570–6

[101] Gough J E, James M R, Nurdin H I and Combes J 2012 Quantum filtering for systems driven by fields in single-photon states or superposition of coherent states *Phys. Rev.* A **86** 043819

[102] Baragiola B Q and Combes J 2017 Quantum trajectories for propagating Fock states *Phys. Rev.* A **96** 023819

[103] Dąbrowska A 2017 Quantum trajectories for environment in superposition of coherent states arXiv:1707.06205

[104] Dąbrowska A, Sarbicki G and Chruściński D 2017 Quantum trajectories for a system interacting with environment in a single-photon state: counting and diffusive processes *Phys. Rev.* A **96** 053819

[105] Carmichael H J 1993b Quantum trajectory theory for cascaded open systems *Phys. Rev. Lett.* **70** 2273

[106] Gardiner C W 1993 Driving a quantum system with the output field from another driven quantum system *Phys. Rev. Lett.* **70** 2269

[107] Gough J and James M R 2009 The series product and its application to quantum feedforward and feedback networks *IEEE Trans. Aut. Control* **54** 2530

[108] Combes J, Kerckhoff J and Sarovar M 2017 The SLH framework for modeling quantum input-output networks *Advances in Physics:* X **2** 784